

**HYDRODYNAMIC MODELING OF DELAWARE BAY WITH
APPLICATIONS TO STORM SURGES AND COASTAL FLOODING:
CURRENT CONDITIONS AND FUTURE SCENARIOS**

by

Andre Paim Ferraz Rodrigues

A thesis submitted to the Faculty of the University of Delaware in partial fulfillment of the requirements for the degree of Master of Science in Marine Studies

Fall 2016

© 2016 Andre Paim Ferraz Rodrigues
All Rights Reserved

**HYDRODYNAMIC MODELING OF DELAWARE BAY WITH
APPLICATIONS TO STORM SURGES AND COASTAL FLOODING:
CURRENT CONDITIONS AND FUTURE SCENARIOS**

by

Andre Paim Ferraz Rodrigues

Approved: _____
Tobias Kukulka, Ph.D.
Professor in charge of thesis on behalf of the Advisory Committee

Approved: _____
Mark A. Moline, Ph.D.
Director of the School of Marine Science and Policy

Approved: _____
Mohsen Badiy, Ph.D.
Acting Dean of the College of Earth, Ocean, and Environment

Approved: _____
Ann L. Ardis, Ph.D.
Senior Vice Provost for Graduate and Professional Education

ACKNOWLEDGMENTS

I thank my advisor, Dr. Tobias Kukulka, for believing in me and for helping me to find my way during my period here. This wouldn't have happened without you.

Funding was supported in part by the Delaware Department of Natural Resources and Environmental Control, in part by the University of Delaware Research Foundation, and in part by the NSF Grant OCE1634578.

This study was supported by computational and staff resources from the Department of Information Technologies at the University of Delaware.

I would also like to thank

- All the professors who taught me during my period at the University of Delaware: Tobias, Fabrice, Pablo, Andreas, Danny, Helga, Corbett, Carlos, Kirby, Tom, Xiao-Hai, Greenberg. Every time you teach something to someone, you give a part of you to that person, and I will bring little pieces of you wherever I go.
- All my friends who helped me in so many ways. Peter, Yi, Pat, Shamin, Dimitrios, Payam, Rob, Joe, Auvi, Dong, Enhui, Zheguang, Wenfang, Feiyun. You all helped in many ways, and I will miss you.

DEDICATION

I want to dedicate this study to my wife: without your support and love and care, I do not know if this would have become reality.

And to my daughter, who teach me every day to find a reason to smile, even in the smallest of things.

TABLE OF CONTENTS

LIST OF TABLES	vii
LIST OF FIGURES	viii
ABSTRACT	xvi

Chapter

1	INTRODUCTION	1
1.1	Delaware Bay Description.....	1
1.2	Bowers - DE	4
1.3	Regional Storms	5
1.4	Modeling Delaware Bay	9
1.5	Sea Level Rise	10
1.6	Research Objectives	14
2	METHODS AND MATERIALS	15
2.1	Model System	15
2.1.1	Model Setup.....	15
2.1.2	Initialization.....	16
2.1.3	Forcing.....	16
2.1.4	Wetting and Drying	17
2.1.5	Model Domain and Grid.....	17
2.1.5.1	Regional Model	17
2.1.5.2	High Resolution Bowers Model	19
2.2	Observations	29
2.3	Large-Scale Models.....	31
3	RESULTS.....	37
3.1	Water Levels during Sandy	37
3.1.1	Evaluating Existing Models	37
3.1.2	Improving Water Level in Regional Model	42
3.1.3	Water Level in High-Resolution Model	56

3.1.3.1	RM-H Forcing	56
3.1.3.2	Observational Forcing	58
3.2	Inundation Processes near Bowers	60
3.2.1	RM-H Forcing	60
3.2.2	Observational Forcing	62
3.3	Sea Level Rise Scenarios.....	63
3.3.1	RM-H Forcing	64
3.3.2	Observational Forcing	69
4	CONCLUSIONS	75
BIBLIOGRAPHY		78
Appendix		
A	ROMS EQUATIONS.....	83
B	OTHER STORM SURGE EVENTS.....	86

LIST OF TABLES

Table 2-1– Water level stations information.	29
Table 3-1– Estimate areas of the Permanently Flooded Area, the Intertidal Zone, and the Sandy Inundated Area, based on the HR-Bowers results generated when forced by the RM-H. The values are shown both when considering the whole grid and also when considering only the area adjacent to Bowers.	69
Table 3-2– Estimate areas of the Permanently Flooded Area, the Intertidal Zone, and the Sandy Inundated Area, based on the HR-Bowers results generated when forced by the water heights measured by the USGS Murderkill at Bowers station. The values are shown both when considering the whole grid and also when considering only the area adjacent to Bowers.	74
Table A-1 - Variables used in the description of the ocean model (adapted from Hedström 2010).	85
Table B-1 - Moment of occurrence and peak value of the three surges analyzed for the NOAA stations at Atlantic City, Lewes, Cape May, Brandywine Shoal Light and Ship John Shoal and for the USGS station at Bowers. Date in local time.	87

LIST OF FIGURES

Figure 1-1 – Map of the state of Delaware with the red pinpoint the position of Bowers.....	4
Figure 1-2 – Satellite image obtained from Google Earth, showing the outline of the towns of Bowers (the bigger one in the north) and South Bowers (the smaller one in the south).	5
Figure 1-3 - Tropical Storms registered by NOAA between the year 2000 and 2015. Adapted from Historical Hurricane Tracks (2016).	7
Figure 1-4 - Water level measurements during Hurricane Sandy at NOAA Tides and Currents’ Lewes Station. The blue line presents the prediction based on the tidal harmonics while the green line presents the measured water levels. Adapted from NOAA Tides and Currents website.....	9
Figure 1-5 – Mean Sea Level Trend calculated from tidal measurements taken by NOAA – Tides and Currents at their Lewes station (#8557380). This figure was adapted from < http://tidesandcurrents.noaa.gov/sltrends/sltrends_station.shtml?stnid=8557380 >	12
Figure 1-6 – Sea level rise scenarios considered by the Delaware Technical Workgroup (adapted from DNREC Sea Level Rise Technical Workgroup, 2009). The “Stable” scenario assumes the current sea level rise rates will remain constant until 2100. The other three scenarios, “High”, “Intermediate” and “Low” assume that sea level will rise by 1.5, 1.0 and 0.5 meters, respectively, until the year 2100. ...	13
Figure 2-1 - Grid cells over bathymetry from the Low Resolution grid.	18
Figure 2-2 – Region covered by the Hurricane Sandy Digital Elevation Model. The red square delimits the four tiles used to create the HR-Bowers grid. Figure adapted from the NCEI Hurricane Sandy DEM webpage: http://www.ngdc.noaa.gov/mgg/inundation/sandy/sandy_geoc.html	21
Figure 2-3 – Plot of the four tiles chosen to be used to create the new grid. Region covered by the Hurricane Sandy Digital Elevation Model.....	22

Figure 2-4 – Plot of the integrated data from the four tiles chosen from the Hurricane Sandy DEM. The orange shade represents the region between 0.0 m and 0.8 m (height a regular high tide) while the dark red shade delimits the region between 0.8 m and 2.0 m (high tide mark during Hurricane Sandy). 23

Figure 2-5 – Plot of the points from RM grid used to delimit the HR-Bowers. The upper-left image presents the RM grid cells and, in blue, the cells chosen for the new grid. The upper-right image presents only the selected cells over the Hurricane Sandy DEM data. The lower-left image shows a zoom over the RM cells selected while the lower-left image shows a zoom of the selected points over the Hurricane Sandy DEM data 24

Figure 2-6 – Plot of the HR-Bowers. Depths in meters. 25

Figure 2-7 – Water bathymetry of the HR-Bowers over the RM grid. Values in meters. Light blue contours are depths from the RM grid while black contours are from HR-Bowers. 26

Figure 2-8 – Grid cells in the HR-Bowers grid v3. Left image shows the bathymetry of the grid while the right image shows the extension of the grid, plotting every 10th point. 27

Figure 2-9 – Comparison between the HR-Bowers grid v2 (left images) and v3 (right images), over Bowers region (top images) and Murderkill River mouth (lower images). Depths are shown in meters, and the positive orientation is the water bathymetry. 28

Figure 2-10 – Position of all the NOAA and USGS stations used in this study. 30

Figure 2-11 - Grid cells of the LM-HYCOM model in our area of interest using an arbitrary color-bar to facilitate the visualization of the cells; each cross mark the center of a cell. The RM grid limits are outlined in red. 33

Figure 2-12 - Grid cells of the A-RTOFS model in our area of interest using an arbitrary color-bar to facilitate the visualization of the cells; each cross mark the center of a cell. The RM grid limits are outlined in red. 34

Figure 2-13 - Plot of the southeast corner of RM grid over HYCOM Consortium grid. The color represents depth (in meters)..... 35

Figure 2-14 - Plot of the southeast corner of RM grid over A-RTOFS grid. The color represents depth (in meters). 36

Figure 3-1 – Sea surface height (top panels) and subtidal water level (bottom panels) at available water level stations inside Delaware Bay (Inner Stations, right panels) and close to the mouth of the Bay (Outer Stations, left panels).	38
Figure 3-2 - Sea surface height (top panel), tidal oscillation (middle panel) and subtidal water oscillation (bottom panel) during Hurricane Sandy at NOAA Station Atlantic City. Each panel shows the observations (black) and model results from the RM (red), LM-HYCOM (green) and LM-ARTOFS (blue).	40
Figure 3-3 - Plot of the Sea Surface Height (top panel), Tidal Oscillation (middle panel) and Subtidal Signal (bottom panel) during Hurricane Sandy at the position of the NOAA station in Lewes. Each panel contains the observations (black) and modeled results from the RM (red), LM-HYCOM (green) and LM-ARTOFS (blue).	41
Figure 3-4 - Plot of the Sea Surface Height (top panel), Tidal Oscillation (middle panel) and Subtidal Signal (bottom panel) during Hurricane Sandy at the position of the NOAA station in Cape May. Each panel contains the observations (black) and modeled results from the RM (red), LM-HYCOM (green) and LM-ARTOFS (blue).	42
Figure 3-5 – Plot of the positions of the stations (South, East, and North) used to analyze the LM-HYCOM and LM-ARTOFS results on top of the bathymetry from RM grid in meters.	44
Figure 3-6 – Plot of the water level and barotropic current from LS-HYCOM (upper panels) and LS-ARTOFS (lower panels) at the Position North (north boundary of the RM grid). Water level is in meters and barotropic current in m/s, with the green line representing the current speed.	45
Figure 3-7 - Plot of the water level and barotropic current from LS-HYCOM (upper panels) and LS-ARTOFS (lower panels) at the Position South (south boundary of the RM grid). Water level in meters and barotropic current in m/s, with the green line representing the current speed.	46
Figure 3-8 - Plot of the water level and barotropic current from LS-HYCOM (upper panels) and LS-ARTOFS (lower panels) at the Position East (east boundary of the RM grid). Water level in meters and barotropic current in m/s, with the green line representing the current speed.	47

Figure 3-9 – Plot of the water levels registered during Hurricane Sandy in Atlantic City versus the four scenarios using LM-HYCOM as forcing: top left panel shows the RM-H-NOBRY, top right panel shows RM-H-WL, bottom left panel shows RM-H-BAR and bottom right panel shows RM-H.....	49
Figure 3-10 – Plot of the water levels registered during Hurricane Sandy in Atlantic City versus the four scenarios using LM-ARTOFS as forcing: top left panel shows the RM-A-NOBRY, top right panel shows RM-A-WL, bottom left panel shows RM-A-BAR and bottom right panel shows RM-A-WLBAR.....	49
Figure 3-11 – Plot of the water levels registered during Hurricane Sandy in Lewes versus the four scenarios using LM-HYCOM as forcing: top left panel shows the RM-H-NOBRY, top right panel shows RM-H-WL, bottom left panel shows RM-H-BAR and bottom right panel shows RM-H-WLBAR.....	50
Figure 3-12 - Plot of the water levels registered during Hurricane Sandy in Lewes versus the four scenarios using LM-ARTOFS as forcing: top left panel shows the RM-A-NOBRY, top right panel shows RM-A-WL, bottom left panel shows RM-A-BAR and bottom right panel shows RM-A-WLBAR.....	50
Figure 3-13 – Plot of the water levels registered during Hurricane Sandy in Cape May versus the four scenarios using LM-HYCOM as forcing: top left panel shows the RM-H-NOBRY, top right panel shows RM-H-WL, bottom left panel shows RM-H-BAR and bottom right panel shows RM-H-WLBAR.....	51
Figure 3-14 – Plot of the water level registered during Hurricane Sandy in Cape May versus the four scenarios using LM-ARTOFS as forcing: top left panel shows the RM-A-NOBRY, top right panel shows RM-A-WL, bottom left panel shows RM-A-BAR and bottom right panel shows RM-A-WLBAR.....	51
Figure 3-15 – Plot of the water level registered at the Ship John Shoal station versus the RM-H results during Hurricane Sandy.....	53
Figure 3-16 - Plot of the water level registered at the Murderkill at Bowers station versus the RM-H results during Hurricane Sandy.....	53

Figure 3-17 – Comparison between the NAM wind product and wind observations for the stations at Cape May, Lewes, Brandywine Shoal Light, and Ship John Shoal. The sticks represent the direction towards where the wind is going while the green line shows the wind speed in m/s..... 55

Figure 3-18 – Plot of the Sea Surface Height (top panel), Tidal Oscillation (middle panel) and Subtidal Signal (bottom panel) at the position of the station Murderkill at Bowers from the USGS. Each panel contains the observations (green) and results of the models RM-H (black) and HR-Bowers (red) being forced by the RM-H at the lateral boundaries. 57

Figure 3-19 –Sea Surface Height (top panel), Tidal Oscillation (middle panel) and Subtidal Signal (bottom panel) at the position of the station Murderkill at Bowers from the USGS. Each panel contains the observations (green) and results of the models RM-H (black) and HR-Bowers (red) being forced by the Murderkill at Bowers water heights. 59

Figure 3-20 –Plot of the flooded area (in gray) during a regular tidal cycle (panels on the left) and during Hurricane Sandy (panels on the right), when the HR-B grid is forced by the results from the RM-WLBAR. The bottom images are a zoom region of Bowers (marked here by the black lines). 62

Figure 3-21 – Plot of the flooded area (in gray) during a regular tidal cycle (panels on the left) and during Hurricane Sandy (panels on the right), using Murderkill at Bowers observations to force the HR-B model. The bottom images are a zoom region of Bowers (marked here by the black lines). 63

Figure 3-22 – Plot of the Sea Surface Height (top panel), Tidal Oscillation (middle panel) and Subtidal Signal (bottom panel) at the position of the station Murderkill at Bowers from the USGS. Each panel contains the observations (black) and modeled results for the scenarios considering the MSL at present day (red), 0.5 m increase in the MSL (green), 1.0 m increase in the MSL (blue), and 1.5 m increase in the MSL (cyan). All the model results here are generated using the results from RM-H as lateral forcing..... 66

Figure 3-23 – Plot of the areas affected by inundation in all four SLR scenarios: upper left panel shows the results of the present day scenario; upper right panel shows the results of the scenario with 0.5 m increase in the MSL; lower left panel shows the results of the scenario with 1.0 m increase in the MSL; and lower right panel shows the results of the scenario with 1.5 m increase in the MSL. Red represents the area which would be inundated by a storm surge like the one generated by Hurricane Sandy; gray is the Intertidal area; dark blue is the area permanently inundated in each scenario; and light blue is the area permanently inundated in the present day. All the results here are generated using the results from RM-H as lateral forcing. 67

Figure 3-24 – Zoom over the Bowers region of plot of the areas affected by inundation in all four SLR scenarios: upper left panel shows the results of the present day scenario; upper right panel shows the results of the scenario with 0.5 m increase in the MSL; lower left panel shows the results of the scenario with 1.0 m increase in the MSL; and lower right panel shows the results of the scenario with 1.5 m increase in the MSL. Red represents the area which would be inundated by a storm surge like the one generated by Hurricane Sandy; gray is the Intertidal area; dark blue is the area permanently inundated in each scenario; and light blue is the area permanently inundated in the present day. All the model results here are generated using the results from RM-H as lateral forcing. 68

Figure 3-25 –Plot of the Sea Surface Height (top panel), Tidal Oscillation (middle panel) and Subtidal Signal (bottom panel) at the position of the station Murderkill at Bowers from the USGS. Each panel contains the observations (black) and modeled results for the scenarios considering the MSL at present day (red), 0.5 m increase in the MSL (green), 1.0 m increase in the MSL (blue), and 1.5 m increase in the MSL (cyan). All the model results here are generated using the observations from the USGS station Murderkill at Bowers as lateral forcing. 71

Figure 3-26 – Plot of the areas affected by inundation in all four SLR scenarios: upper left panel shows the results of the present day scenario; upper right panel shows the results of the scenario with 0.5 m increase in the MSL; lower left panel shows the results of the scenario with 1.0 m increase in the MSL; and lower right panel shows the results of the scenario with 1.5 m increase in the MSL. In all images the red represents the area which would be inundated by a storm surge like the one generated by Hurricane Sandy; gray is the Intertidal area; dark blue is the area permanently inundated in each scenario; and light blue is the area permanently inundated in the present day. All the model results here are generated using the observations from the USGS station Murderkill at Bowers as lateral forcing. 72

Figure 3-27 – Zoom over the Bowers region of plot of the areas affected by inundation in all four SLR scenarios: upper left panel shows the results of the present day scenario; upper right panel shows the results of the scenario with 0.5 m increase in the MSL; lower left panel shows the results of the scenario with 1.0 m increase in the MSL; and lower right panel shows the results of the scenario with 1.5 m increase in the MSL. In all of the red represents the area which would be inundated by a storm surge like the one generated by Hurricane Sandy; gray is the Intertidal area; dark blue is the area permanently inundated in each scenario; and light blue is the area permanently inundated in the present day. All the model results here are generated using the observations from the USGS station Murderkill at Bowers as lateral forcing. 73

Figure B-1 – Sea surface height (top panels) and subtidal water level (bottom panels) at available water level stations inside Delaware Bay (Inner Stations, right panels) and close to the mouth of the Bay (Outer Stations, left panels) during Hurricane Sandy (October 2012). 88

Figure B-2 – Sea surface height (top panels) and subtidal water level (bottom panels) generated by Regional Model at the measurement locations inside Delaware Bay (Inner Stations, right panels) and close to the mouth of the Bay (Outer Stations, left panels) during Hurricane Sandy (October 2012). 88

Figure B-3 – Comparison between the wind observations for the stations at Cape May, Lewes, and Ship John Shoal during Hurricane Sandy. The sticks represent the direction towards where the wind is going while the green line shows the wind speed in m/s. 89

Figure B-4 – Sea surface height (top panels) and subtidal water level (bottom panels) at available water level stations inside Delaware Bay (Inner Stations, right panels) and close to the mouth of the Bay (Outer Stations, left panels) during the storm surge in December of 2012. 90

Figure B-5 – Sea surface height (top panels) and subtidal water level (bottom panels) generated by Regional Model at the measurement locations inside Delaware Bay (Inner Stations, right panels) and close to the mouth of the Bay (Outer Stations, left panels) during during the storm surge in December of 2012. 90

Figure B-6 – Comparison between the wind observations for the stations at Cape May, Lewes, and Ship John Shoal during the storm surge in December of 2012. The sticks represent the direction towards where the wind is going while the green line shows the wind speed in m/s. 91

Figure B-7 – Sea surface height (top panels) and subtidal water level (bottom panels) at available water level stations inside Delaware Bay (Inner Stations, right panels) and close to the mouth of the Bay (Outer Stations, left panels) during the negative storm surge in February of 2012. 92

Figure B-8 – Sea surface height (top panels) and subtidal water level (bottom panels) generated by Regional Model at the measurement locations inside Delaware Bay (Inner Stations, right panels) and close to the mouth of the Bay (Outer Stations, left panels) during during the storm surge in February of 2012. 92

Figure B-9 – Comparison between the wind observations for the stations at Cape May, Lewes, and Ship John Shoal during the negative storm surge in February of 2012. The sticks represent the direction towards where the wind is going while the green line shows the wind speed in m/s. 93

ABSTRACT

This study is aimed at better understanding storm surges and associated flooding at Delaware Bay coastal regions, considering present day sea levels and future sea level rise. To simulate realistic storm surges we employ a nested regional hydrodynamic modeling approach. An established regional model (RM) for the Delaware Bay and its adjacent coastal shelf is first forced at its lateral boundaries with realistic water levels and depth averaged currents. Imposing this remote forcing in the RM is critical for accurately modeling the timing and magnitude of the storm surge. Then we use water levels and currents from the RM to drive a high resolution local model, with horizontal resolution down to 10 m, for a region close to Bowers, Delaware, that is susceptible to coastal flooding. As a test case we apply this modeling framework for Hurricane Sandy (2012). To investigate the influence of sea level rise on future storm surge events, we consider three different sea level rise scenarios assuming present-day bathymetry and topography. To analyze the impact of a storm surge like the generated by Hurricane Sandy, we added the sea level rise suggested in each scenario to the mean sea level of our simulation. The wind forcing was the same in all scenarios. These scenarios showed that even a SLR of 0.5 m could turn South Bowers into a tidally inundated area with the rest of the town being very susceptible to storm surges, while in the worst case scenario, a part of the town would be permanently under water and the rest of it would be inundated daily, forcing the whole town to be moved.

Chapter 1

INTRODUCTION

Storm surges and coastal flooding pose severe coastal hazards. Understanding them is of great importance for the protection of Delaware's coastline. Future sea level is projected to rise, but the impact of sea level rise on storm surges and coastal flooding are uncertain. To improve our understanding of inundation processes due to storms, we propose to A) simulate a realistic storm surge inside Delaware Bay, B) analyze the coastal inundation process in a selected region and C) analyze how possible sea level rise scenarios would impact that region.

1.1 Delaware Bay Description

Delaware Bay is an area of regional key importance both economically and ecologically. Its waters allow access to Port of Philadelphia, Port of Wilmington, Port of Camden and Port of Chester, respectively the 19th, 21th, 27th and 28th busiest U.S. ports by container volume in 2012, handling approximately 560.000 twenty-foot equivalent units (TEU) altogether (USACE 2014); approximately 85% of all oil shipped to the east coast of the USA pass through Delaware Bay and the ports of Delaware River rank #1 in perishables and #3 in steel imports in the USA. It is also one of 14 strategic ports in the U.S. Coast transporting military supplies and

equipment by vessels to support troops overseas (Philadelphia Port Brochure, 2008; U.S. Department of Transportation, Maritime Administration, 2005).

Ecologically, the area is an important stopover and wintering habitat for a great number of migrating birds, with so many as 200,000 arriving in one single day (Clark et al., 1993; Baker et al., 2004). It is also the home of the greatest horseshoe crab spawning event in the world when tens of thousands of horseshoe crabs lay their eggs on its beaches. This event attracts many different bird species, which come to the region to feed on the eggs (Berkson and Shuster Jr, 1999).

Delaware Bay is the drowned river valley of the Delaware River, a coastal plain which stretches 210 km till its mouth and has a water surface area of 2,070 km². Outside of Delaware Bay, the continental shelf has a width around 130 km. It has a total mean freshwater discharge estimated to be about 550 m³/sec, from which 58% comes from Delaware River itself, and 14% comes from Schuylkill River (Glibert et al. 2010). As any other coastal area, the Bay is subject to changes in its coastline due to natural processes like erosion and accretion, or due to human activities (Phillips, 1986). Sea Level Rise also play a whole in this and might cause the drowning of marsh banks (Schwimmer & Pizzuto, 2000);

Oceanographically, the bay is described as weakly stratified and well mixed with greater density variability on the lateral axis than on the vertical. Spring freshets caused by the ice melting during spring can result in moderate stratification, which persists for 2-8 weeks between late February and April, sometimes also affecting the summer months (Glibert et al. 2010; Garvine, 1991). Along the main axis of the bay, the salinity decreases almost linearly from Delaware River towards the ocean (Garvine et al., 1992). However, the salinity distribution is not homogeneous laterally: Wong

and Münchow (1995) show the existence of two branches of less saline water in the shallow regions on both side of the bay being separated by a saltier water in the middle of the bay.

The currents inside the Bay are mainly forced by the tides with both the winds and the discharge of fresh water playing a smaller role in the process. The water leaving the bay turns anti-cyclonically and flows south, forming the Delaware Coastal Current (Münchow and Garvine, 1993).

Garvine et al. (1992) describes how increased tidal currents on the inner shelf generate enhanced tidal amplitudes inside the bay. The tides can generate currents of 70-80 cm/s in and out to the Bay. According to National Oceanic and Atmospheric Administration (NOAA) Tides and Currents (2016), the main tidal components derived from Lewes station are:

- M2 (Principal Lunar Semidiurnal), with amplitude of 0.62 m;
- N2 (Larger Lunar Elliptic Semidiurnal) with amplitude of 0.13 m;
- S2 (Principal Solar Semidiurnal) and K1 (Lunar Diurnal) with an amplitude of 0.10 m each.

The direction of the predominant wind over the Bay oscillates seasonally coming from South during summer, Northwest during autumn, North-Northwest during winter, and Southwest during spring. Average wind speeds are around 4.7 m/s, with higher values during winter (around 5.5 m/s) and smaller ones during summer (around 3.7 m/s). Inside the bay, the dominant southerly winds observed offshore rotate counterclockwise, aligning with the axis of the water body (Hughes and Veron, 2015).

1.2 Bowers - DE

Inside Delaware Bay, the focus of this work will be in the town of Bowers, sometimes also called Bowers Beach, located in Kent County, Delaware. According to the Census of Population and Housing (available from <http://www.census.gov/prod/www/decennial.html>) the population in 2010 was of 335 people, and it covers an area of 0.3 square miles. It is encircled by Saint Johns River in the north, Murderkill River in the south and Delaware Bay in the east. Figures 1-1 shows the location of Delaware Bay and Bowers within it, while Figure 1-2 is a satellite image showing the outline of Bowers and South Bowers and also the two rivers around it. Both images obtained from Google (2015).

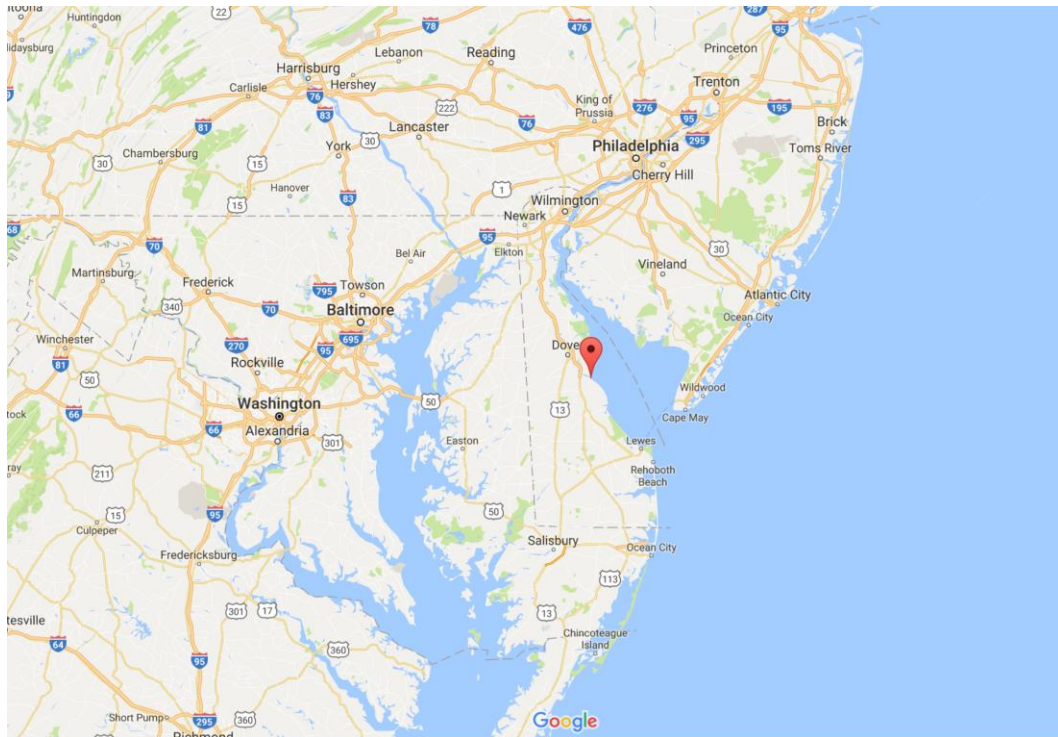


Figure 1-1 – Map of the state of Delaware with the red pinpoint the position of Bowers.



Figure 1-2 – Satellite image obtained from Google Earth, showing the outline of the towns of Bowers (the bigger one in the north) and South Bowers (the smaller one in the south).

1.3 Regional Storms

With its high economic and environmental importance, it is only natural to worry about the impact coastal storms can have over Delaware Bay and its inhabitants. The two main types of coastal storms in the region are Hurricanes and Nor'easters. Both can hit the East Coast of the United States with strong winds, waves, and precipitation, generating as result floods, surges, beach erosion, loss of vegetation and severe damage to property along the coast (Zhang et al., 2000; Wu et al., 2002).

Hurricanes usually generate stronger winds, precipitation, and surges, but affect a relatively small extension of coastline (around hundreds of kilometers) and have a smaller temporal span (affecting the coast during periods of tens of hours).

They usually occur between the months of August and October (but some have been registered as early as May and as late as December) and are generated in lower latitudes.

On the other hand, Nor'easters are large atmospheric low-pressure systems, which generate smaller wind speeds (compared to Hurricanes) but intense precipitation (in the form of snow or rainfall). Their longer duration (several days), wider affected region (around thousands of kilometers) and greater persistence also allow them to generate big waves and considerable storm surges and flooding events. They usually occur between October and May (although they may happen any time of the year) and are formed along the northeastern coast of the United States, where the warm waters of the Gulf Stream meet with cold air masses coming from Canada (Davis and Dolan, 1993; National Hurricane Center, 2016).

Between the years 2000 and 2015, 8 Hurricanes have been tracked by around Delaware coast (National Oceanic and Atmospheric Administration, 2016), as can be seen in Figure 1-3 below. One was a Hurricane Level 1, one Tropical Storm and five Extratropical Cyclones (one of them being Hurricane Sandy).

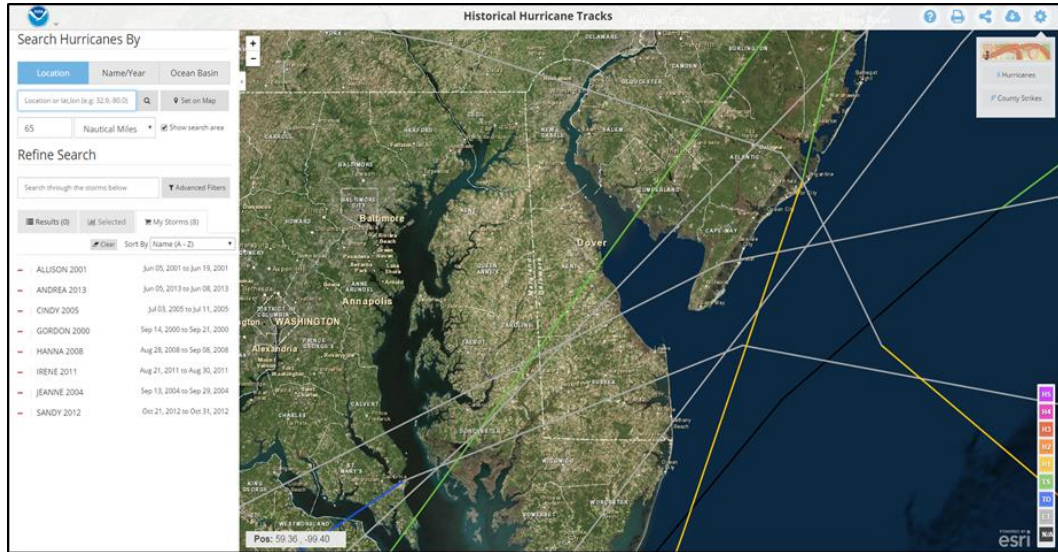


Figure 1-3 - Tropical Storms registered by NOAA between the year 2000 and 2015. Adapted from Historical Hurricane Tracks (2016).

One of the more dangerous effects of a coastal storm, the storm surge is an anomalous variation in the water level beyond the predicted astronomical tides caused, mainly, by the winds. Other factors which affect the occurrence of storm surges are atmospheric pressure, geometry and depth of the basin, continental shelf width and radiation stress (momentum transfer from waves breaking). On the other hand, the presence of wetlands, vegetation on dry land inundated (both increasing bottom friction) and the geometry of the basin might attenuate the intensity of a storm surge (Ebbersole, 2014; Resio and Westerink, 2008). Below is presented a simple, linear and steady-station equation from Resio and Westerink (2008) to relate the influence of the shelf width and water depth on wind driven surges:

$$\zeta \propto \left(\frac{\tau_s}{gh} \right) W \quad \text{Equation 1}$$

Where ζ is the surge height, τ_s is the wind stress, g is the gravitational acceleration, h is the depth of the water column, and W is the shelf width.

As for the wind stress:

$$\tau_s = c_d \rho_a U_{10}^2 \quad \text{Equation 2}$$

Where c_d is the coefficient of drag, ρ_a is the air density, and U_{10} is the wind speed.

As an example, Hurricane Katrina (2005) killed 1833 people, most of them as a direct or indirect result of its storm surge which reached up to 7.6 –8.5 m (Lott and Ross 2006, and National Hurricane Center, 2016). Along the East Coast, the hurricane that caused most damage was Hurricane Sandy. It was less deadly than Katrina (killing 200 people on the U.S. mainland) and caused fewer damages (US\$148 billion for Katrina and US\$97 billion for Sandy). Figure 1-4 below presents the predicted and the measured water levels during Hurricane Sandy by the NOAA Tides and Currents` (2016) at Lewes` station (#8557380).

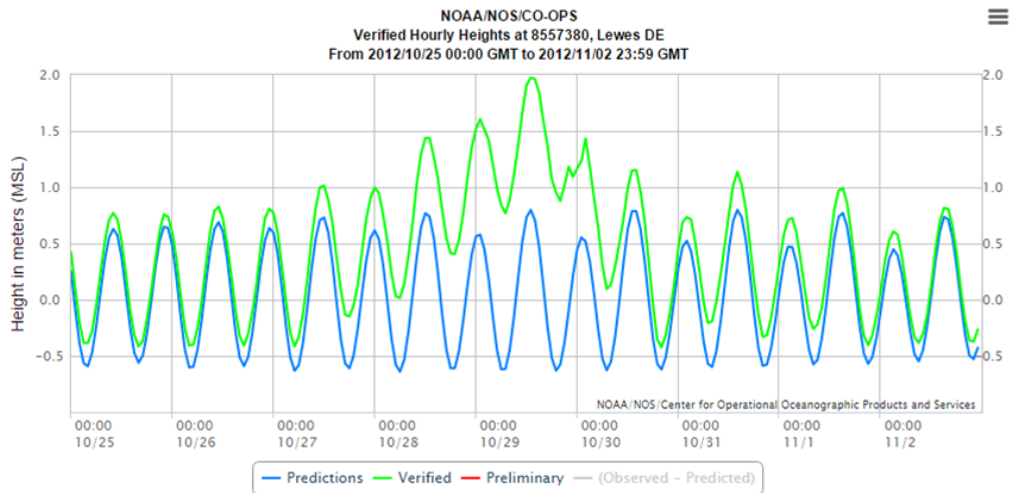


Figure 1-4 - Water level measurements during Hurricane Sandy at NOAA Tides and Currents' Lewes Station. The blue line presents the prediction based on the tidal harmonics while the green line presents the measured water levels. Adapted from NOAA Tides and Currents website.

1.4 Modeling Delaware Bay

Numerical modeling presents itself as an important tool to help understand and prepare for storms. Successful modeling efforts have been carried out in the region in the past. Whitney (2003) and later Whitney and Garvine (2006) created a realistic simulation of the buoyant outflow from Delaware Bay using the hydrodynamic model “ECOM3d”; the model was forced using tidal data at the boundaries, wind forcing over the whole grid and river discharge from Delaware River. Qin et al (2005) implemented SWAN over Delaware Bay to simulate the waves at a station in the middle of the bay still using the same grid and bathymetry. Chen (2010) produced a similar study but used the coupling toolkit MCT to do the coupling between the waves models SWAN and the hydrodynamic model ROMS. Castellano (2011) worked on running the same grid as Whitney (2003) using the hydrodynamic model “ROMS”

[reference or refer to methods section if more detail there] but for longer periods (from January 2006 until December 2009), applying a more realistic river discharge. Jurisa & Chant (2013) analyzed the relationship between the wind conditions along the shelf and the outflow from Delaware Bay. Recently, Jenkins (2015) analyzed the influence of remotely generated waves against locally generated waves inside the bay, while considering the impact of the currents on waves.

The DBOFS and ESPRESSO are two operational models covering Delaware Bay. DBOFS (Delaware Bay Operational Forecast System) is a ROMS based nowcast and forecast system implemented to provide short-term predictions of current, sea surface height, temperature, and salinity for the Delaware Bay waters (Schmalz, 2011). It is operated by the National Center for Environmental Prediction (NCEP) from National Oceanographic and Atmospheric Administration (NOAA) since September 2010. ESPRESSO (Experimental System for Predicting Shelf and Slope Optics) is a ROMS based nowcast and forecast system focusing on the shelf waters of the Middle Atlantic Bight (Wilkin, 2012). It was developed by the Rutgers University Oceanic Modeling Group (RU-OMG). This system assimilates daily Coastal Ocean Dynamics Applications RADAR (CODAR) velocities and sea surface height and water temperature from multiple satellite platforms, while also making use of *in situ* temperature and salinity data from Autonomous Underwater Glider Vehicles (AUGV) and ships of opportunity. The horizontal resolution is 5 km. Its domain represents Delaware Bay using three cells at the mouth of the bay and six cells at its widest part.

1.5 Sea Level Rise

As a first step to investigate the impact of sea level rise on coastal inundation processes in the Bowers region, we will consider several sea level rise scenarios

devised by the Delaware Department of Natural Resources and Environmental Control (DNREC). DNREC created a technical workgroup dedicated to evaluating the scientific knowledge and provide realistic sea level rise estimates for the Delaware coast. According to their reports (DNREC Sea Level Rise Technical Workgroup, 2009 and Delaware Sea Level Rise Advisory Committee, 2013), four scenarios were considered of how much sea level rise is expected to take place until the year 2100.

The first one is based on measurements at tide stations conducted by NOAA Tides and Currents (2016) and simply assumes that the current rate of sea level rise along the last century will be constant throughout the next century (“Stable scenario”). Figure 1-5 presents the statically analyzed data from the station at Lewes (#8557380) starting during the late 1910s and showing an increase of 3.40 +/- 0.24 mm per year. Integrating the data from all the stations available either inside Delaware Bay or in its proximities, DNREC arrived at a value of 3.35 mm per year for the historic sea level rise.

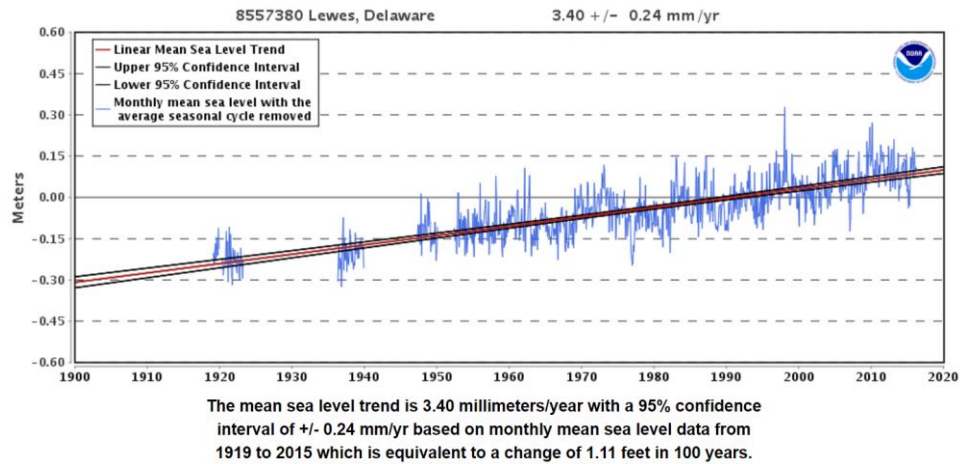


Figure 1-5 – Mean Sea Level Trend calculated from tidal measurements taken by NOAA – Tides and Currents at their Lewes station (#8557380). This figure was adapted from http://tidesandcurrents.noaa.gov/sltrends/sltrends_station.shtml?stnid=8557380

The next three proposed scenarios assume that the sea level will rise by 0.5, 1.0 and 1.5 meters by the year 2100. They are called, respectively “Low”, “Intermediate” and “High” related to the elevation rates. Figure 1-6 bellow presents the evolution of all four scenarios along the 21st century.

For this work, we propose to use the scenarios “Low”, “Intermediate”, and “High”; the “Stable” scenario proposes a rise too small, especially when considering that the modeling setup only computes cells with more than 10 cm of water in them; in this case, the stable scenario would produce results too close to the present day. For the other three scenarios, we will add their sea level rise to the present day mean water level and later compare to a present day simulation. These scenarios will be run for a Sandy-like storm surge inundation event to analyze how it would affect Delaware Bay

in the future. To model more realistically the projected changes in the future, shoreline and bathymetry changes would also need to be considered. This, however, is beyond the scope of this thesis.

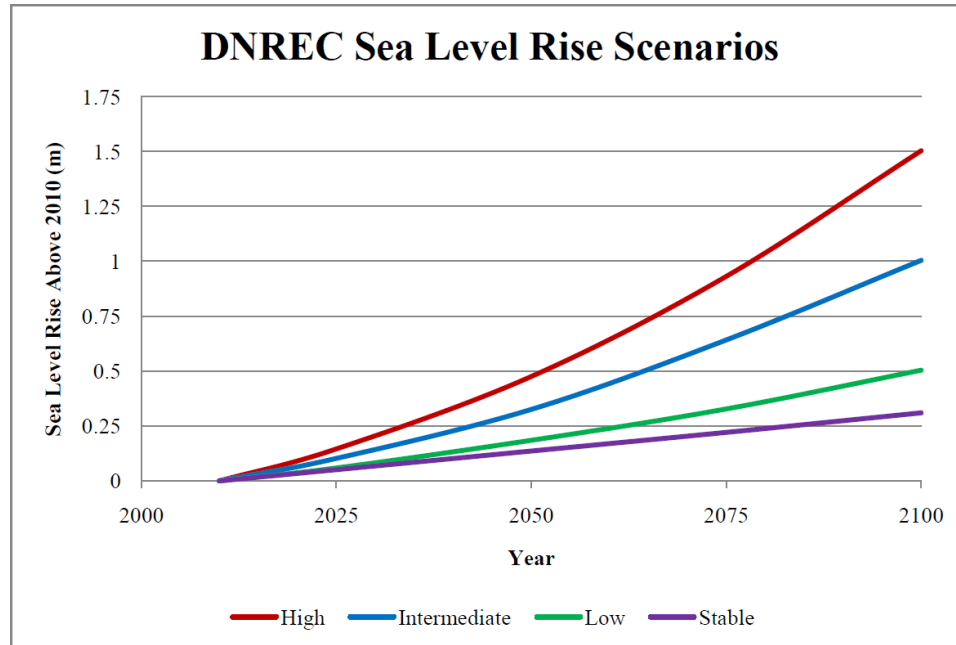


Figure 1-6 – Sea level rise scenarios considered by the Delaware Technical Workgroup (adapted from DNREC Sea Level Rise Technical Workgroup, 2009). The “Stable” scenario assumes the current sea level rise rates will remain constant until 2100. The other three scenarios, “High”, “Intermediate” and “Low” assume that sea level will rise by 1.5, 1.0 and 0.5 meters, respectively, until the year 2100.

1.6 Research Objectives

Delaware Bay and its coast are vulnerable to inundation processes caused by storm surges. Considering the projected sea level rise, this vulnerability is likely to increase in the future. By employing a hydrodynamic model, the proposed work will improve the understanding of flooding processes in Delaware Bay and will provide an important first step to make informed coastal management decisions.

The research objectives are:

A. Simulate storm surges inside Delaware Bay

Realistically model storm surges inside Delaware Bay through the implementation of realistic lateral boundary forcing obtained from a larger scale model. The results will be validated against water level data measured inside the bay. We hypothesize that remote forcing is essential for accurately predicting storm surges.

B. Analyze susceptibility to surge inside the bay

As a first step to model and better understand coastal inundation processes in Delaware Bay, we develop a high-resolution hydrodynamic model for a selected region that is susceptible to flooding. We hypothesize that detailed knowledge of the bathymetry and boundary forcing used to drive the high-resolution model are critical for accurately predicting inundation dynamics.

C. Simulate storm surges considering sea level rise scenarios

To improve the understanding of how sea level rise affects inundation processes in Delaware Bay and associated coastal vulnerability, we will simulate the high-resolution region from Objective B imposing different future sea level rise scenarios. We hypothesize inundation processes are likely much more severe in the future compared to the present sea level.

Chapter 2

METHODS AND MATERIALS

2.1 Model System

For this study, we use the Coupled-Ocean-Atmosphere-Wave-Sediment Transport Modeling System (COAWST, Warner et al. 2010), which is a coupled system consisting of: an ocean model (Regional Ocean Modeling System – ROMS, Moore *et al* 2004); a wave model (Simulating Waves Nearshore – SWAN, Booij et al., 1999); an atmospheric model (Weather Research and Forecasting – WRF, Skamarock et al., 2005); and a sediment transport model (Community Sediment Transport Model, Sherwood, 2002). The models are coupled through the Model Coupling Toolkit (MCT, Warner et al, 2008). This system allows all models to exchange prognostic fields of key variables, increasing the skill of the models and allowing for more integrated results. The setup initially used is based on the one developed by Jenkins (2015) and will be discussed next.

2.1.1 Model Setup

The model setup used in this work will be based on the one developed by Jenkins (2015), which is based on the use of realistic data to force the model such as wind (from model analysis), tide (from amplitude and phase of nine tidal harmonics), river output (estimated from measurements) and remote waves (from global model results). Such setup produced satisfactory sea surface height (SSH) with no noticeable

phase error between modeled and observed water levels. Also, the comparison between the amplitude of the nine tidal components analyzed (M2, S2, M4, M6, K2, K1, N2, O1 and Q1) show reasonable agreement, with a mean difference of about 2 cm between the model and observed tidal height data. However, this model does not account for storm surges that are generated by remote forcing. This configuration will be used as a base for the present work and will be presented in more depth below.

2.1.2 Initialization

The initialization files were created from the results generated by Jenkins (2015), providing the initial state for the ocean for the following variables: Free Surface Elevation, Momentum, Vertically Integrated Momentum and Salinity.

2.1.3 Forcing

The previous model has been forced by spatially varying wind stress, tidal forcing at the lateral boundaries and a point-source of river discharge (Jenkins 2015). Some details as follows.

- Wind Stress – Space varying wind stress calculated according to Large & Pond 1981 based on wind data from North American Meso-scale (NAM) reanalysis (nomads.ncdc.noaa.gov).
- Tide – Amplitude and phase of nine tidal constituents (M2, S2, K2, N2, K1, O1, Q1, M4, M6) derived from ADCIRC tidal database (Luettich et al. 1992) as described in Castellano (2011);
- River discharge – applied at the head of the Delaware River in the grid with information obtained from USGS gauge in Delaware River at Trenton, New Jersey (<http://waterdata.usgs.gov/usa/nwis/uv?01463500>).

2.1.4 Wetting and Drying

The wetting and drying process is very common at the interface between ocean and land. Near-shore water level changes due to waves, daily tides, or storm surges, result in wetting of initially dry land locations and in drying of inundated regions when water retrieves. The capability to reproduce this phenomenon is essential in a model expecting to simulate flooding processes.

The model ROMS includes wetting and drying capabilities (Warner *et al.*, 2013). The wetting and drying method works based on a user defined minimum depth value called D_{crit} . Every time step, the model will compute the total water depth at the cell center, which is calculated as being the sum between the local bathymetry and the free surface displacement. If the total water depth is lower than D_{crit} the cell is considered “dry” and no flux of water is allowed out of the cell. In this study, the D_{crit} was set to 0.10 m since that is the value recommended by the developers of the model in a test case similar to our scenario.

2.1.5 Model Domain and Grid

2.1.5.1 Regional Model

The grid of the Regional Model for Delaware Bay and Adjacent Continental Shelf (RM) comprehends Delaware Bay and the adjacent oceanic region. It has 150 x 300 grid cells with the points over land not being considered in the computation. It extends from land until the 100 m isobaths and has 240 km from East to West versus 340 km from North to South, beginning on the coast around 39.5° N and ending in front of the Chesapeake Bay (which is not considered in this domain), around 37.0° N.

The highest horizontal resolution is around 0.8 km in the entrance of the Bay while the lowest resolution is about 8 km in the oceanic corners.

The grid and its bathymetry were obtained from Whitney (2003). The west boundary is closed (continent) while the north, south, and boundaries are open. Bellow, Figure 2-1 presents all the grid points considered as water (i.e. all the points where the model makes computations) with the colors representing the model's bathymetry.

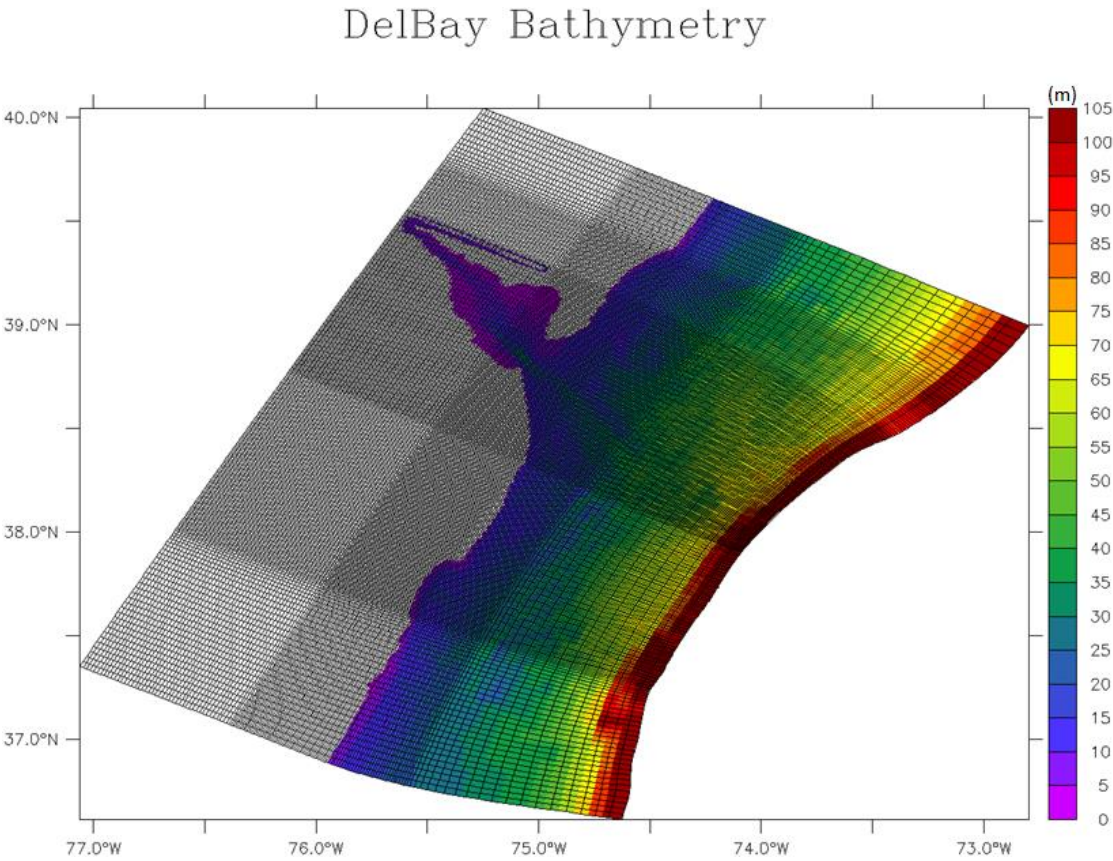


Figure 2-1 - Grid cells over bathymetry from the Low Resolution grid.

2.1.5.2 High Resolution Bowers Model

As the first step to model and better understand coastal inundation processes in Delaware Bay, we developed a High-Resolution Hydrodynamic Model for the Region of Bowers – DE (HR-Bowers), which is susceptible to storm surge flooding (as will be shown later). This new grid has resolution increased enough as to be able to represent the rivers and lowlands in the area. The Bowers region was chosen as part of an effort from Delaware Department of Natural Resources and Environmental Control (DNREC) to investigate in-depth different Delaware coastal regions.

To provide bathymetric and topographic information for this new grid, we will use the Hurricane Sandy Digital Elevation Model (DEM) from National Centers for Environmental Information (NCEI – NOAA, available at http://www.ngdc.noaa.gov/mgg/inundation/sandy/sandy_geoc.html) which has data with resolution varying from 3 arc-seconds (in the ocean far from the coast) till 1/9 arc-second (over the coast). This DEM was created as part of a planned framework, developed under the Disaster Relief Appropriations Act of 2013 (aka "Sandy Supplemental") to support improved hurricane forecasting and warning efforts (Eakins, 2015). According to personal communication with a Scientist from the NCEI (Kelly Carignam, on October of 2016), it was created through the integration of high-resolution data from the following sources:

- Two NOAA LIDAR datasets: 2012 USGS Lidar Post-Sandy (DE,MD,NC,NY,VA); and 2014 USGS CMGP Lidar Post Sandy (DE & MD) (available at <https://coast.noaa.gov/dataregistry/search/collection/info/coastallidar>):
- USGS National Map of Elevation (available at <http://nationalmap.gov/elevation.html>)

- NOS Hydrographic Survey Data (available at <http://www.ngdc.noaa.gov/mgg/bathymetry/hydro.html>).

These datasets were referenced horizontally to the North American Datum of 1983 (NAD83) and vertically to the North American Vertical Datum of 1988 (NAVD 88) being integrated together afterward. The final product is presented in tiles with $0.25^\circ \times 0.25^\circ$.

It is important to notice that the topography / bathymetry used here represent a specific moment in time and not necessarily the present morphology in the region. River channels can frequently change due to erosion and deposition processes. To be able to simulate the inundation accurately in coastal regions, it is essential to have realistic bathymetry both in the Bay and in the rivers, through which the water will first flow inland during a storm surge. Uncertainties in the bathymetry and topography of the area can lead to errors and cause the results to be unrealistic.

To ensure that we are using the most up-to-date dataset available for the region, field survey data from the rivers around Bowers Beach will be used. This dataset was provided by the Center for Applied Coastal Research (CACR) at the University of Delaware (Jim Kirby, personal communication, July, 2016). The usage of this information is seen by us as the first step towards the objective of producing a grid with greater resolution (compared to RM grid) and which better represents our area of interest.

The tiles used to generate the new grid are:

- ncei19_n39x00_w075x50_2014v1;
- ncei19_n39x00_w075x25_2014v1;
- ncei19_n39x25_w075x50_2014v1;
- ncei19_n39x25_w075x25_2014v1;

Figure 2-2 shows all the tiles available to be used from the NCEI-NOAA website, highlighting the four tiles used to generate HR-Bowers grid, while Figure 2-3 shows a plot of the data in the selected tiles.

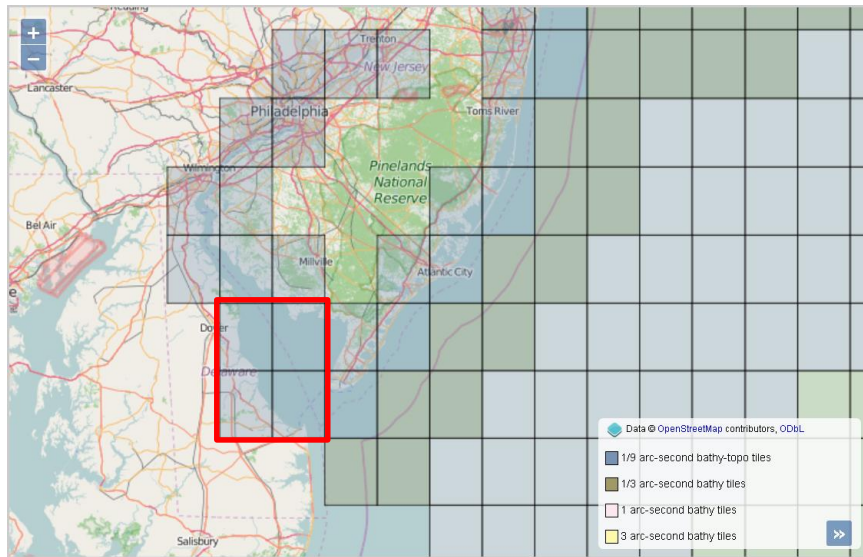


Figure 2-2 – Region covered by the Hurricane Sandy Digital Elevation Model. The red square delimits the four tiles used to create the HR-Bowers grid. Figure adapted from the NCEI Hurricane Sandy DEM webpage:
http://www.ngdc.noaa.gov/mgg/inundation/sandy/sandy_geoc.html

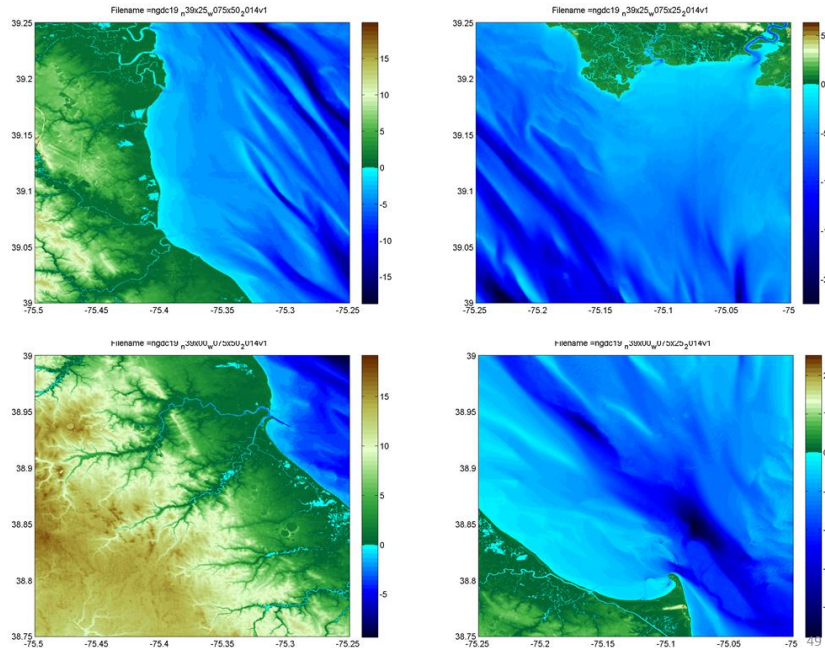


Figure 2-3 – Plot of the four tiles chosen to be used to create the new grid. Region covered by the Hurricane Sandy Digital Elevation Model.

Figure 2-4 shows the integrated data from the four tiles plotted with a fast inundation analysis: in orange is shaded the region between 0.0 m and 0.8 m, which represents the area inundated during a regular tide cycle; in dark red is shaded the region between 0.8 m and 2.0 m, which represents the area inundated during a storm surge like the one generated by Hurricane Sandy.

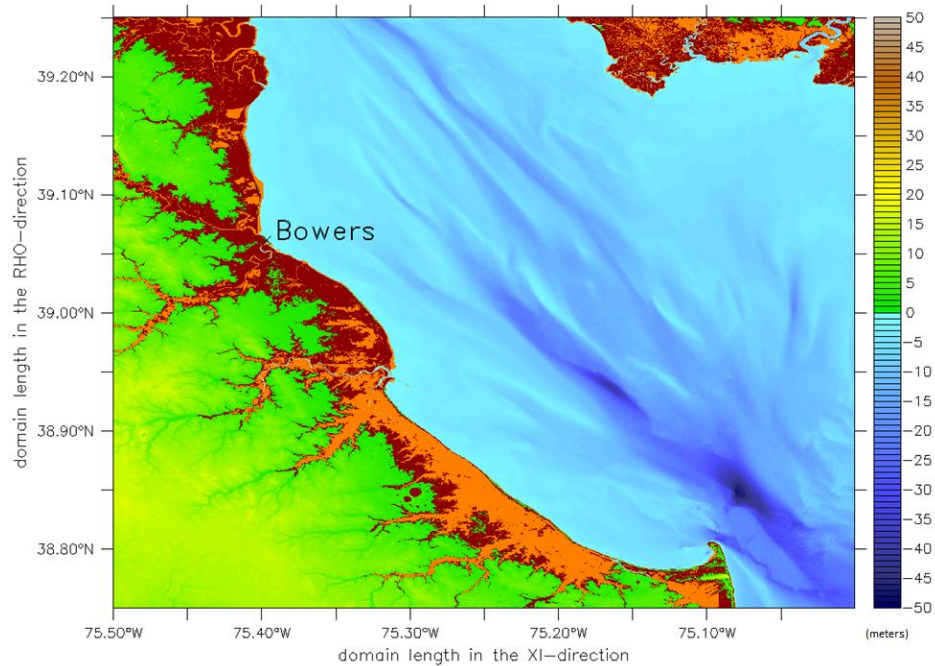


Figure 2-4 – Plot of the integrated data from the four tiles chosen from the Hurricane Sandy DEM. The orange shade represents the region between 0.0 m and 0.8 m (height a regular high tide) while the dark red shade delimits the region between 0.8 m and 2.0 m (high tide mark during Hurricane Sandy).

This new HR-Bowers grid will be forced at the lateral boundaries using the output from the RM. Therefore, we decided to define the new grid's borders aligned with the RM grid points. Figure 2-5 shows the process of defining these points. The upper-left image presents the center of the RM cells and, in blue, the cells chosen to delimit the new grid. The upper-right image presents only the selected points over the Hurricane Sandy DEM data. The lower-left image shows a zoom over the RM selected grid cells while the lower-left image shows a zoom of the selected points over the Hurricane Sandy DEM data. The chosen region contains 25 x 40 grid cells. To generate the new grid, we have adapted a version of the script

"create_sandy_application.m" which was created by John Warner and released as part of the package distributed with COAWST (<http://woodshole.er.usgs.gov/operations/modeling/COAWST/>). This script creates a regularly spaced Mercator grid.

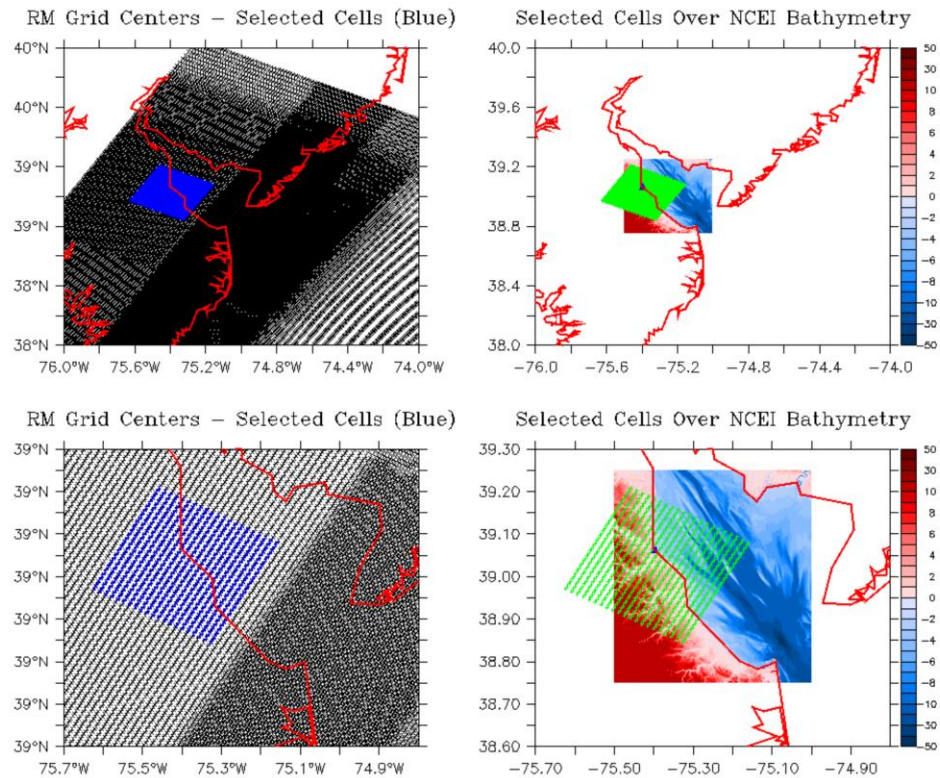


Figure 2-5 – Plot of the points from RM grid used to delimit the HR-Bowers. The upper-left image presents the RM grid cells and, in blue, the cells chosen for the new grid. The upper-right image presents only the selected cells over the Hurricane Sandy DEM data. The lower-left image shows a zoom over the RM cells selected while the lower-right image shows a zoom of the selected points over the Hurricane Sandy DEM data

After defining which points would be used, we increased the original resolution 20 times by adding 19 points regularly spaced between every two points.

This increase allows us to simulate the storm surge in a much smaller scale, making the model capable of representing the channel from the rivers in the region. Figure 2-6 shows the bathymetry of HR-Bowers grid v2. This grid has curvilinear coordinates and is formed by 500 x 800 grid cells, with a resolution of about 80x50 meters.

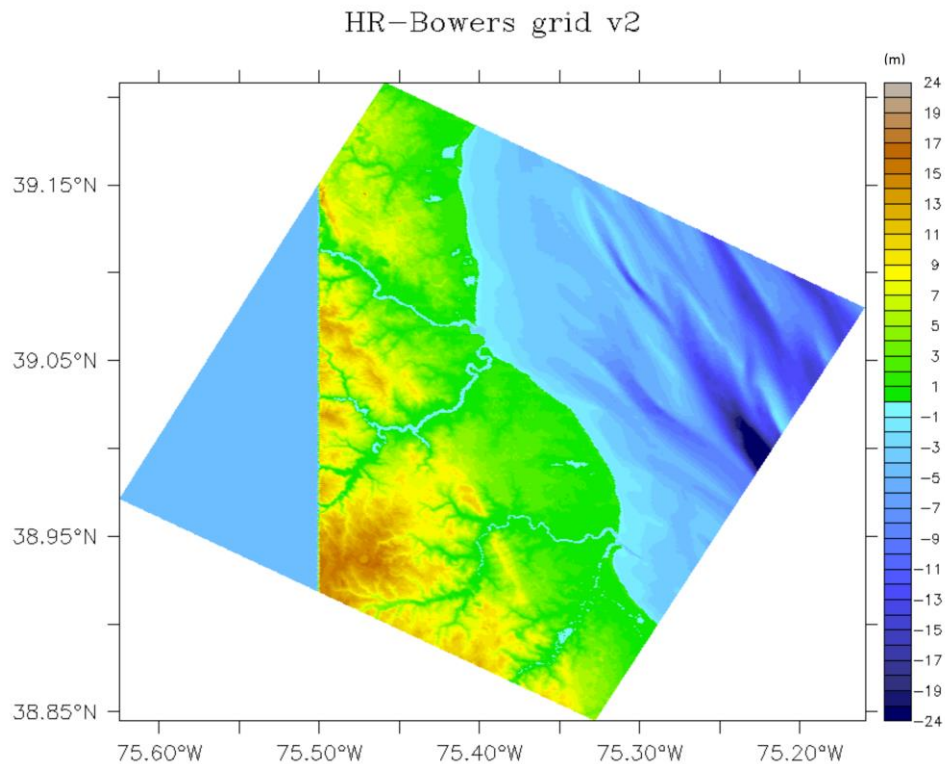


Figure 2-6 – Plot of the HR-Bowers. Depths in meters.

Figure 2-7 presents a comparison between the bathymetries from the RM and the HR-Bowers. Increasing so much the resolution could lead to marked differences in the depth at any point, especially when considering that we used a new product for the bathymetry in the HR-Bowers. If that was the case, it could hinder the use of the depth-averaged currents from the RM. However, the depths in both grids agree very

well, with the three main channels in the area being represented similarly in both grids.

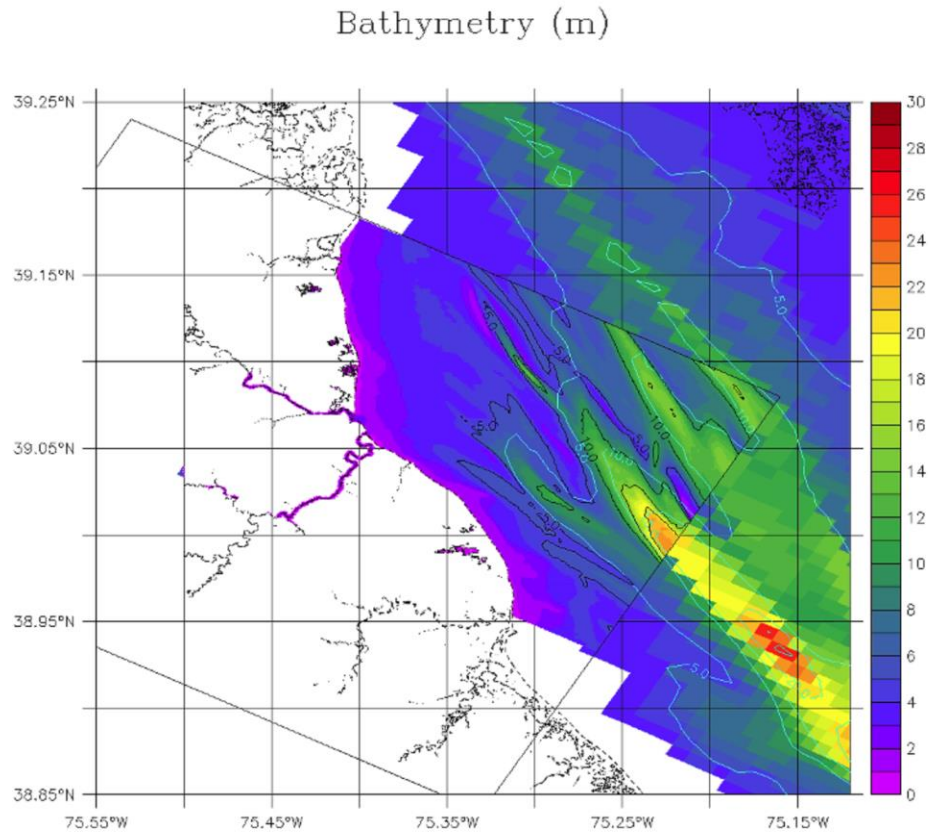


Figure 2-7 – Water bathymetry of the HR-Bowers over the RM grid. Values in meters. Light blue contours are depths from the RM grid while black contours are from HR-Bowers.

After running a few sensitivity tests, it became clear that the new increased resolution was still not enough to capture the rivers around Bowers. To improve that, we used the GridBuilder toolkit (available at <http://austides.com/downloads/>) to increase the amount of cells in the center of the grid at the expense of the cells closer

to the borders. Figure 2-8 shows the final configuration of the grid, with the denser amount of cells over Bowers. In this Figure, the left image is showing every 10th point of the grid. The biggest cells now have a horizontal resolution of 200 m x 110 m while the smallest cells have a horizontal resolution of 12 m x 6.5 m.

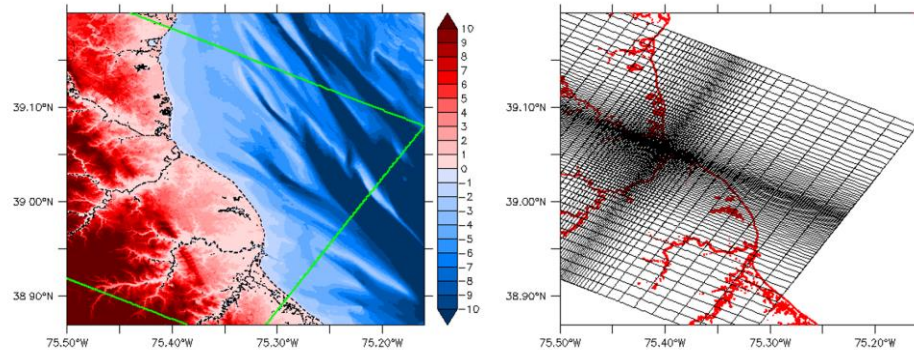


Figure 2-8 – Grid cells in the HR-Bowers grid v3. Left image shows the bathymetry of the grid while the right image shows the extension of the grid, plotting every 10th point.

Figure 2-9 presents a comparison between the resolution in the HR-Bowers v2 (left panel) and HR-Bowers v3 (right panel) near the mouth of Murderkill River. This shows that in a place where the grid v2 had 2 cells, grid v3 can have as many as 8 cells instead, allowing to resolve the river dynamics. From now on, every time we refer to the model HR-Bowers it will be the Grid v3. The increase in the resolution allowed for a better representation of the bathymetry in the area.

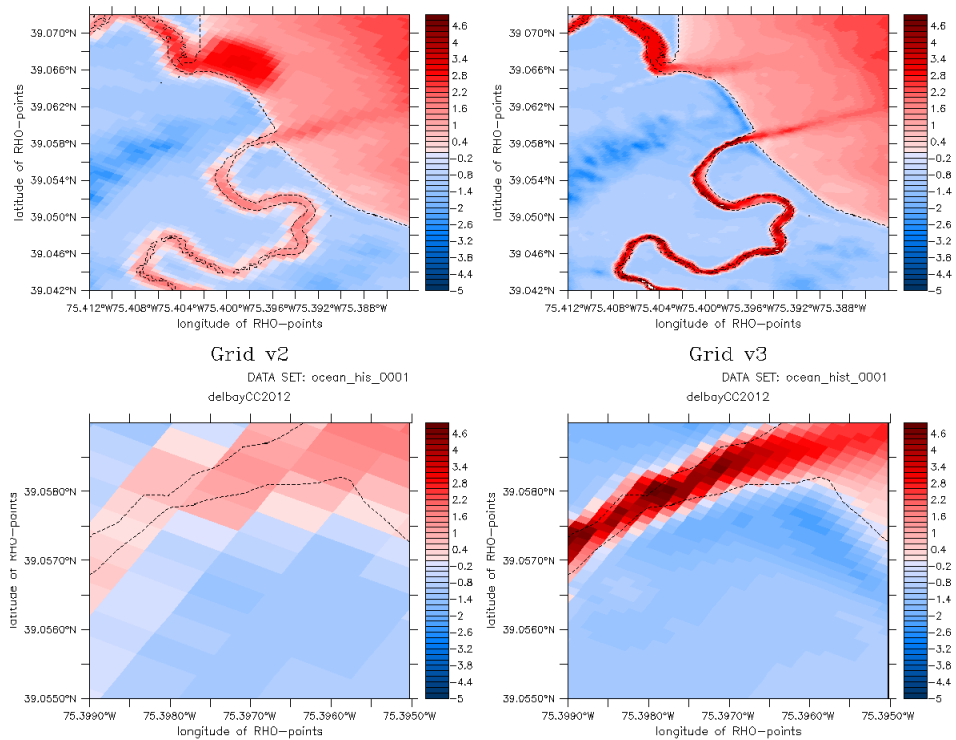


Figure 2-9 – Comparison between the HR-Bowers grid v2 (left images) and v3 (right images), over Bowers region (top images) and Murderkill River mouth (lower images). Depths are shown in meters, and the positive orientation is the water bathymetry.

The HR-Bowers setup differs from the RM since it is not forced by tidal harmonics or by river input. The only forcings are wind stresses based on the same NAM product used in the RM discussed above and the barotropic currents and water levels obtained from the coarser RM, or by the observations at USGS stations Murderkill at Bowers, as discussed below.

2.2 Observations

Water level observations from NOAA - Tides and Currents (2016) and USGS - Water Data for the Nation (2016) stations inside Delaware Bay are used in this work (Figure 2-10). Also, some of the NOAA stations have wind measurements which we investigate below. Table 2-1 presents the name of every station used in this study and also contains its position, who the owner is, the code, state where the station is positioned and if that station also has meteorological measurements.

Table 2-1– Water level stations information.

Name	State	Code	Owner	Wind	Longitude	Latitude
Atlantic City	NJ	8534720	NOAA	No	74° 25.1' W	39° 21.3' N
Cape May	NJ	8536110	NOAA	Yes	74° 57.6' W	38° 58.1' N
Lewes	DE	8557380	NOAA	Yes	75° 7.1' W	38° 47' N
Brandywine Shoal Light	DE	8555889	NOAA	Yes	75° 6.8' W	38° 59.1' N
Ship John Shoal	NJ	8537121	NOAA	Yes	75° 22.5' W	39° 18.3' N
Murderkill River at Bowers	DE	01484085	USGS	No	75°23.856' W	39°03.498' N

All stations have data available for the year of 2012, with output every 6 minutes or every hour, with the exception of NOAA – Brandywine Shoal Light, which was destroyed on the 29th of October of 2012 during Hurricane Sandy; the station went back online on the 11th of November of 2014. The precision in the longitude and latitude are the ones provided by the owner of each station. The datum used is the

Mean Sea Level, which is the arithmetic mean of the hourly heights observed, referenced to the North American Vertical Datum of 1988.

In this work, we will refer to the stations at Atlantic City, Cape May, and Lewes as Outer Stations while the ones at Brandywine Shoal Light, Bowers and Ship John Shoal will be called Inner Stations, see Figure 2-10.

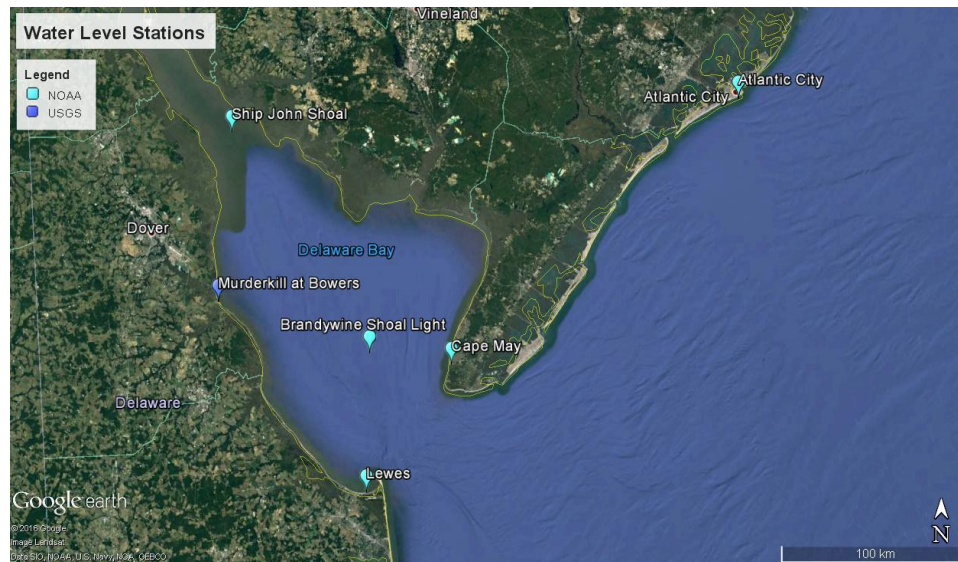


Figure 2-10 – Position of all the NOAA and USGS stations used in this study.

2.3 Large-Scale Models

To more realistically model storm surges in Delaware Bay we impose remote forcing from a large scale model, i.e. currents and water levels due to larger scale dynamics not captured by our limited size RM domain (see Figure 2-1). We will consider two Large-Scale Models (LMs): the global HYCOM-Consortium and the regional Atlantic Real-Time Ocean Forecast System (ARTOFS), both described by Chassignet et al. (2009). The datasets were generated using the Hybrid Coordinate Ocean Model (HYCOM; Bleck 2002). These model will be referred as LM-HYCOM and LM-ARTOFS, respectively.

Among the many LM-HYCOM datasets (available at hycom.org), we have chosen the Global 1/12° Reanalysis – Experiment 19.1 (GLBu0.08/expt_19.1) which is made available on a uniform grid (called GLBu0.08) with a resolution of 0.08° (which corresponds to approximately 7 km at the entrance of Delaware Bay). Model output is available every 3 hours and includes Sea Surface Elevation, Water Temperature, Water Salinity and 3D Velocity Fields.

The A-RTOFS (available at <http://polar.ncep.noaa.gov/ofs/>) is run on a curvilinear coordinate's grid with a resolution of 0.055° (which corresponds to approximately 5 km resolution at the entrance of Delaware Bay). It provides hourly fields of Sea Surface Elevation, Water Temperature, Water Salinity, 3D and Vertically Integrated Velocity Fields, Mixed Layer Depth, among others.

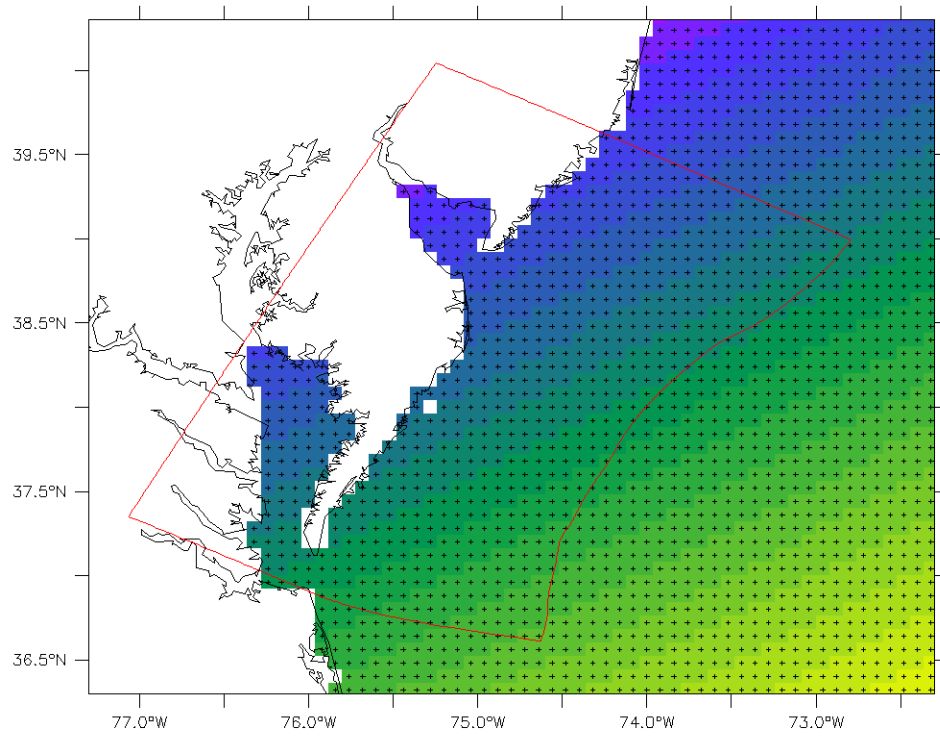
To obtain the low-frequency signal from those variables, we will apply twice a moving average filter with length of 24 hours (24 points in A-RTOFS and 8 points in HYCOM-Consortium), first forward and then backward in the time domain. This approach produces a smooth time series, with only the low-frequency oscillations.

After filtering, both datasets were interpolated to the RM grid showed in section 3.1 and formatted to be read by ROMS.

With these data fields, four different scenarios were considered to force the RM:

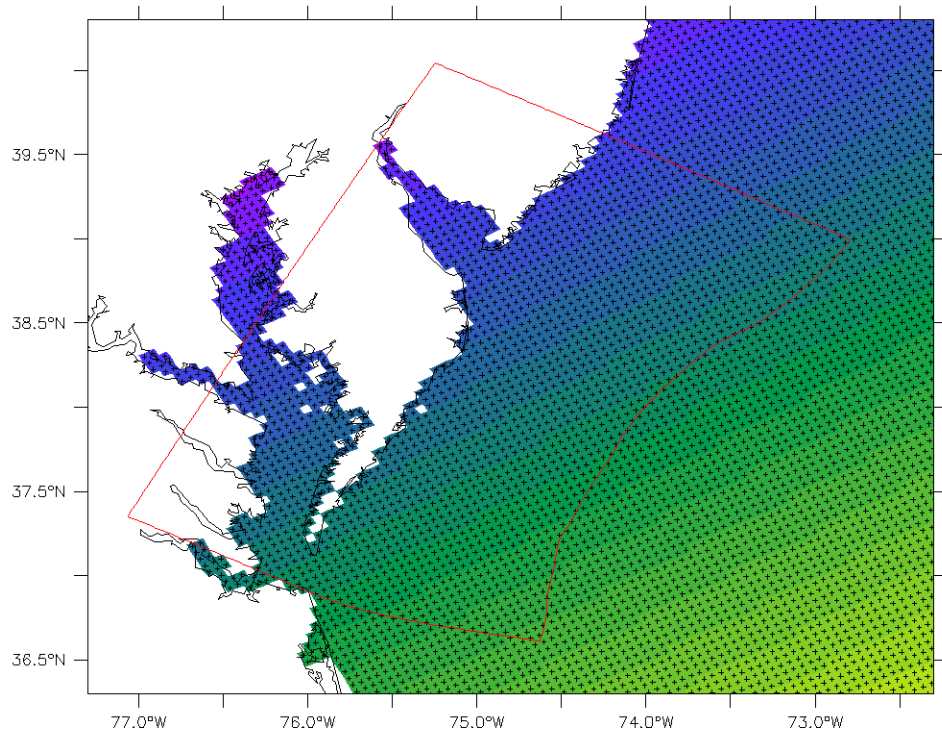
- NoBry – no imposed external forcing information at the boundary;
- WL – forcing the boundary with Surface Elevation only;
- BAR - forcing the boundary with Depth-Averaged Velocity only;
- BAR-WL - forcing the boundary with both the Surface Elevation and Depth-Averaged Velocity only.

Figures 2-11 and 2-12 below present the outline of the RM grid over the water cells from the LM-HYCOM grid and the ARTOFS grid, respectively. Also, figures 2-13 and 2-14 show a comparison of the cell size at the southeast corner of the RM grid against, again, LM-HYCOM cells and the A-RTOFS cells, respectively. Both model grids have similar cell sizes at the domain borders of the RM grid, which facilitates using the LM output as RM boundary conditions.



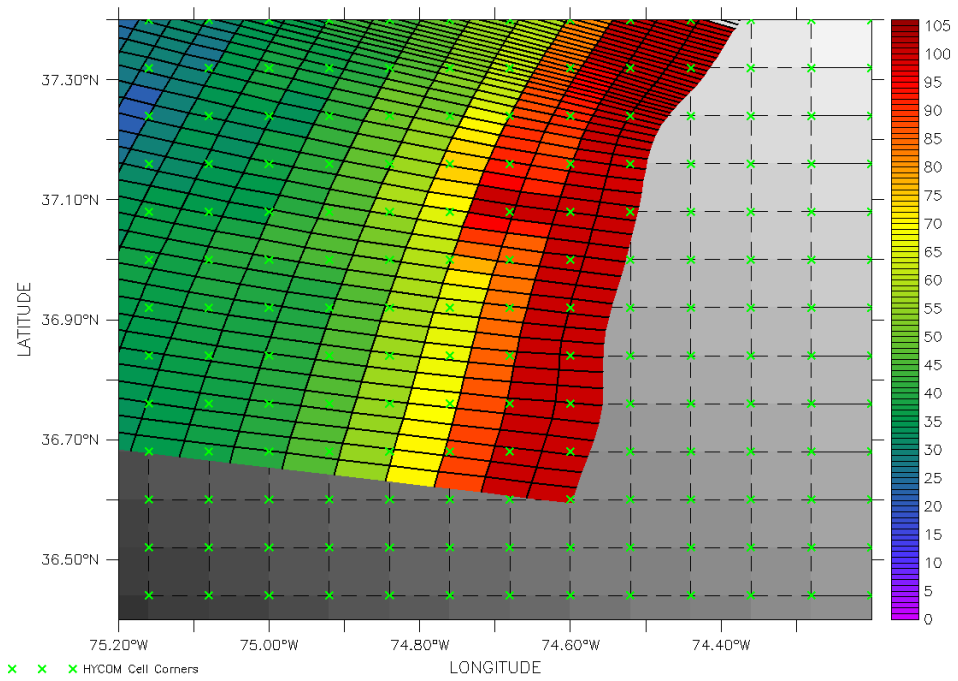
HYCOM-CONSORTIUM Grid Cells

Figure 2-11 - Grid cells of the LM-HYCOM model in our area of interest using an arbitrary color-bar to facilitate the visualization of the cells; each cross mark the center of a cell. The RM grid limits are outlined in red.



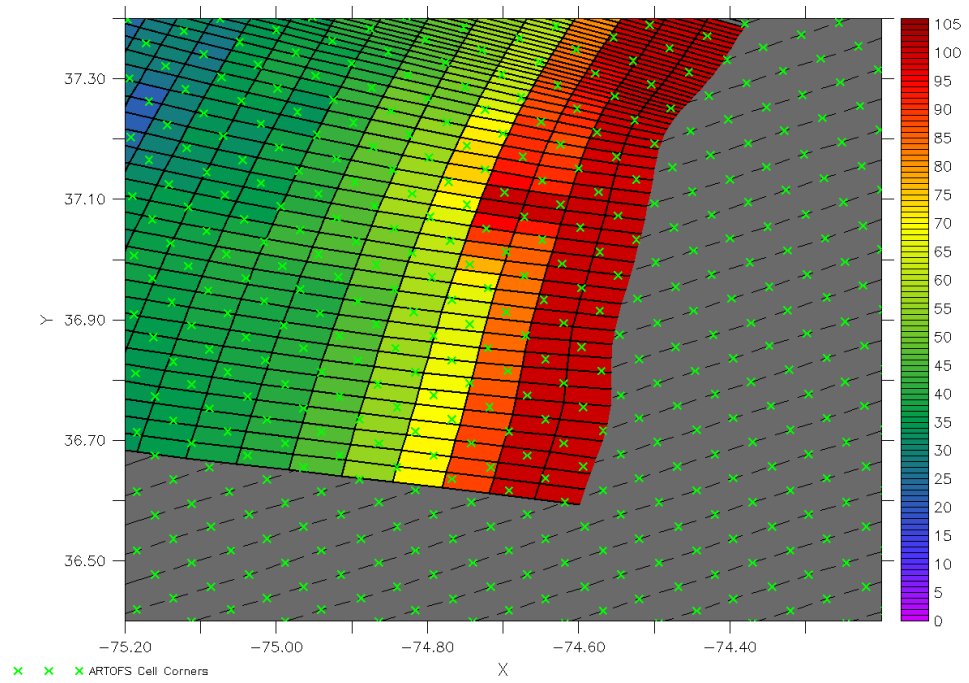
A-RTOfS Grid Cells

Figure 2-12 - Grid cells of the A-RTOfS model in our area of interest using an arbitrary color-bar to facilitate the visualization of the cells; each cross mark the center of a cell. The RM grid limits are outlined in red.



Delbay grid (depth in m) over HYCOM grid

Figure 2-13 - Plot of the southeast corner of RM grid over HYCOM Consortium grid. The color represents depth (in meters).



Delbay grid (depth in m) over ARTOFS grid

Figure 2-14 - Plot of the southeast corner of RM grid over A-RTOFS grid. The color represents depth (in meters).

Chapter 3

RESULTS

In this chapter, we will first evaluate modeled water levels during Hurricane Sandy (section 3.1) and then examine associated, modeled inundation processes near the Bowers region (section 3.2). Finally, we will explore changes in water levels and flooding for different sea-level rise scenarios (section 3.3).

3.1 Water Levels during Sandy

We will first evaluate three existing models, Regional Model (RM, based on Jenkins, 2015), LM-ARTOFS and LM-HYCOM, based on tide gauge observations during Hurricane Sandy, then discuss the improvement of modeled water levels using the RM setup forced with water level and depth-averaged current at the lateral boundaries. Finally, we will assess modeled water levels for the HR-Bowers model setup.

3.1.1 Evaluating Existing Models

The timing and magnitude of maximum sea levels caused by the storm surge due to Hurricane Sandy were different for each tide gauge station. Figures 3-1 presents the measurements at each of them during the surge event. The station at Brandywine Shoal Light was destroyed during Hurricane Sandy, having data available only until the 29th of October. All measurements presented here are based on the Mean Sea Level datum.

With the objective of analyzing the storm surge movement inside Delaware Bay, we will look at the subtidal oscillation present in the water level measurements of these stations calculated here by the application of a 24h-moving average filter. The NOAA stations at Lewes and Cape May hit peak surge at 10:00h and 14:00h of Oct/29 respectively. The station in Atlantic City registered its peak surge at 15:00h the same day. These three stations registered surges between 1.20m and 1.32m. The NOAA station farther up in the Bay, Ship John Shoal, measured the peak of the surge early next day, with a value of 0.96m. Finally, the USGS station at Bowers was the first one to hit the peak, at 7:00h on Oct/29 with observed sea level of 0.90m.

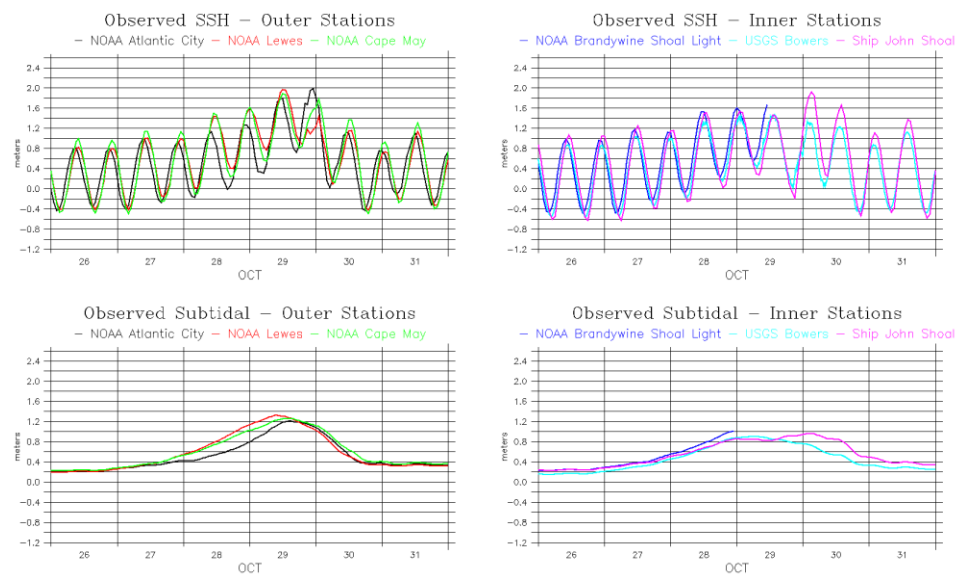


Figure 3-1 – Sea surface height (top panels) and subtidal water level (bottom panels) at available water level stations inside Delaware Bay (Inner Stations, right panels) and close to the mouth of the Bay (Outer Stations, left panels).

Using these observations as a basis, we evaluate how the RM captures water levels during Hurricane Sandy. We also investigate the performance of the two large-

scale models, LM-HYCOM and LM-ARTOFS. In Figures 3-2, 3-3, and 3-4 below, the upper panel presents the observed and modeled sea surface height; the lower panel shows the subtidal oscillation; and the middle panel contains the tidal signal, obtained simply by subtracting the subtidal oscillation from the sea surface height. Each figure compiles all those datasets (NOAA observations, RM, LM-HYCOM, and LM-ARTOFS) for each of the outer stations. LM-HYCOM does not simulate tides, and for that reason, we do not present them in the tidal signal panel.

The RM setup models the tides well, due to the realistic tidal constituents imposed at the lateral boundaries. However, this setup generates almost no surge, which suggests that large-scale remote forcing is critical. On the other hand, both large scale models capture well the increase in the mean water level (low frequency), although not being able to reproduce the tides: LM-HYCOM has no tides in its formulations and LM-ARTOFS, although including tides in its formulation, does not generate realistic tidal oscillations. Also, LM-ARTOFS mean sea level consistently overpredicts the observations, while LM-HYCOM generates closer values albeit slightly under-predicting the observations

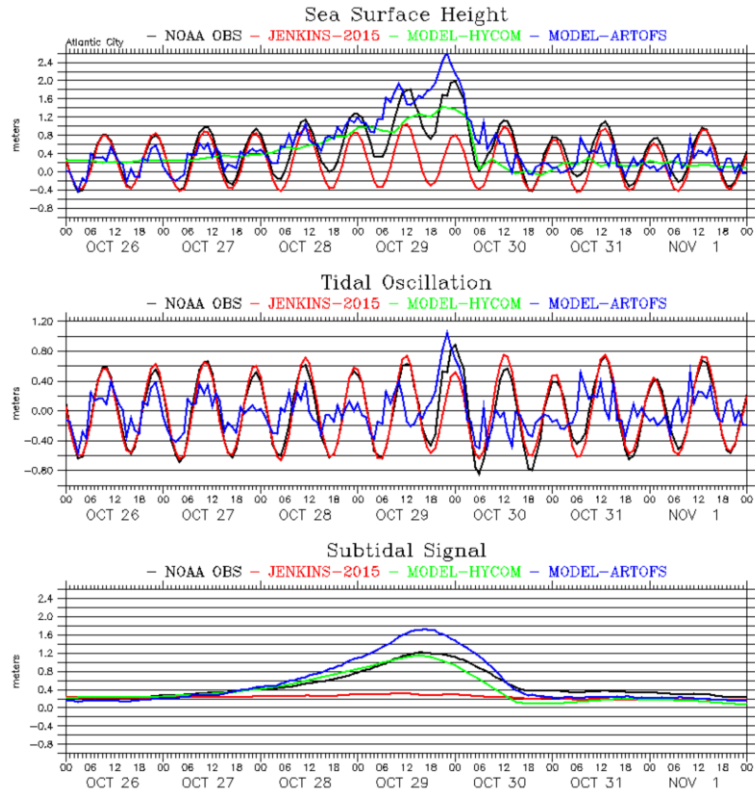


Figure 3-2 - Sea surface height (top panel), tidal oscillation (middle panel) and subtidal water oscillation (bottom panel) during Hurricane Sandy at NOAA Station Atlantic City. Each panel shows the observations (black) and model results from the RM (red), LM-HYCOM (green) and LM-ARTOFS (blue).

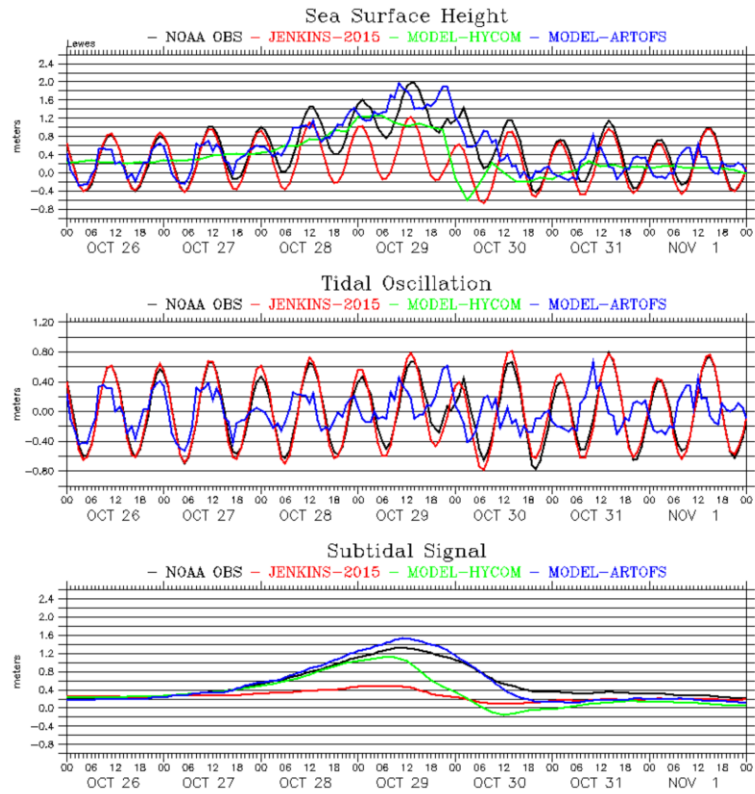


Figure 3-3 - Plot of the Sea Surface Height (top panel), Tidal Oscillation (middle panel) and Subtidal Signal (bottom panel) during Hurricane Sandy at the position of the NOAA station in Lewes. Each panel contains the observations (black) and modeled results from the RM (red), LM-HYCOM (green) and LM-ARTOFS (blue).

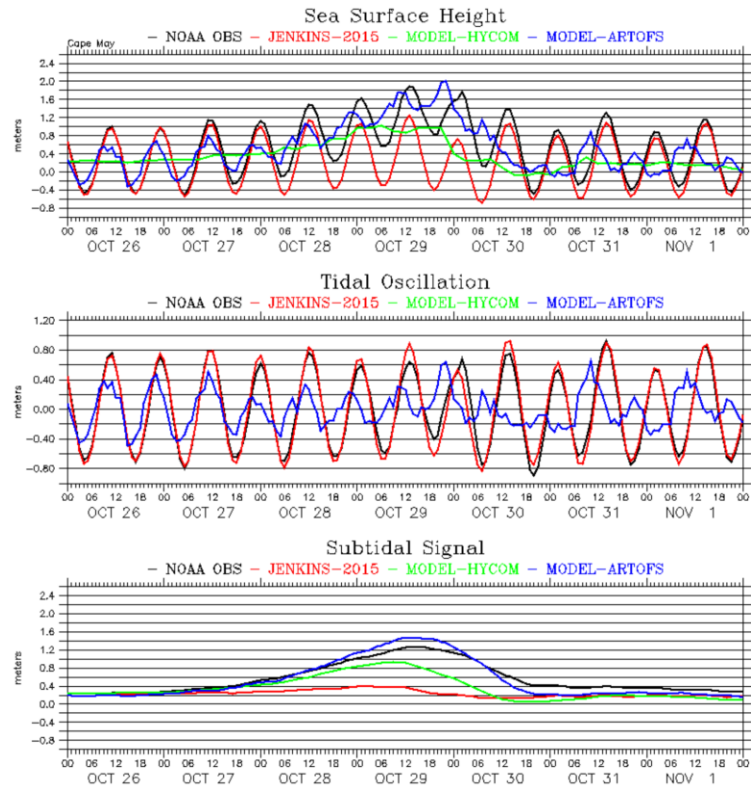


Figure 3-4 - Plot of the Sea Surface Height (top panel), Tidal Oscillation (middle panel) and Subtidal Signal (bottom panel) during Hurricane Sandy at the position of the NOAA station in Cape May. Each panel contains the observations (black) and modeled results from the RM (red), LM-HYCOM (green) and LM-ARTOFS (blue).

3.1.2 Improving Water Level in Regional Model

Although the Regional Model (RM, based on Jenkins, 2015) results represented rather well the tidal elevation, this setup was not capable of representing subtidal sea surface elevation, i.e., storm surges. It is not a surprise since storm surges are generated by large-scale phenomena, like Nor'easters and Hurricanes, which develop through a region much bigger than the domain utilized. To represent appropriately the sea level oscillation generated by these kinds of events inside our domain, we propose a two steps approach: the application of the tidal forcing

described in Section 2.1.3 to generate the high-frequency tides and the use of the low-frequency signal extracted from LM-ARTOFS or from LM-HYCOM to force the lateral boundaries.

Before applying the results from the Large Scale models to specify the boundary conditions in our Regional Model, we examine how those models represent Hurricane Sandy and what kind of signal they could pass on to the RM. With this objective, we choose one point in each boundary of the RM grid and present the water level and a stick plot of the depth-averaged current of both models. Figure 3-5 below shows the position of each boundary station (called North, South, and East in reference to the position of the respective boundary in regards to the grid) over the grid's bathymetry. Figures 3-6, 3-7, and 3-8 present each point results. In these plots, the Y axis is measured in days from Jan/01/2012, and each plot covers the span between Oct/25/2012 and Nov/02/2012, with Sandy making landfall on Oct/29/2012 (day 302). Both the water levels and the currents show very similar pattern along the north and the south boundaries, with a little more variations at the east boundary, where LM-HYCOM generates relatively small surge water levels but relatively strong currents. LM-ARTOFS has the opposite response, with higher surge water levels but weaker currents.

Boundary Stations

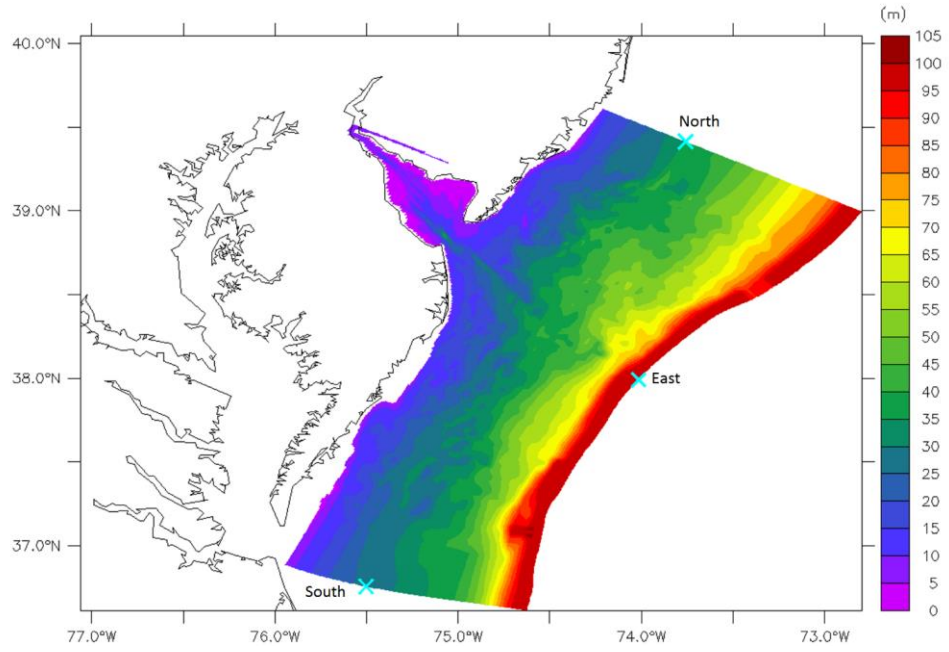


Figure 3-5 – Plot of the positions of the stations (South, East, and North) used to analyze the LM-HYCOM and LM-ARTOFS results on top of the bathymetry from RM grid in meters.

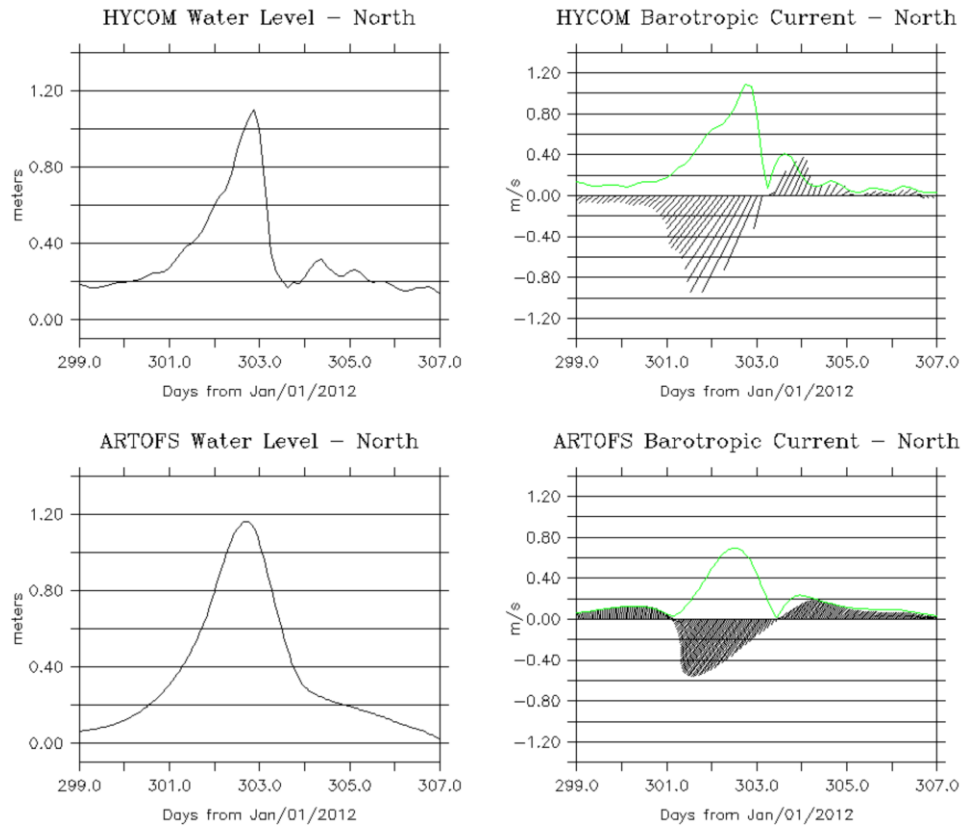


Figure 3-6 – Plot of the water level and barotropic current from LS-HYCOM (upper panels) and LS-ARTOFS (lower panels) at the Position North (north boundary of the RM grid). Water level is in meters and barotropic current in m/s, with the green line representing the current speed.

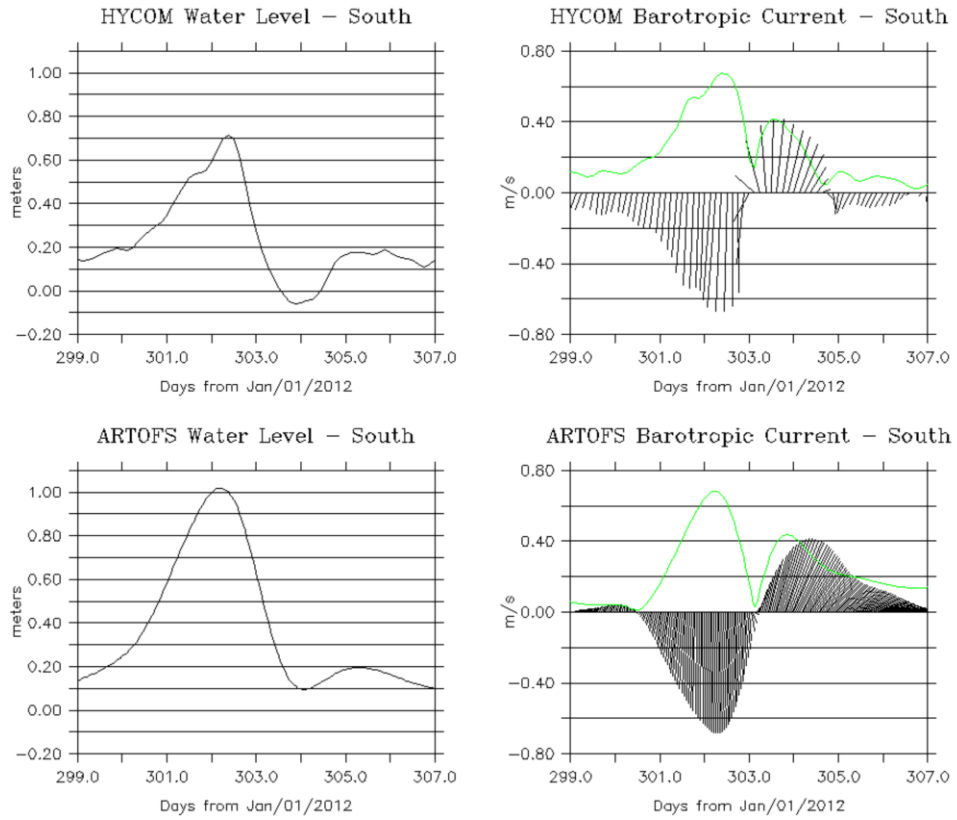


Figure 3-7 - Plot of the water level and barotropic current from LS-HYCOM (upper panels) and LS-ARTOFS (lower panels) at the Position South (south boundary of the RM grid). Water level in meters and barotropic current in m/s, with the green line representing the current speed.

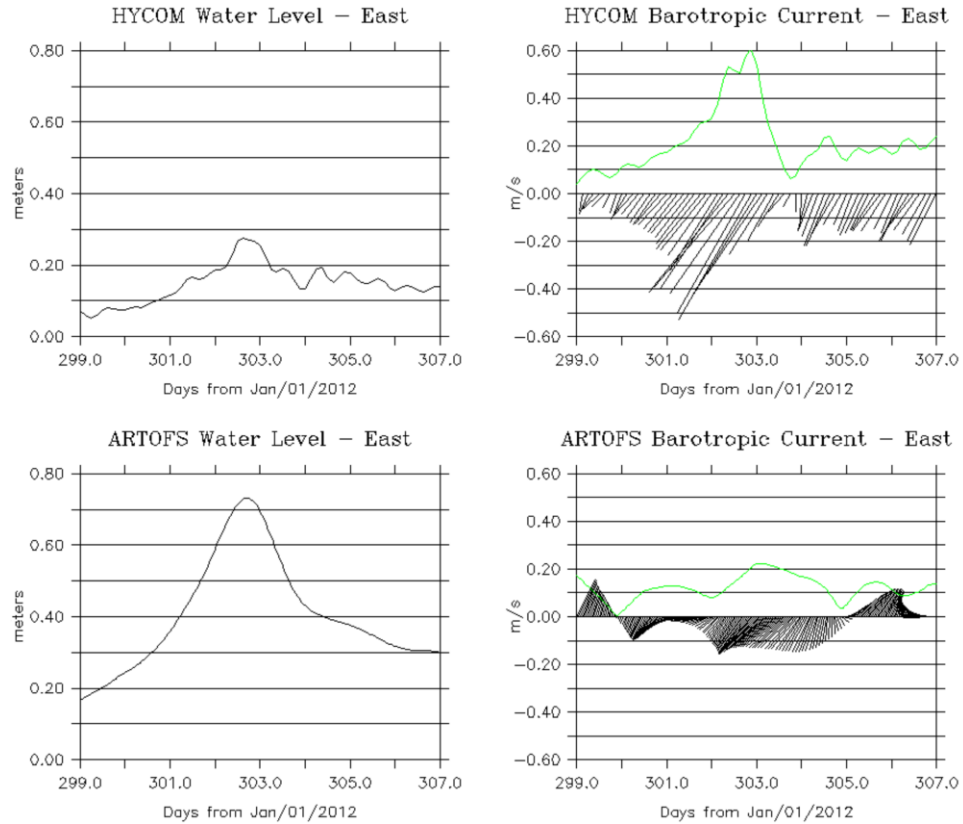


Figure 3-8 - Plot of the water level and barotropic current from LS-HYCOM (upper panels) and LS-ARTOFS (lower panels) at the Position East (east boundary of the RM grid). Water level in meters and barotropic current in m/s, with the green line representing the current speed.

To understand the sensitivity to imposing boundary conditions from LMs, we design different RM test cases with and without water levels (WLs) and barotropic currents (BAR) from the large-scale models:

- RM-NoBRY – no use of boundary forcing (setup like Jenkins, 2015);
- RM-WL – forced with Water Level at the boundaries;
- RM-BAR – forced with Barotropic Current at the boundaries;

- RM-WLBAR – forced with Water Level and Barotropic Current at the boundaries.

Figures 3-9, 3-10, 3-11, 3-12, 3-13, and 3-14 below present the results generated by each one of the four scenarios during Hurricane Sandy and a comparison with the observations from the NOAA Tides and Currents (2016) stations in Atlantic City, Lewes and Cape May (outer stations). The results presented here are for the RM, previously presented in Section 2.1.5; the NOBRY scenario is exactly like the previous Jenkins (2015) setup, while in the other three scenarios we have added the boundary forcing described to each case. In each figure, the top four images are the results generated by the RM being forced by the LM-HYCOM while the bottom four images are the results generated using the LM-ARTOFS as forcing.

In the LM-HYCOM scenarios, it is clear that the WLBAR is the best setup both for representing the hurricane storm surge and the regular tidal cycles observed in the days before the hurricane arrival. As for the scenarios forced using LM-ARTOFS results, we note an inconsistent response. The scenarios WL and WLBAR can recreate well a regular tidal cycle, but the WL scenario underestimates the hurricane surge while the WLBAR scenario overestimates the surge. As for the BAR, it represents well the hurricane surge but does not capture realistically the regular tidal cycle, showing an increase in the mean water level in the days before the hurricane, which is observed neither for the data nor the other sensitivity scenarios. Therefore, we chose to force the lateral boundaries of our RM with the results from the LM-HYCOM. We will call this setup RM-H.

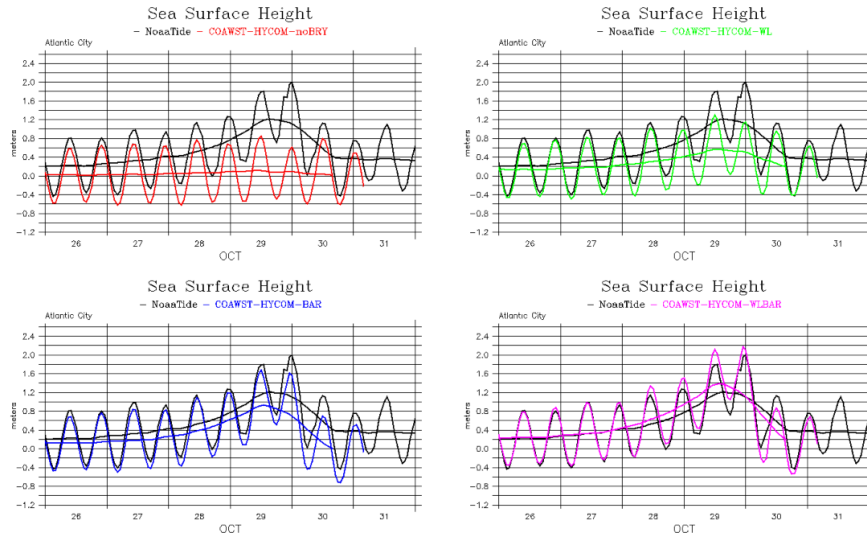


Figure 3-9 – Plot of the water levels registered during Hurricane Sandy in Atlantic City versus the four scenarios using LM-HYCOM as forcing: top left panel shows the RM-H-NOBRY, top right panel shows RM-H-WL, bottom left panel shows RM-H-BAR and bottom right panel shows RM-H.

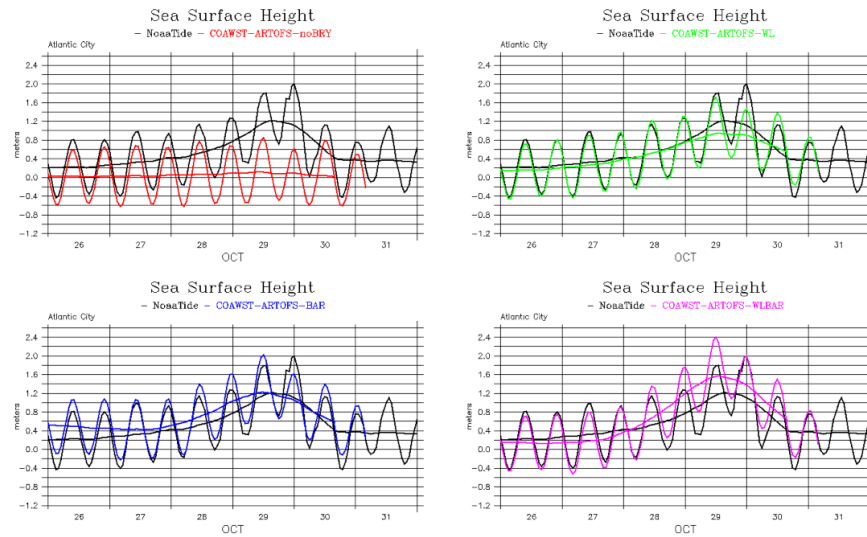


Figure 3-10 – Plot of the water levels registered during Hurricane Sandy in Atlantic City versus the four scenarios using LM-ARTOFS as forcing: top left panel shows the RM-A-NOBRY, top right panel shows RM-A-WL, bottom left panel shows RM-A-BAR and bottom right panel shows RM-A-WLBAR.

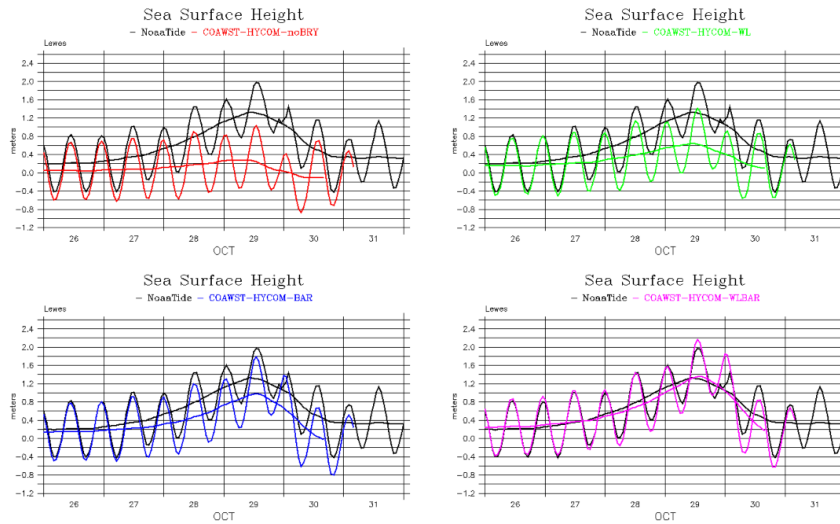


Figure 3-11 – Plot of the water levels registered during Hurricane Sandy in Lewes versus the four scenarios using LM-HYCOM as forcing: top left panel shows the RM-H-NOBRY, top right panel shows RM-H-WL, bottom left panel shows RM-H-BAR and bottom right panel shows RM-H-WLBAR.

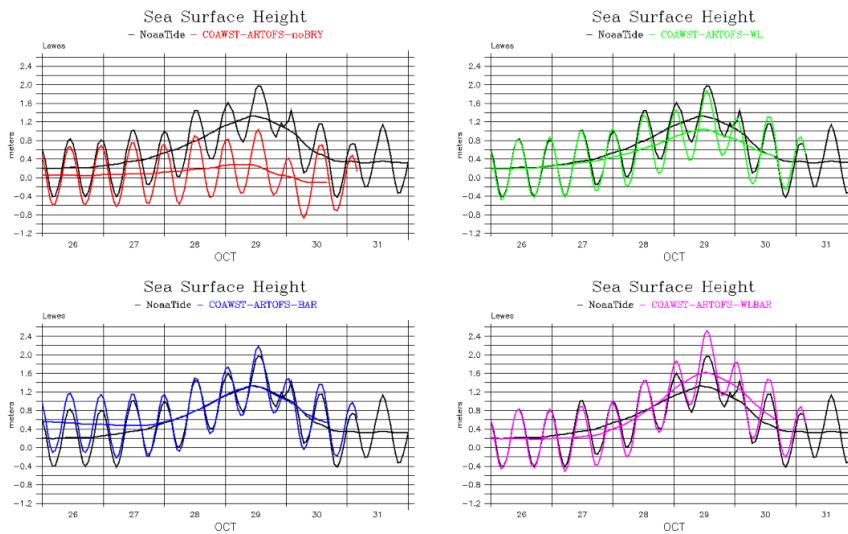


Figure 3-12 - Plot of the water levels registered during Hurricane Sandy in Lewes versus the four scenarios using LM-ARTOFS as forcing: top left panel shows the RM-A-NOBRY, top right panel shows RM-A-WL, bottom left panel shows RM-A-BAR and bottom right panel shows RM-A-WLBAR.

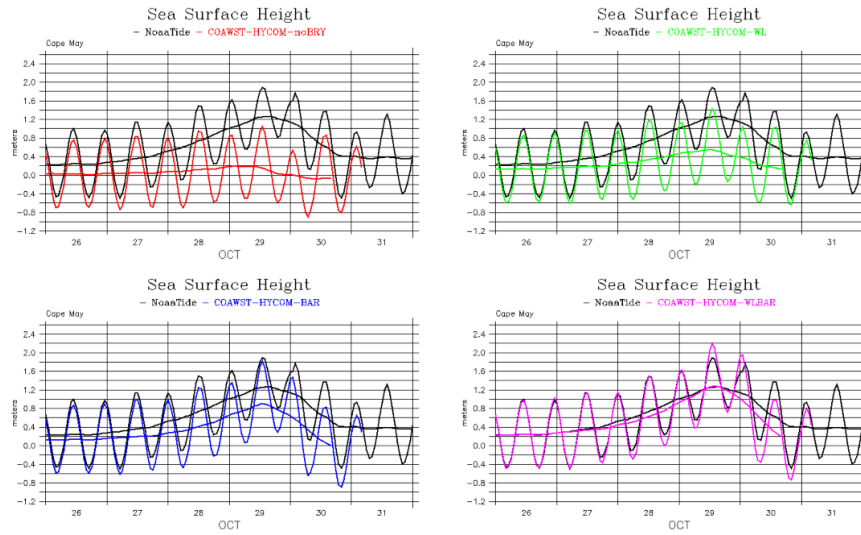


Figure 3-13 – Plot of the water levels registered during Hurricane Sandy in Cape May versus the four scenarios using LM-HYCOM as forcing: top left panel shows the RM-H-NOBRY, top right panel shows RM-H-WL, bottom left panel shows RM-H-BAR and bottom right panel shows RM-H-WLBAR.

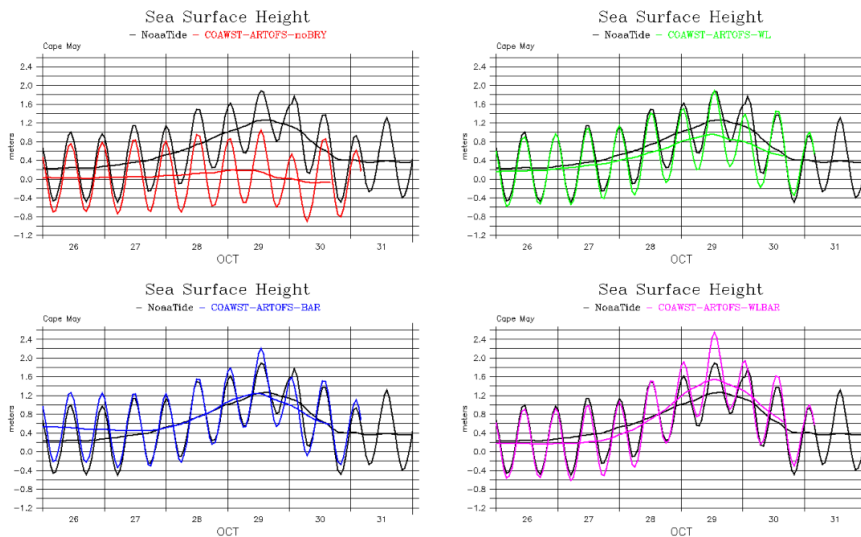


Figure 3-14 – Plot of the water level registered during Hurricane Sandy in Cape May versus the four scenarios using LM-ARTOFS as forcing: top left panel shows the RM-A-NOBRY, top right panel shows RM-A-WL, bottom left panel shows RM-A-BAR and bottom right panel shows RM-A-WLBAR.

After choosing the RM-H-WLBAR setup as the one to be used (which will be called, from now on, simply RM-H), we compare how those results fare against observations closer to the Bowers region (stations Murderkill at Bowers and Ship John Shoal, as seen in Figure 2-12). Figures 3-15 and 3-16 contain the comparison between the results generated by RM-H against the observations in the Inner Stations. In this case, the model performs reasonably in reproducing the regular tidal cycles before Sandy's surge. However, it over-predicts the effects of the surge, especially during the second tidal cycle of the 29th of October, when the model generates a peak around 2.2 m in both stations, while the observations stay around 1.4 m. The Ship John Shoal station has its peak water height during the first tidal cycle of the next day (30th of October), registering a value very close to the simulated (both around 2.0 m). In the following low tide and high tide, the model results are considerably lower than the observed water heights, but, after this point, the model simulates well observed water levels. For the Murderkill at Bowers station, the model consistently generates higher water levels than the measurements, even at moments when the other stations have registered water levels consistent with the observations.

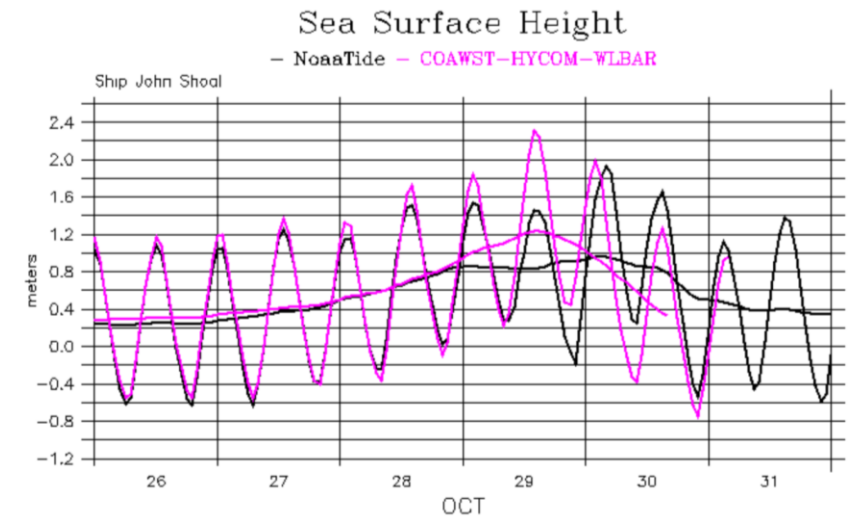


Figure 3-15 – Plot of the water level registered at the Ship John Shoal station versus the RM-H results during Hurricane Sandy.

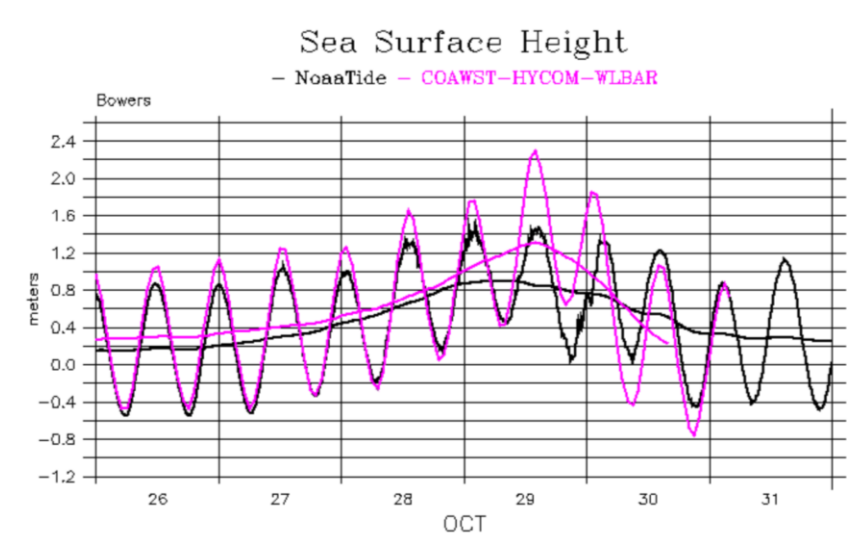


Figure 3-16 - Plot of the water level registered at the Murderkill at Bowers station versus the RM-H results during Hurricane Sandy.

The differences between the observations and modeled water heights inside Delaware Bay could be due to a problem in the measurement themselves. It is important to keep in mind possible instrument failures during extreme events, either by a faulty sensor not properly registering the conditions or by the destruction of an instrument, as happened to the Brandywine Shoal Light tide gauge. However, according to the USGS hydrologist Wendy McPherson (personal communication, September 19, 2016), the measurements taken at the Bowers at Murderkill station are probably correct since, during this event, since the observed water levels are consistent with an independent measurement from a storm surge sensor also installed at Bowers. Below we discuss that strong winds over the bay may contribute to the spatiotemporal variations of observed water levels inside the bay.

This moves our eyes to the model being the problem, what could be caused by a less than ideal forcing being applied. One likely explanation is that the wind product is not accurate enough in reproducing strong winds inside Delaware Bay during the Hurricane. Figure 3-17 presents a comparison between the observations at four NOAA stations with available meteorological measurements versus the NAM product winds for the same position. The NAM represents well the observed wind direction; even when considering the smaller temporal resolution, it is still able to reproduce the rotation and timing of the wind from North to South at each station. The wind speeds are in good agreement before and after the Hurricane. However, the peak wind speeds during the Hurricane Sandy are under-predicted by almost 10m/s (observations around 25 m/s and wind forcing around 15 m/s). This higher speed value could lead to a wind stress almost three times higher, according to Equation 2, and changes local surge dynamics as Equation 1 suggests (see Section 1.3). These high winds from North

could contribute to the lower storm surge and spatiotemporal water level variability in the bay not captured by wind forcing used in RM-H. A more thorough comparison of the winds and water levels, measured and modeled, is shown in Appendix – B. Additional analyses were also conducted for two other storm surge events which happened during the year of 2012, one in February and the other in December.

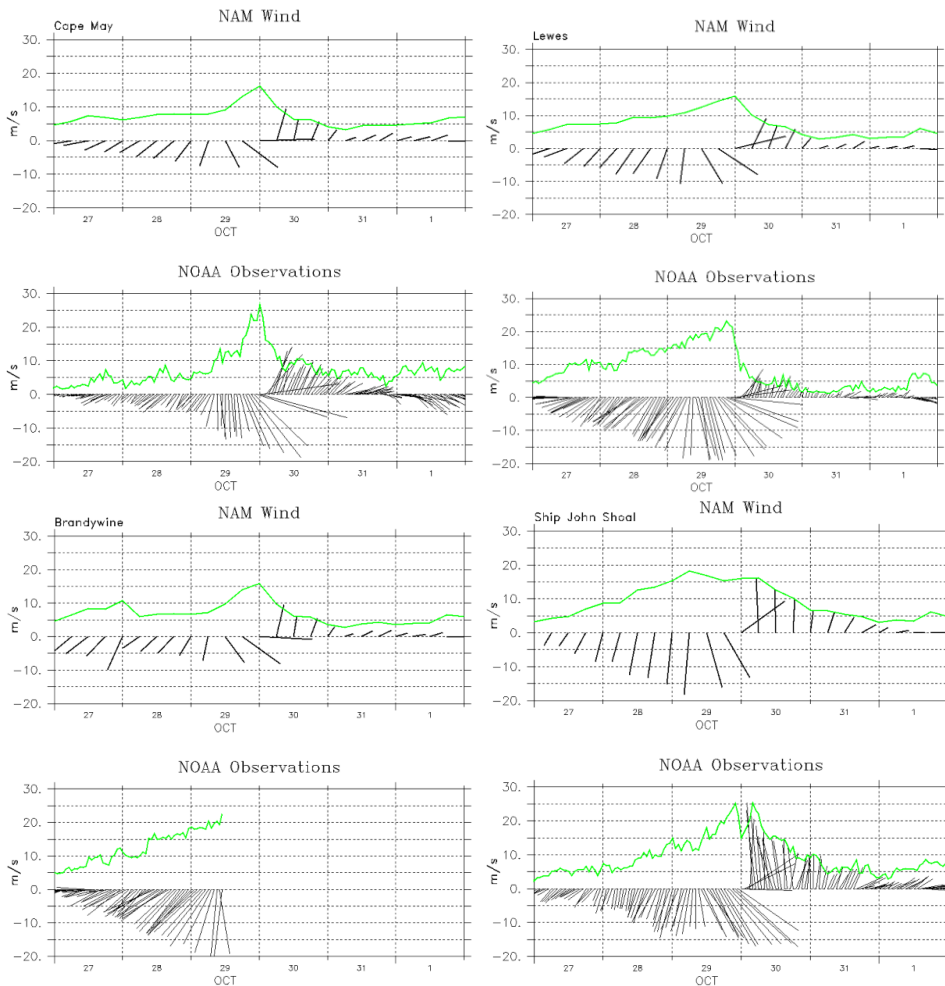


Figure 3-17 – Comparison between the NAM wind product and wind observations for the stations at Cape May, Lewes, Brandywine Shoal Light, and Ship John Shoal. The sticks represent the direction towards where the wind is going while the green line shows the wind speed in m/s.

3.1.3 Water Level in High-Resolution Model

This section presents the results generated using the HR-Bowers grid, previously presented in Section 2.1.6. It is a more resolved grid focusing on the region of Bowers and its two rivers, Saint Jones and Murderkill (Figure 1-2). Section 3.1.3.1 will show the results generated by the new grid when forced by the RM-H results on its lateral boundaries. Section 3.1.3.2 will show the results generated by the new grid when being forced by water level measurements taken at the Murderkill at Bowers station to closely model the observed surge at Bowers.

3.1.3.1 RM-H Forcing

To analyze the water levels generated for the region around Bowers, we compare the results from HR-Bowers and RM-H against the observations in the station at Murderkill at Bowers. Figure 3-18 presents that comparison showing water level, tidal oscillation, and the subtidal signal.

The comparison shows good agreement in the days before and after the hurricane, but differences are observed during the days 29th and 30th of October, when the hurricane was affecting the region. During this period, the subtidal signal is considerably lower (about 0.4 m), and even the tidal amplitude is affected, being smaller in the observations than in the model. This consistency with the RM-H results suggests that the storm surge response is likely not sensitive to the higher spatial resolution in the HR-Bowers grid.

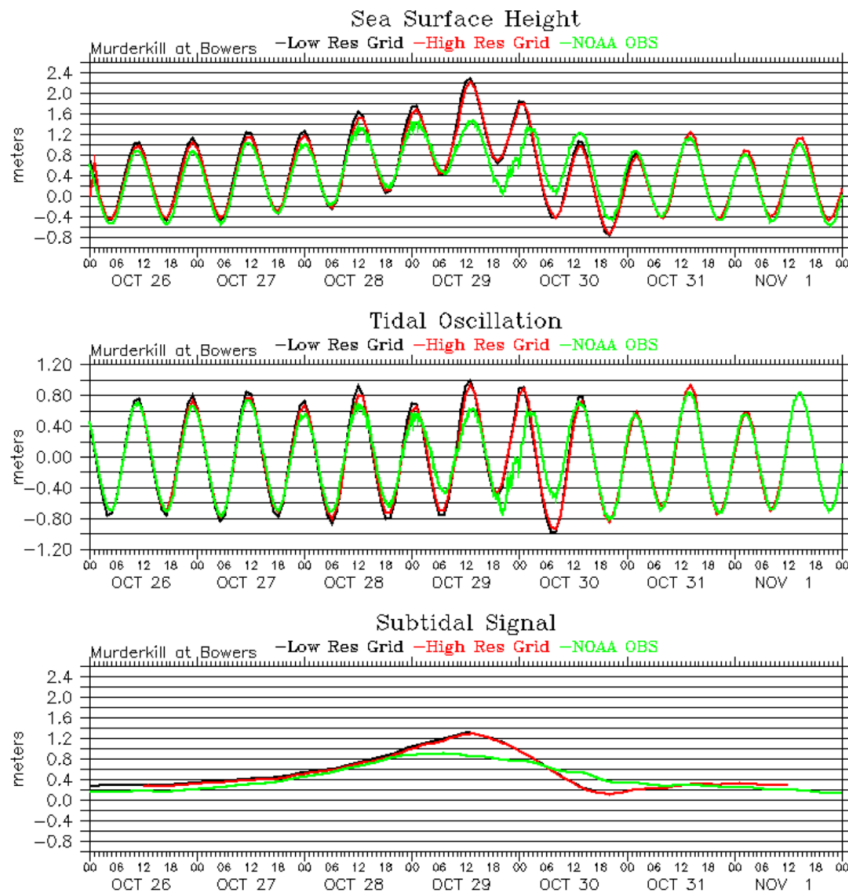


Figure 3-18 – Plot of the Sea Surface Height (top panel), Tidal Oscillation (middle panel) and Subtidal Signal (bottom panel) at the position of the station Murderkill at Bowers from the USGS. Each panel contains the observations (green) and results of the models RM-H (black) and HR-Bowers (red) being forced by the RM-H at the lateral boundaries.

3.1.3.2 Observational Forcing

As presented previously (in Figure 3-16), the measured water levels at the USGS station in Murderkill at Bowers are considerably lower than the ones observed in every other station inside Delaware Bay. As seen in the previous Section, the water heights generated by HR-Bowers forced with RM-H are also considerably higher than the observations, and consistent with the water levels generated by the RM. For that reason, we propose an experimental scenario where the HR-Bowers model will be set like the previous scenarios but using the water level measurements from the station Murderkill at Bowers as lateral boundary condition for the sea surface height. This way we will be able to reproduce the observations more closely. For a matter of consistency, we also apply the barotropic current from RM-H at the lateral boundaries, although sensitivity runs without imposing barotropic currents indicate that modeled water levels do not strongly depend on these current boundary conditions. Figure 3-19 presents the comparison between the water levels generated by the HR-Bowers model versus the observations, as well as the tidal oscillation and the subtidal signal. In this new setup, the model results and the observations agree well at the Murderkill at Bowers station. The only noticeable difference is in the tides, with the model's results having a slightly smaller amplitude, which may be attributed to a loss of energy due to bottom shear stress.

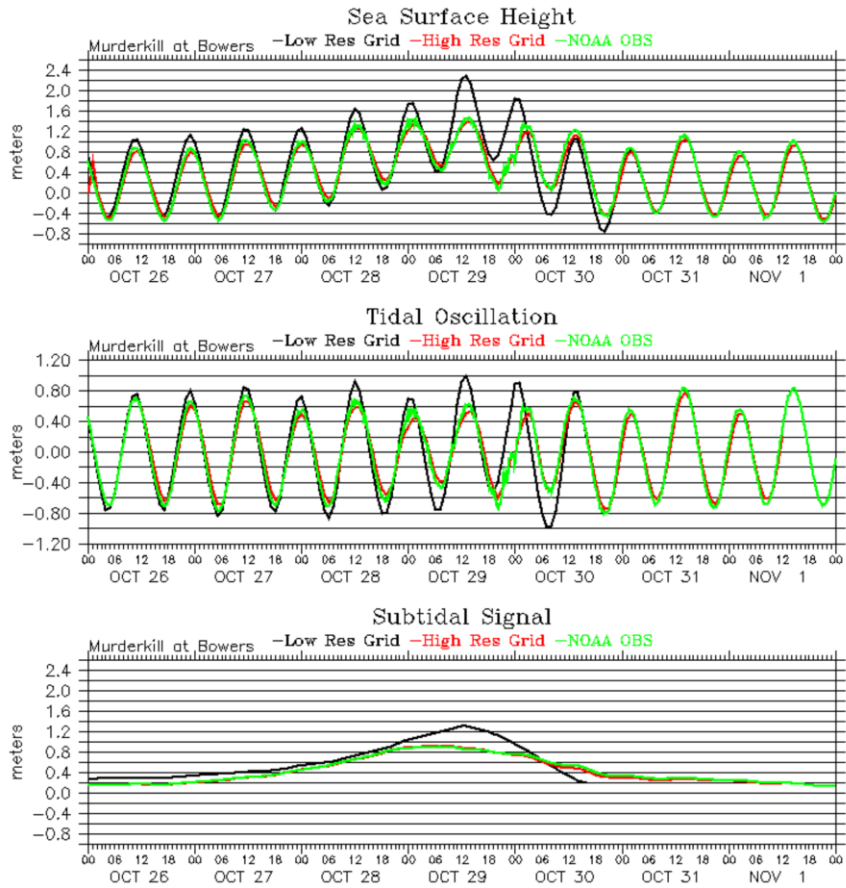


Figure 3-19 –Sea Surface Height (top panel), Tidal Oscillation (middle panel) and Subtidal Signal (bottom panel) at the position of the station Murderkill at Bowers from the USGS. Each panel contains the observations (green) and results of the models RM-H (black) and HR-Bowers (red) being forced by the Murderkill at Bowers water heights.

3.2 Inundation Processes near Bowers

This section will show the results of the inundation caused by Hurricane Sandy over the Bowers region simulated by the HR-Bowers grid. Section 3.2.1 will show the results generated when the model is forced by the RM-H water level and barotropic currents results on its lateral boundaries. Section 3.2.2 will show the results generated by a setup just like in the previous scenario, except in this case the model is forced by the water level measurements taken at the Murderkill at Bowers station.

3.2.1 RM-H Forcing

Every day, the tides are responsible for the inundation of a strip of land close to the shoreline. This area which is covered by water during High Tide and exposed during Low Tide is called Intertidal Zone. When a region is affected by a storm surge, like the one generated by Hurricane Sandy, the inundated area will be greater.

Figure 3-20 presents a comparison between the Intertidal Zone during a regular tide (in this case, a tidal cycle three days before the Spring Tide) and the area flooded by Hurricane Sandy. The area in light blue represents locations that are permanently inundated (ocean) and the area in gray covers the Intertidal Zone. The black outline represents the extent of the towns of Bowers and South Bowers as shown in Figure 1-3. The figures will be shown for the whole grid and for a zoomed in area defined roughly as a $0.04^\circ \times 0.04^\circ$ showing Bowers, South Bowers, Murderkill river, Saint Jones river and the marsh area north of Saint Jones.

Considering the whole grid, the model generated an intertidal zone of 30 km^2 ; in the region around Bowers, the Intertidal Zone covers 2.26 km^2 . However, during Hurricane Sandy, the area inundated in the whole grid was 114 km^2 , with 12.3 km^2 being covered in the Bowers region. In this scenario, the whole city of Bowers was

flooded during the Hurricane. According to reports the storm surge flooded at least a part of the city. O'malleys (2012) is a little piece from a local news outlet showing footage of the flooded streets of Bowers and residents stating that "it wasn't bad", while Mac Davis (2012) is a video published on Youtube showing South Bowers flooded after Hurricane Sandy. These pieces can work as a confirmation that the town was flooded, however, it is hard to estimate how much of it was affected based only on footage and without knowing exactly where are the spots shown. Moreover, it is hard to separate how much in this flood was due to the storm surge and how much was due to the rain. A possible way to validate these results could be to compare them to satellite or aerial images from after the hurricane, and try to establish which areas were inundated. Also, a comparison against images from a storm surge when there was no significant precipitation could help to evaluate how much of the flood observed was due to rain associated with the Hurricane Sandy. However, this is beyond the scope of this project.

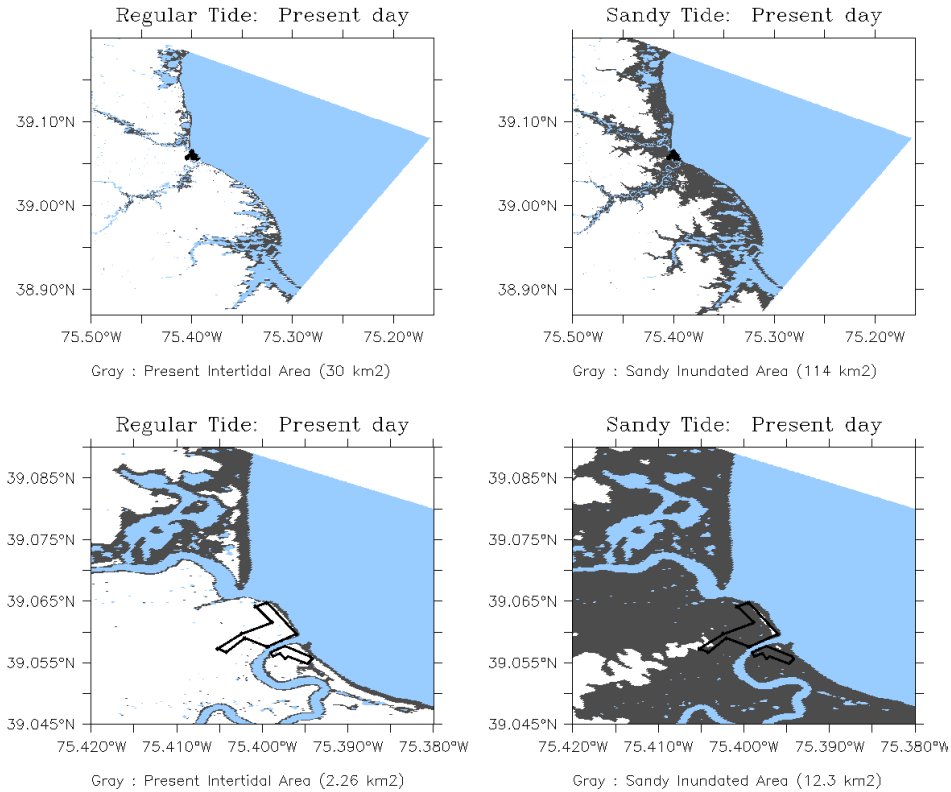


Figure 3-20 –Plot of the flooded area (in gray) during a regular tidal cycle (panels on the left) and during Hurricane Sandy (panels on the right), when the HR-B grid is forced by the results from the RM-WLBAR. The bottom images are a zoom region of Bowers (marked here by the black lines).

3.2.2 Observational Forcing

As expected, the scenario using the modified forcing (water level data from the Murderkill at Bowers station) generates smaller tides and storm surge. Figure 3-21 presents a comparison between the Intertidal Zone during a regular tide (in this case, a tidal cycle three days before the Spring Tide) and the area flooded by Hurricane Sandy. The color and line scheme is as described in the previous section.

In this scenario, inside the whole grid, the model generated an intertidal zone of 12.7 km²; in the region around Bowers, the intertidal zone covered only 0.9 km².

During Hurricane Sandy, the area inundated in the whole grid was 89.7 km², with 9.3 km², being covered in the Bowers region. In this scenario, only South Bowers was flooded during the Hurricane.

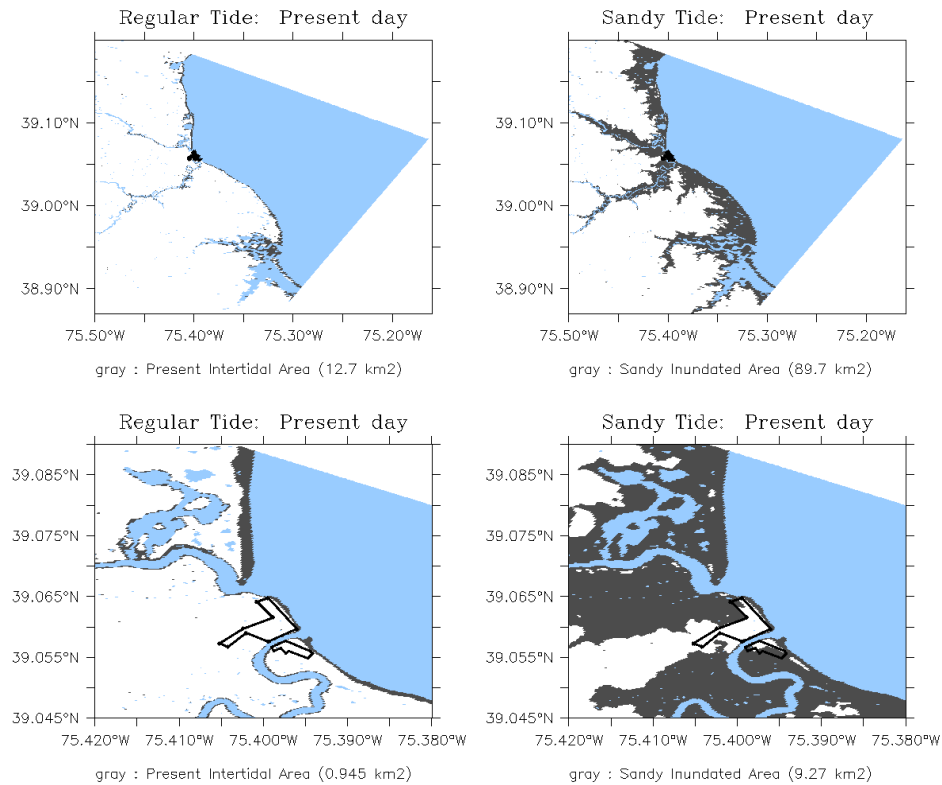


Figure 3-21 – Plot of the flooded area (in gray) during a regular tidal cycle (panels on the left) and during Hurricane Sandy (panels on the right), using Murderkill at Bowers observations to force the HR-B model. The bottom images are a zoom region of Bowers (marked here by the black lines).

3.3 Sea Level Rise Scenarios

The changes in the Mean Sea Level (MSL) of the ocean are a real threat to the coastal communities and habitats. The Sea Level Rise (SLR) expected to take place within the next century has the potential to destroy present marsh and beach areas, changing the ecological outlook of Delaware Bay Intertidal Zone. It also can force

humans to move away from present inhabited areas, leaving behind developments. In this scenario, the occurrence of a Hurricane forced storm surge is also something to take into consideration and to prepare for. For that reason, it is important to have estimates of which regions might be affected in order to allow for planned retreats and to rebuild in safer areas.

As a tool to analyze which areas are more at risk of being inundated during a daily tide or during a storm surge in the vicinities of Bowers, we run HR-Bowers grid considering four different SLR scenarios: one using the present MSL; one considering an increase of 0.5 m in the MSL; one considering an increase of 1.0 m in the MSL; and the last one considering an increase of 1.5 m in the MSL, corresponding to 0.5m SLR, 1.0m SLR, and 1.5m SLR scenarios, respectively (see section 1.5). To simulate a surge for those scenarios, we will use the storm surge generated by Hurricane Sandy added to the SLR scenario. We have selected Hurricane Sandy because it generated an extreme storm surge, with record high surge water levels for some of the affected stations, like Ship John Shoal and Cape May (Fanelli *et al.*, 2013). The following sections will present the results of these three sea level rise scenarios being run considering the two different setups previously proposed: the first being forced by the RM-H results (Section 3.3.1) and the second being forced by the water height measurements taken by the Murderkill at Bowers station (Section 3.3.2).

3.3.1 RM-H Forcing

This Section presents the results generated for the three new SLR scenarios compared to the present day scenario, when being forced by the results from RM-H at the lateral boundaries.

Figure 3-22 presents the water height registered by the USGS station Murderkill at Bowers and the results for the four SLR scenarios. The comparison between the observation and the present day scenario are like the one presented in Section 3.1.3.1. The tidal oscillation panel in the figure shows how the astronomical tides are the same in all SLR scenarios. The only difference between said scenarios is the increase in the MSL, as showed by the sea surface height and subtidal oscillation.

Figures 3-23 and 3-24 present a plot of the region affected by flooding in each scenario, with the second figure being a zoom over the region of Bowers. Meanwhile, Table 3-1 contains, for all four scenarios, estimates of the Permanently Flooded Area, the Intertidal Zone and the Sandy Inundated Area, i.e., the area which would be inundated by a surge similar to the one caused by Hurricane Sandy. In the scenario 0.5 m SLR, South Bowers would be part of the Intertidal Zone, being flooded by daily tides; with 1.0 m SLR, Bowers would also become inundated on a daily basis; in the 1.5 m SLR scenario, South Bowers would be permanently under water. In these simulations, river widths expand with increasing MSL. However, it is important to note that we assume present-day topography/bathymetry of the area without any changes over time. Coastal processes, like accretion and erosion, and land changes by humans to protect certain regions would likely change the local topography/bathymetry and the associated flooded area.

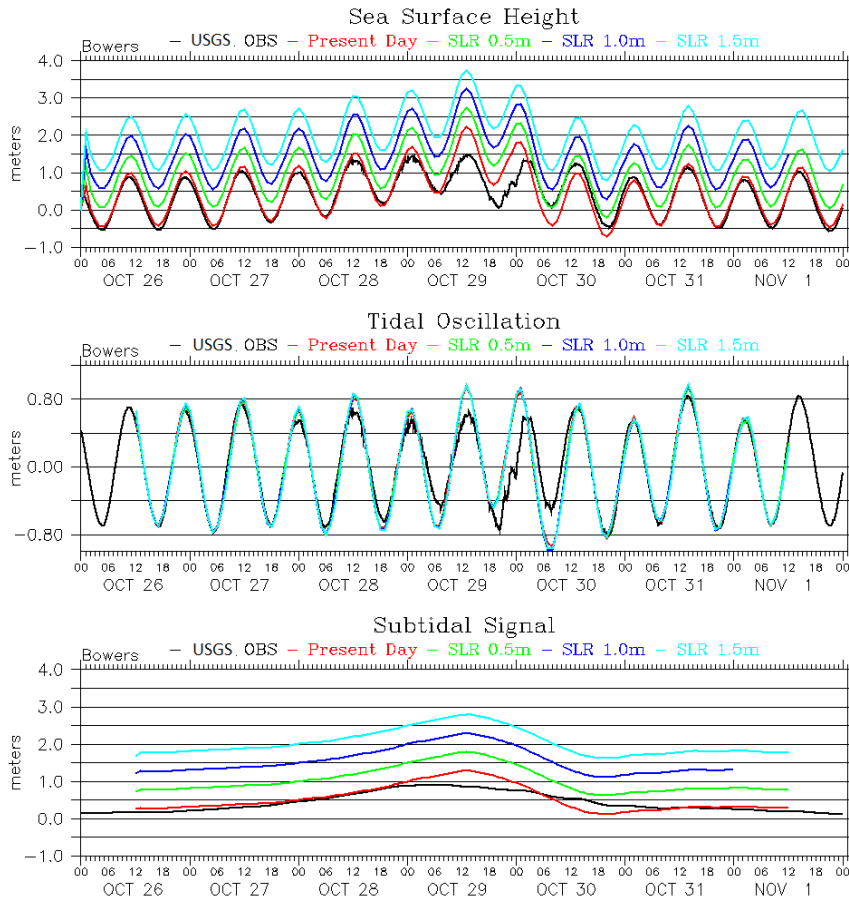


Figure 3-22 – Plot of the Sea Surface Height (top panel), Tidal Oscillation (middle panel) and Subtidal Signal (bottom panel) at the position of the station Murderkill at Bowers from the USGS. Each panel contains the observations (black) and modeled results for the scenarios considering the MSL at present day (red), 0.5 m increase in the MSL (green), 1.0 m increase in the MSL (blue), and 1.5 m increase in the MSL (cyan). All the model results here are generated using the results from RM-H as lateral forcing.

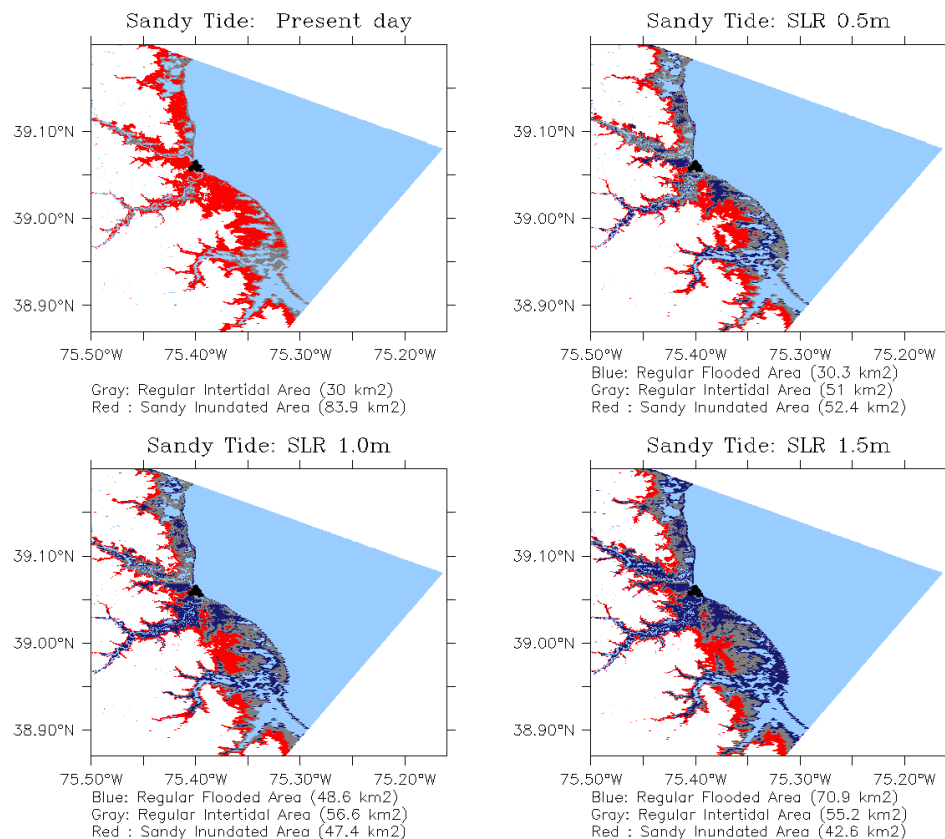


Figure 3-23 – Plot of the areas affected by inundation in all four SLR scenarios: upper left panel shows the results of the present day scenario; upper right panel shows the results of the scenario with 0.5 m increase in the MSL; lower left panel shows the results of the scenario with 1.0 m increase in the MSL; and lower right panel shows the results of the scenario with 1.5 m increase in the MSL. Red represents the area which would be inundated by a storm surge like the one generated by Hurricane Sandy; gray is the Intertidal area; dark blue is the area permanently inundated in each scenario; and light blue is the area permanently inundated in the present day. All the results here are generated using the results from RM-H as lateral forcing.

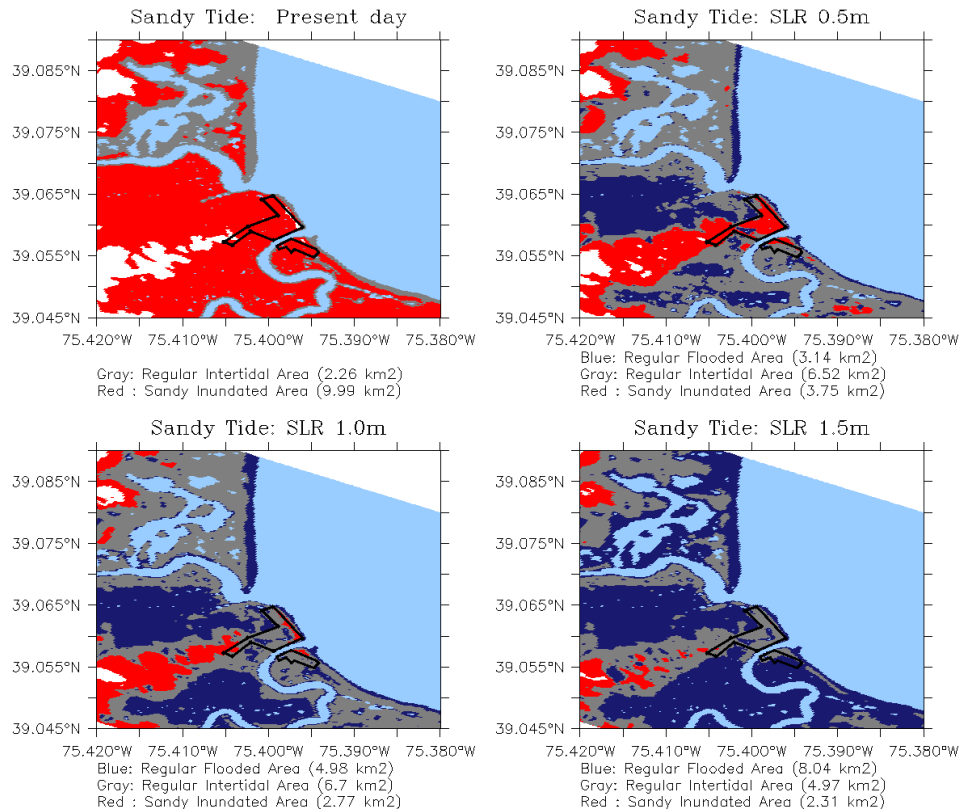


Figure 3-24 – Zoom over the Bowers region of plot of the areas affected by inundation in all four SLR scenarios: upper left panel shows the results of the present day scenario; upper right panel shows the results of the scenario with 0.5 m increase in the MSL; lower left panel shows the results of the scenario with 1.0 m increase in the MSL; and lower right panel shows the results of the scenario with 1.5 m increase in the MSL. Red represents the area which would be inundated by a storm surge like the one generated by Hurricane Sandy; gray is the Intertidal area; dark blue is the area permanently inundated in each scenario; and light blue is the area permanently inundated in the present day. All the model results here are generated using the results from RM-H as lateral forcing.

Table 3-1– Estimate areas of the Permanently Flooded Area, the Intertidal Zone, and the Sandy Inundated Area, based on the HR-Bowers results generated when forced by the RM-H. The values are shown both when considering the whole grid and also when considering only the area adjacent to Bowers.

	Permanently Flooded		Intertidal Zone		Sandy Inundated Area	
	Area in km ² (Blue)		Area in km ² (Gray)		in km ² (Red)	
	Whole domain	Bowers region	Whole domain	Bowers region	Whole domain	Bowers region
Present Day	-	-	30	2.3	83.9	10
SLR 0.5 m	30.3	3.1	51	6.5	52.4	3.7
SLR 1.0 m	48.6	5.0	56.6	6.7	47.4	2.8
SLR 1.5 m	70.9	8.0	55.2	5.0	42.6	2.3

3.3.2 Observational Forcing

This Section presents the results generated for the four SLR scenarios when being forced by the water height measurements from the USGS station Murderkill at Bowers at the lateral boundaries (see section 3.1.3.2).

Figure 3-25 presents the water height measured at the USGS station Murderkill at Bowers versus the results for the four SLR scenarios. The comparison between the observation and the present day scenario are like the one presented in Section 3.1.3.2. As in the previous section, the tidal oscillation panel shows how the astronomical tides are the same in all SLR scenarios while the sea surface height and subtidal oscillation show that the only difference in each scenario is the increase in the MSL.

Figures 3-26 and 3-27 present the region affected by flooding in each scenario, with the second figure being a zoom over the region of Bowers, while Table 3-2 contains the estimated values, for all four scenarios, of the Permanently Flooded Area, the Intertidal Zone and the Sandy Inundated Area, which is the area which a surge similar to the one caused by Hurricane Sandy would inundate. In this scenario, a storm surge like the one generated by Hurricane Sandy would only affect a part of South Bowers. In the 0.5 m SLR, Bowers would be affected by a Sandy-like event. Only in the 1.0 m SLR and 1.5 m SLR we see the area becoming flooded by the daily tide.

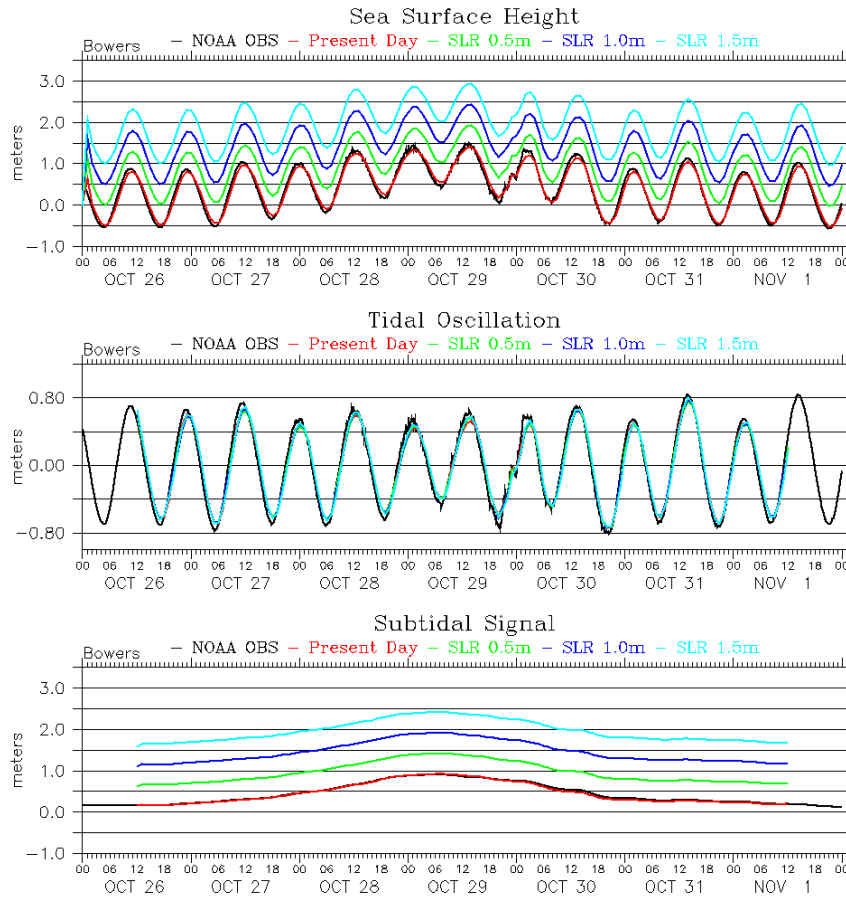


Figure 3-25 –Plot of the Sea Surface Height (top panel), Tidal Oscillation (middle panel) and Subtidal Signal (bottom panel) at the position of the station Murderkill at Bowers from the USGS. Each panel contains the observations (black) and modeled results for the scenarios considering the MSL at present day (red), 0.5 m increase in the MSL (green), 1.0 m increase in the MSL (blue), and 1.5 m increase in the MSL (cyan). All the model results here are generated using the observations from the USGS station Murderkill at Bowers as lateral forcing.

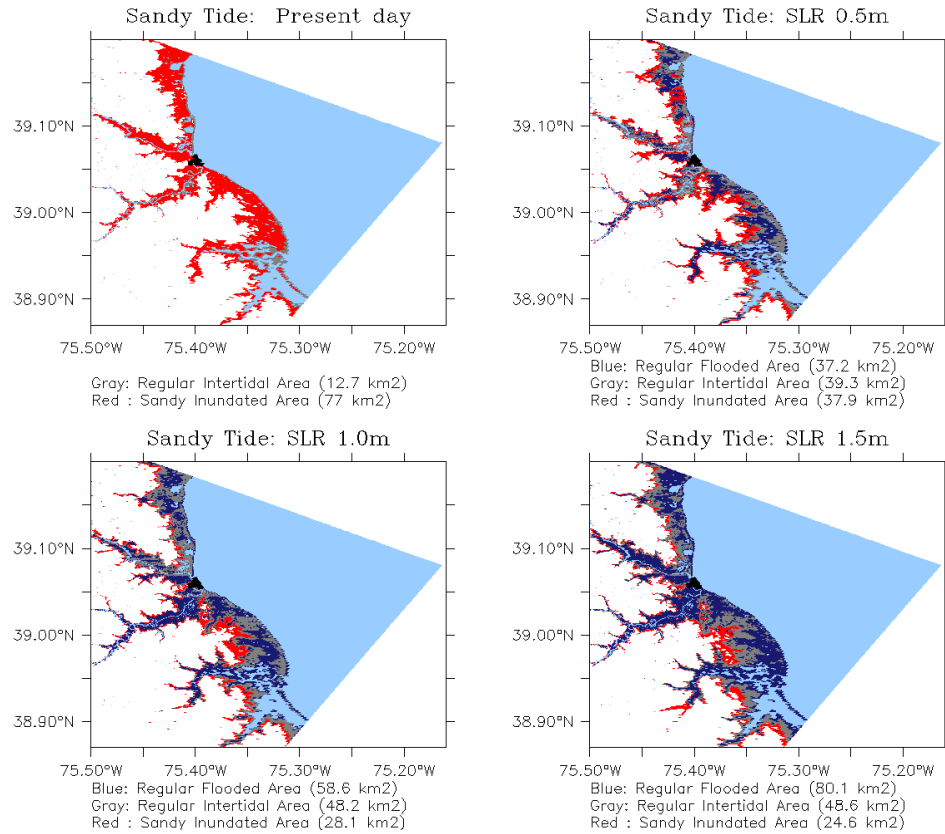


Figure 3-26 – Plot of the areas affected by inundation in all four SLR scenarios: upper left panel shows the results of the present day scenario; upper right panel shows the results of the scenario with 0.5 m increase in the MSL; lower left panel shows the results of the scenario with 1.0 m increase in the MSL; and lower right panel shows the results of the scenario with 1.5 m increase in the MSL. In all images the red represents the area which would be inundated by a storm surge like the one generated by Hurricane Sandy; gray is the Intertidal area; dark blue is the area permanently inundated in each scenario; and light blue is the area permanently inundated in the present day. All the model results here are generated using the observations from the USGS station Murderkill at Bowers as lateral forcing.

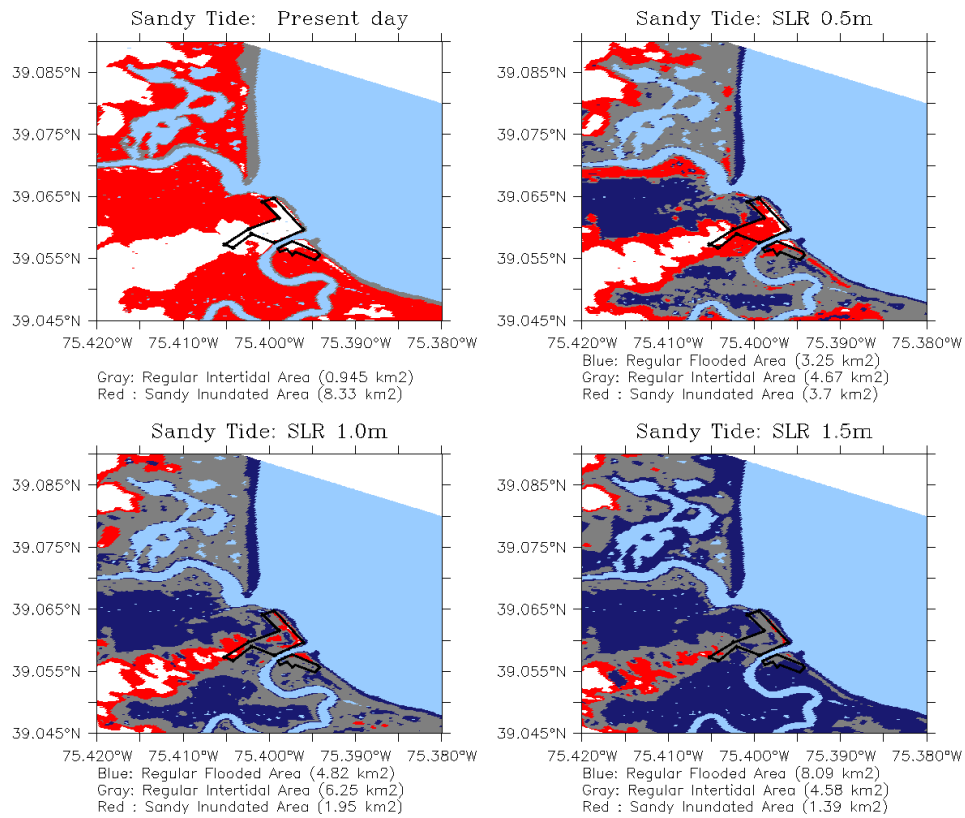


Figure 3-27 – Zoom over the Bowers region of plot of the areas affected by inundation in all four SLR scenarios: upper left panel shows the results of the present day scenario; upper right panel shows the results of the scenario with 0.5 m increase in the MSL; lower left panel shows the results of the scenario with 1.0 m increase in the MSL; and lower right panel shows the results of the scenario with 1.5 m increase in the MSL. In all of the red represents the area which would be inundated by a storm surge like the one generated by Hurricane Sandy; gray is the Intertidal area; dark blue is the area permanently inundated in each scenario; and light blue is the area permanently inundated in the present day. All the model results here are generated using the observations from the USGS station Murderkill at Bowers as lateral forcing.

Table 3-2– Estimate areas of the Permanently Flooded Area, the Intertidal Zone, and the Sandy Inundated Area, based on the HR-Bowers results generated when forced by the water heights measured by the USGS Murderkill at Bowers station. The values are shown both when considering the whole grid and also when considering only the area adjacent to Bowers.

Values in km ²	Permanently Flooded Area (Blue)		Intertidal Zone (Gray)		Sandy Inundated Area (Red)	
	Grid	Bowers	Grid	Bowers	Grid	Bowers
Present Day	-	-	12.7	0.9	77	8.3
SLR 0.5 m	37.2	3.2	39.3	4.7	37.9	3.7
SLR 1.0 m	58.6	4.8	48.2	6.2	28.1	1.9
SLR 1.5 m	80.1	8.1	48.6	4.6	24.6	1.4

Comparing the results of the scenarios being forced by RM-H against the scenarios being forced by the observations from Murderkill at Bowers, we notice that the Permanently Flooded Area increases with each new SLR scenario. Also, the permanently flooded area is higher in the observation forced scenario. This happens because the scenario forced by observations has a smaller tidal amplitude, therefore, the lowest water level is higher than the lowest water level in scenario forced by the RM-H.

Regarding the Intertidal Zone and the Sandy Inudated area, they are both bigger in the scenario forced by the RM-H, both also being caused by the bigger tidal amplitude.

Chapter 4

CONCLUSIONS

The objective of this study was to simulate a storm surge inside of Delaware Bay, more specifically in the area of Bowers – DE, and to simulate how future sea level rise could impact the inundated area in such events. To understand coastal inundation processes, we have employed a hydrodynamic modeling system using a nested approach.

A previously developed Regional Model (Jenkins, 2015) has first been forced by realistic water levels and barotropic currents at the lateral boundaries from two Large Scale Models: LM-ARTOFS and LM-HYCOM. Comparing the results against tidal gauge stations inside and around Delaware Bay, LM-HYCOM was established as the best forcing. The addition of water level and barotropic current forcing considerably increased the capacity of the model to reproduce a storm surge entering Delaware Bay.

The next step was to develop a High-Resolution grid for the region of Bowers (HR-Bowers), to be able to analyze the flooding. We created the new grid based on a subset of the original RM grid, increasing 20 times the horizontal resolution and going from a resolution of about 1.600 m to 80 m around Bowers. Next, we increase the concentration of cells focusing in the rivers around Bowers and getting to a resolution of 12 m in that area.

The results from the HR-Bowers model being forced by RM setup did not generate water levels in accordance with the observations in Murderkill at Bowers

station, producing higher water levels than the ones observed. To increase the capacity of the model to reproduce those results, we decided to force the model's lateral boundaries with water level measurements from the Bowers station. This new setup produced results in accordance with the observations

Finally, to analyze the impact of future Sea Level Rise (SLR) over the tidal flooding and storm surge effects on the region of Bowers, we run the HR-Bowers grid using both scenarios (the one forced by the RM and the one forced by observations) with an increase in the Mean Sea Level (MSL) of 0.5 m, 1.0 m, and 1.5 m. These SLR scenarios showed that even an increase of only 0.5 m in the MSL could turn South Bowers into a tidally inundated area with the rest of the town being very susceptible to storm surges. In the worst case scenario, a part of the town would be permanently under water, and the rest of it would be inundated daily, forcing the whole town to be moved.

We would like to suggest further studies to create a grid of Delaware Bay with intermediate resolution, which could try to better represent the spatialtemporal differences between the observations in each station inside the bay. However, that may not be accomplished without the application of a more realistic wind product capable of reproducing the strong winds observed which may play a critical role in predicting the timing and magnitude of the local surge inside the bay. One idea could be to use the observations, in the same way as was done with the water levels. However, since there are no wind measurements in the Bowers region, that would require a more thorough examination of the observations available and analysis of how to better apply those results to this case

The application of realistic water level and barotropic current at the lateral boundaries of our Regional Model showed a great improvement in the capability of simulating storm surges entering Delaware Bay. The High-Resolution model also showed that it is a valuable tool to analyze systematically flooding events due to storm surges, and in preparing for the impacts of future Sea Level Rise.

BIBLIOGRAPHY

- Baker, A. J., Gonzalez, P. M., Piersma, T., Niles, L. J., de Lima Serrano do Nascimento, I., Atkinson, P. W., ... & Aarts, G. (2004). Rapid population decline in red knots: fitness consequences of decreased refuelling rates and late arrival in Delaware Bay. *Proceedings of the Royal Society of London, Series B: Biological Sciences*, 271(1541), 875-882.
- Berkson, J., & Shuster Jr, C. N. (1999). The horseshoe crab: the battle for a true multi-use resource. *Fisheries*, 24(11), 6-10.
- Bleck, R. (2002). An oceanic general circulation model framed in hybrid isopycnic-Cartesian coordinates. *Ocean modelling*, 4(1), 55-88.
- Booij, N., Ris, R. C., & Holthuijsen, L. H. (1999). A third-generation wave model for coastal regions: 1. Model description and validation. *Journal of geophysical research: Oceans*, 104(C4), 7649-7666.
- Castellano, P. (2011). Validation of a hydrodynamic model of Delaware Bay and the adjacent coastal region (Master dissertation, University of Delaware).
- Chassignet, E. P., Hurlburt, H. E., Metzger, E. J., Smedstad, O. M., Cummings, J. A., Halliwell, G. R., ... & Tolman, H. L. (2009). US GODAE: global ocean prediction with the HYbrid Coordinate Ocean Model – HYCOM (No. NRL/JA/7304-08-8335). Naval Research Lab Stennis Space Center Ms Oceanography Div.
- Chen, Y. (2010). Coupling of wave and circulation models for predicting storm-induced waves, surges, and coastal inundation (Doctoral dissertation, University of Delaware).
- Clark, K. E., Niles, L. J., & Burger, J. (1993). Abundance and distribution of migrant shorebirds in Delaware Bay. *Condor*, 694-705.
- Davis, R. E., & Dolan, R. (1993). Nor'easters. *American Scientist*, 81(5), 428-439.

- Delaware Sea Level Rise Advisory Committee. (2013). Delaware Sea Level Rise Adaptation Effort: Preparing for Tomorrow's High Tide - Recommendations for Adapting to Sea Level Rise in Delaware. Retrieved from <http://www.dnrec.delaware.gov/coastal/Pages/DESLRAdvisoryCommittee.aspx>
- DNREC Sea Level Rise Technical Workgroup. (2009). Recommended Sea Level Rise Scenarios for Delaware. Dover, DE: Department of Natural Resources and Environmental Control. Retrieved from <http://www.dnrec.delaware.gov/coastal/Documents/SeaLevelRise/Final%20and%20Signed%20DNREC%20SLR%20scenarios.pdf>
- Eakins, B. W., Danielson, J. J., Sutherland, M. G., & Mclean, S. J. (2015). A framework for a seamless depiction of merged bathymetry and topography along U. S. coasts. Paper presented at U.S. HYDRO Conference Proceedings. National Harbor, MD, March 16-19, 2015
- Ebersole, B. A. (2014). Basic Storm Surge, Wave, and Flooding Principles. In: Engineering Investigations of Hurricane Damage: Wind versus Water (pp. 22-40). ASCE.
- Fanelli, C., Fanelli, P., & Wolcott, D. (2013). NOAA Water Level and Meteorological Data Report—Hurricane Sandy. US Department of Commerce, National Oceanic and Atmospheric Administration, National Ocean Service Center for Operational Oceanographic Products and Services, 62.
- Garvine, R. W. (1991). Subtidal frequency estuary-shelf interaction: Observations near Delaware Bay. *Journal of Geophysical Research: Oceans*, 96(C4), 7049-7064.
- Garvine, R. W., McCarthy, R. K., & Wong, K. C. (1992). The axial salinity distribution in the Delaware estuary and its weak response to river discharge. *Estuarine, Coastal and Shelf Science: Estuarine*, 35(2), 157-165.
- Glibert, P. M., Madden, C. J., Boynton, W., Flemer, D., Heil, C., & Sharp, J. (2010). Nutrients in estuaries a summary report of the national estuarine experts' workgroup 2005–2007. – Chapter 5 – 3. Delaware Estuary - EPA <http://water.epa.gov/scitech/swguidance/standards/criteria/nutrients/upload/Nutrients-in-Estuaries-November-2010.pdf>.
- Google Inc. (2015). Google Earth Pro (Version 7.1.5.1557) [Software]. Available from: <https://www.google.com/earth/>
- Hedström, K. (2000). Technical manual for a coupled sea-ice/ocean circulation model. OCMS study MMS, 97-0017.

- Hughes, C. P., & Veron, D. E. (2015). Characterization of Low-Level Winds of Southern and Coastal Delaware. *Journal of Applied Meteorology and Climatology*, 54(1), 77-93.
- Jenkins III, R. (2015) Surface wave analysis based on a hydrodynamic modeling system for the Delaware coastal environment. (Masters Dissertation - University of Delaware).
- Jurisa, J. T., & Chant, R. J. (2013). Impact of offshore winds on a buoyant river plume system. *Journal of Physical Oceanography*, 43(12), 2571-2587.
- Large, W. G., & Pond, S. (1981). Open ocean momentum flux measurements in moderate to strong winds. *Journal of physical oceanography*, 11(3), 324-336.
- Lott, N., & Ross, T. (2006). Tracking and evaluating U. S. billion dollar weather disasters, 1980-2005. Preprints. AMS Forum: Environmental Risk and Impacts on Society: Successes and Challenges, Atlanta, GA, Amer. Meteor. Soc., 1.2.
- Luetlich Jr, R. A., Westerink, J. J., & Scheffner, N. W. (1992). "ADCIRC: an advanced three-dimensional circulation model for shelves coasts and estuaries, report 1: theory and methodology of ADCIRC-2DDI and ADCIRC-3DL", Dredging Research Program Technical Report DRP-92-6, U.S. Army Engineers Waterways Experiment Station, Vicksburg, MS, 137p
- Mac Davis (2012, November 01) Hurricane Sandy Flooding - Driving Into South Bowers Beach Delaware [Video File] Retrieved from: <https://www.youtube.com/watch?v=EZThraMZ41Q&index=12&list=PLKizUK42xnRBNhdm9ygOFXv2JCt9sEZc2>
- Moore, A. M., Arango, H. G., Di Lorenzo, E., Cornuelle, B. D., Miller, A. J., & Neilson, D. J. (2004). A comprehensive ocean prediction and analysis system based on the tangent linear and adjoint of a regional ocean model. *Ocean Modelling*, 7(1), 227-258.
- Münchow, A., & Garvine, R. W. (1993). Buoyancy and wind forcing of a coastal current. *Journal of Marine Research*, 51(2), 293-322.
- National Hurricane Center. 2016. Tropical Cyclone Climatology. Retrieved June 16, 2016, from <<http://www.nhc.noaa.gov/climo/>>
- National Historical Hurricane Tracks. 2016 National Oceanic and Atmospheric Administration. Retrieved June 16, 2016, from <<https://coast.noaa.gov/hurricanes/>>

- National Hurricane Center. 2016. Tropical Cyclone Climatology. Retrieved June 16, 2016, from <<http://www.nhc.noaa.gov/climo/>>
- O'malley, S. (2012, October, 30). Flooding in Bowers Beach cuts off roadway; damage still considered minimal. Retrieved from <http://www.newsworks.org/index.php/local/delaware-feature/46294-flooding-in-bowers-beach-cuts-off-roadway-damage-still-considered-minimal10>
- Tides and Currents. 2016. National Oceanic and Atmospheric Administration. Retrieved June 16, 2016, from <<http://tidesandcurrents.noaa.gov/>>
- National Oceanic and Atmospheric Administration. 2016. Retrieved June 16, 2016, from <<http://www.noaa.gov/>>
- Philadelphia Regional Port Authority. "Philadelphia Regional Port Authority: Marketing Brochure - 2008" Philadelphia Regional Port Authority. 2008. Accessed March 08, 2016. <http://www.philaport.com/marketing/brochure2008.pdf>
- Qin, W., Kirby, J. T., & Badiey, M. (2005). Application of the spectral wave model SWAN in Delaware Bay. Research Report No. CACR-05-09.
- Resio, D. T., & Westerink, J. J. (2008). Modeling the physics of storm surges. *Physics Today*, 61(9), 33.
- Schmalz, R. A. (2011). Skill Assessment of the Delaware River and Bay Operational Forecast System (DBOFS). US Department of Commerce, National Oceanic and Atmospheric Administration, National Ocean Service, Office of Coast Survey, Coast Survey Development Laboratory.
- Sherwood, C. R., Harris, C. K., Geyer, W. R., & Butman, B. (2002). Toward a community coastal sediment transport modeling system: the second workshop. *Eos, Transactions American Geophysical Union*, 83(51), 604-604.
- Skamarock, W. C., Klemp, J. B., Dudhia, J., Gill, D. O., Barker, D. M., Wang, W., & Powers, J. G. (2005). A description of the advanced research WRF version 2 (No. NCAR/TN-468+ STR). National Center for Atmospheric Research Boulder Co Mesoscale and Microscale Meteorology Div.
- U.S. Department of Transportation, Maritime Administration. (June 2005) Report to Congress on the Performance of Ports and the Intermodal System. Washington, DC: U.S. Department of Transportation, Maritime Administration.

- USACE. "U.S. Waterborne Container Traffic by Port/Waterway in 2012." U.S. Waterborne Container Traffic by Port/Waterway in 2012. December 29, 2014. Accessed March 08, 2016. <http://www.navigationdatacenter.us/wcsc/by_porttons12.html>.
- U.S. Geological Survey. 2016. USGS Water Data for the Nation. Retrieved June 16, 2016, from <<http://waterdata.usgs.gov/nwis>>
- Warner, J. C., Perlin, N., & Skillingstad, E. D. (2008). Using the Model Coupling Toolkit to couple earth system models. *Environmental Modelling & Software*, 23(10), 1240-1249.
- Warner, J. C., Armstrong, B., He, R., & Zambon, J. B. (2010). Development of a coupled ocean-atmosphere-wave-sediment transport (COAWST) modeling system. *Ocean modelling*, 35(3), 230-244.
- Warner, J. C., Defne, Z., Haas, K., & Arango, H. G. (2013). A wetting and drying scheme for ROMS. *Computers & Geosciences*, 58, 54-61.
- Whitney, M. M. (2003) Simulating the Delaware coastal current. (Doctoral Dissertation - University of Delaware).
- Whitney, M. M., & Garvine, R. W. (2006). Simulating the Delaware Bay buoyant outflow: Comparison with observations. *Journal of Physical Oceanography*, 36(1), 3-21.
- Wilkin, J., Zavala-Garay, J., & Levin, J. Integrating modeling and data assimilation using ROMS with a Coastal Ocean Observing System for the US Middle Atlantic Bight. In Workshop Report: The Australian Coastal and Oceans Modelling and Observations Workshop (ACOMO 2012) (p. 3).
- Wong, K. C., & Münchow, A. (1995). Buoyancy forced interaction between estuary and inner shelf: observation. *Continental Shelf Research*, 15(1), 59-88.
- Wu, S. Y., Yarnal, B., & Fisher, A. (2002). Vulnerability of coastal communities to sea-level rise: a case study of Cape May County, New Jersey, USA. *Climate Research*, 22(3), 255-270.
- Zhang, K., Douglas, B. C., & Leatherman, S. P. (2000). Twentieth-century storm activity along the US east coast. *Journal of Climate*, 13(10), 1748-1761.

Appendix A

ROMS EQUATIONS

ROMS is a three-dimensional, free surface, terrain following, numerical model that solve the Reynolds averaged Navier-Stokes equations using the hydrostatic and Boussinesq assumptions (Hedström, 2010). The governing equations in Cartesian coordinates are:

$$\frac{\partial u}{\partial t} + \vec{v} \cdot \nabla u - fv = -\frac{\partial \phi}{\partial x} - \frac{\partial}{\partial z} \left(\overline{u'w'} - \nu \frac{\partial u}{\partial z} \right) + F_u + D_u \quad (1)$$

$$\frac{\partial v}{\partial t} + \vec{v} \cdot \nabla v + fu = -\frac{\partial \phi}{\partial y} - \frac{\partial}{\partial z} \left(\overline{v'w'} - \nu \frac{\partial v}{\partial z} \right) + F_v + D_v \quad (2)$$

$$\frac{\partial \phi}{\partial z} = \frac{-\rho g}{\rho_0} \quad (3)$$

The continuity equation is:

$$\frac{\partial u}{\partial x} + \frac{\partial v}{\partial y} + \frac{\partial w}{\partial z} = 0 \quad (4)$$

The scalar transport is given by:

$$\frac{\partial C}{\partial t} + \vec{v} \cdot \nabla C + fu = -\frac{\partial}{\partial z} \left(\overline{C'w'} - v_{\theta} \frac{\partial C}{\partial z} \right) + F_c + D_c \quad (5)$$

And at last, the equation of state is:

$$\rho = \rho(T, S, P) \quad (6)$$

The prescription of the vertical boundary condition is as follow:

$z = \zeta(x, y, t)$	$K_m \frac{\partial u}{\partial z} = \tau_s^x(x, y, t)$	(7)
	$K_m \frac{\partial v}{\partial z} = \tau_s^y(x, y, t)$	(8)
	$K_c \frac{\partial C}{\partial z} = \frac{Q_c}{\rho_0 C_p}$	(9)
	$w = \frac{\partial \zeta}{\partial t}$	(10)

Table A-1 - Variables used in the description of the ocean model (adapted from Hedström 2010).

Variable	Description
$C(x, y, z, t)$	Scalar quantity, i.e., temperature, salinity, nutrient concentration
D_u, D_v, D_c	Optional horizontal diffusive terms
F_u, F_v, F_c	Forcing/source terms
$f(x, y)$	Coriolis parameter
g	Acceleration of gravity
$h(x, y)$	Depth of sea floor below mean sea level
$H_z(x, y, z)$	Vertical grid spacing
ν, ν_θ	Molecular viscosity and diffusivity
K_M, K_C	Vertical eddy viscosity and diffusivity
P	Total pressure $P \approx -\rho_0 g z$
$\phi(x, y, z, t)$	Dynamic pressure $\phi = (P/\rho_0)$
$\rho_0 + \rho(x, y, z, t)$	Total in situ density
Q_c	Surface concentration flux
$S(x, y, z, t)$	Salinity
t	Time
$T(x, y, z, t)$	Temperatures
τ_s^x, τ_s^y	Surface wind stress
u, v, w	The (x, y, z) components of vector velocity \vec{v}
x, y	Horizontal coordinates
z	Vertical coordinates
$\zeta(x, y, t)$	Surface elevation

Appendix B

OTHER STORM SURGE EVENTS

In an effort to better understand storm surges in Delaware Bay, we examine two other surge events which happened in 2012: the first was a negative surge on the 26th of February and the second a positive surge on the 22nd of December. In both cases, the spatial variability of the surge in the bay is smaller than during Hurricane Sandy. During the positive surge on December, all stations registered the peak surge during the first hours of the day with values around 0.6m for Atlantic City, Cape May, and Bowers, while Lewes registered 0.53m and Ship John Shoal 0.76m. During the negative surge of February, all stations registered the peak surge around 6:00 with values between -0.60m -0.76m.

Figures B-1, B-4, and B-7 present the water level measurements during each storm surge; Figures B-2, B-5, and B-8 present the water level results generated by the RM for each storm surge; Figures B-3, B-6, and B-9 present the wind measurements during the same surge events. Table B- presents all the timing and height of peak surge in each surge event for every station. The station at Brandywine Shoal Light was destroyed during Hurricane Sandy.

Looking at the surges of December and February, the measured water level height and timing were close at different stations. However, observed water levels during the Sandy surge show a greater spatial variability in the Bay. Possibly, relatively strong, persistent winds in the Bay caused this variability during Sandy (Figure 4-1). During the other two events (Figures 4-4 and 4-7), the wind direction

continuously changed between south and north winds in periods of about 24 hours, so that the water level response to wind forcing likely differs from that observed during Sandy.

Table B-1 - Moment of occurrence and peak value of the three surges analyzed for the NOAA stations at Atlantic City, Lewes, Cape May, Brandywine Shoal Light and Ship John Shoal and for the USGS station at Bowers. Date in local time.

	Feb Surge		Dec Surge		Sandy	
	Time	Peak (m)	Time	Peak (m)	Time	Peak (m)
Atlantic City	Feb/26 6:00	-0.66	Dec/21 0:00	0.57	Oct/29 15:00	1.20
Lewes	Feb/26 7:00	-0.66	Dec/21 2:00	0.53	Oct/29 10:00	1.32
Cape May	Feb/26 8:00	-0.60	Dec/21 2:00	0.62	Oct/29 14:00	1.26
Bowers	Feb/26 5:00	-0.75	Dec/21 2:00	0.58	Oct/29 7:00	0.90
Ship John Shoal	Feb/26 6:00	-0.76	Dec/21 3:00	0.76	Oct/30 3:00	0.96

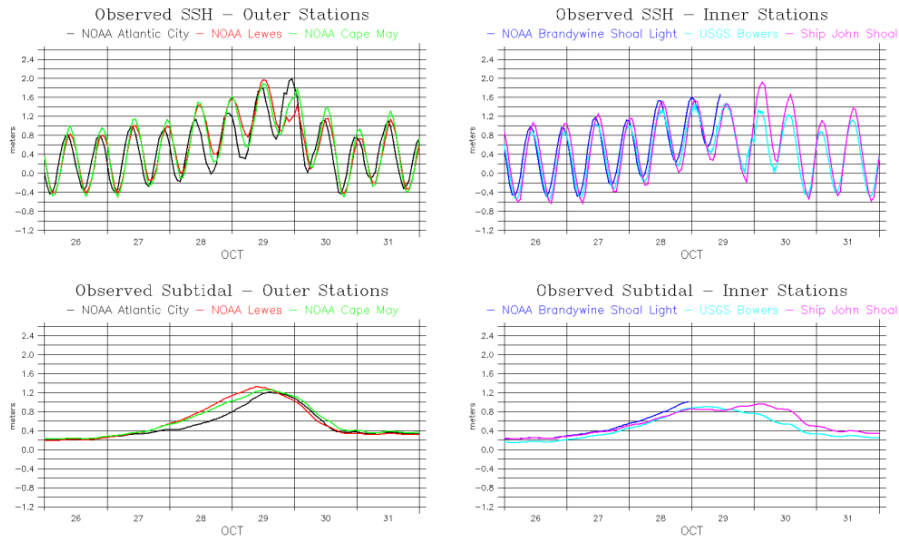


Figure B-1 – Sea surface height (top panels) and subtidal water level (bottom panels) at available water level stations inside Delaware Bay (Inner Stations, right panels) and close to the mouth of the Bay (Outer Stations, left panels) during Hurricane Sandy (October 2012).

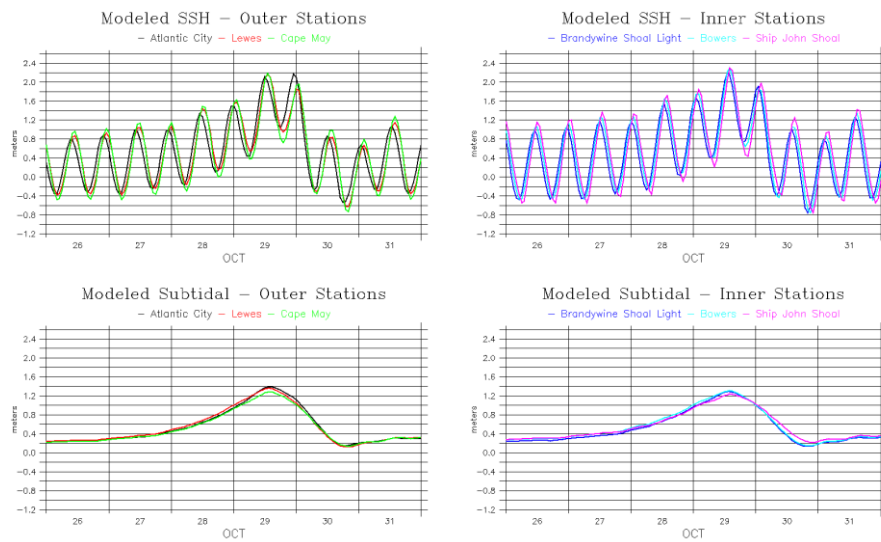


Figure B-2 – Sea surface height (top panels) and subtidal water level (bottom panels) generated by Regional Model at the measurement locations inside Delaware Bay (Inner Stations, right panels) and close to the mouth of the Bay (Outer Stations, left panels) during Hurricane Sandy (October 2012).

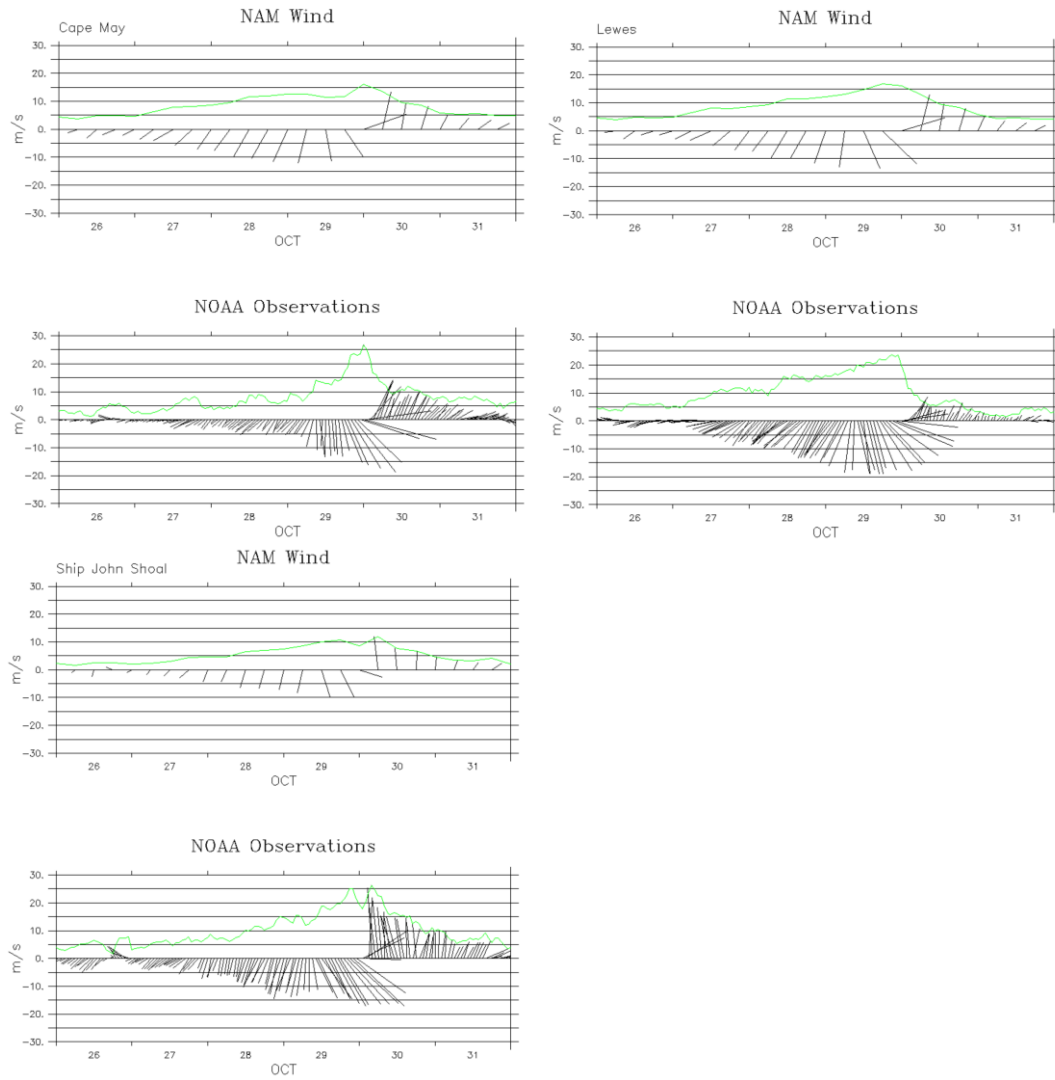


Figure B-3 – Comparison between the wind observations for the stations at Cape May, Lewes, and Ship John Shoal during Hurricane Sandy. The sticks represent the direction towards where the wind is going while the green line shows the wind speed in m/s.

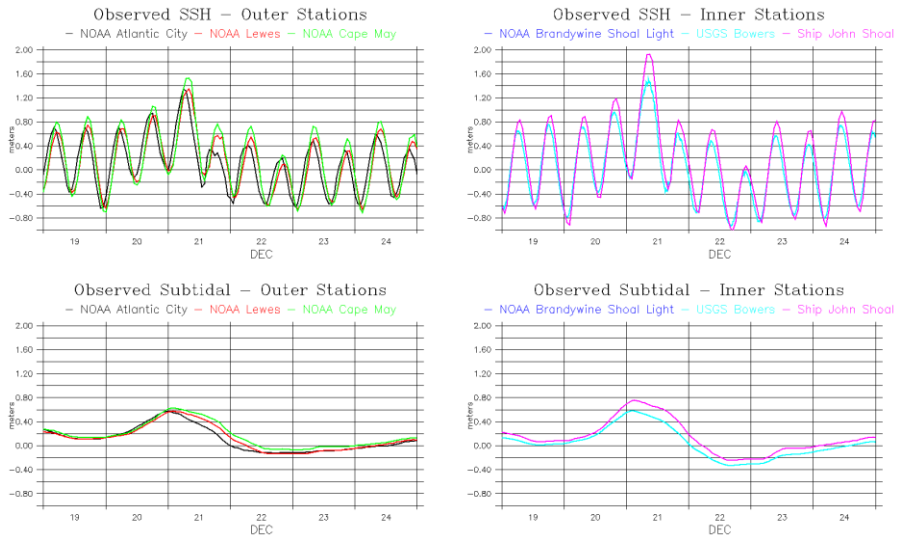


Figure B-4 – Sea surface height (top panels) and subtidal water level (bottom panels) at available water level stations inside Delaware Bay (Inner Stations, right panels) and close to the mouth of the Bay (Outer Stations, left panels) during the storm surge in December of 2012.

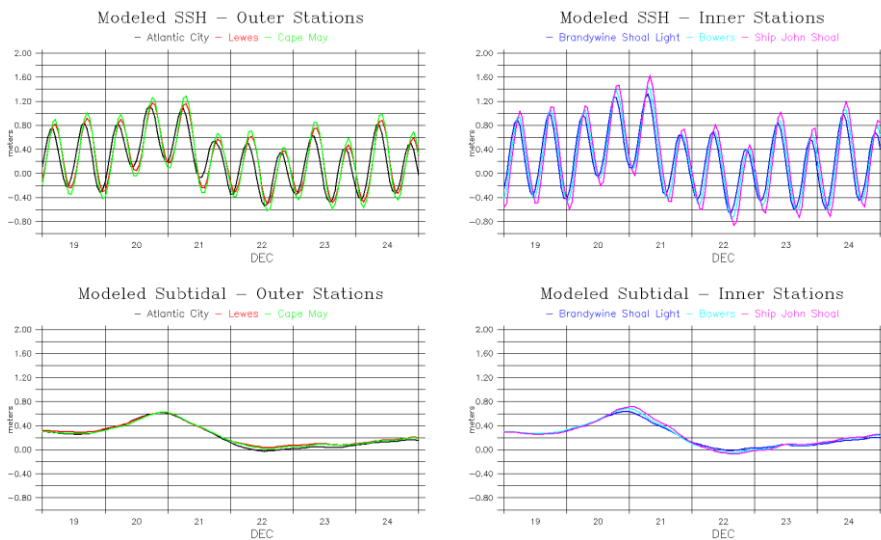


Figure B-5 – Sea surface height (top panels) and subtidal water level (bottom panels) generated by Regional Model at the measurement locations inside Delaware Bay (Inner Stations, right panels) and close to the mouth of the Bay (Outer Stations, left panels) during during the storm surge in December of 2012.

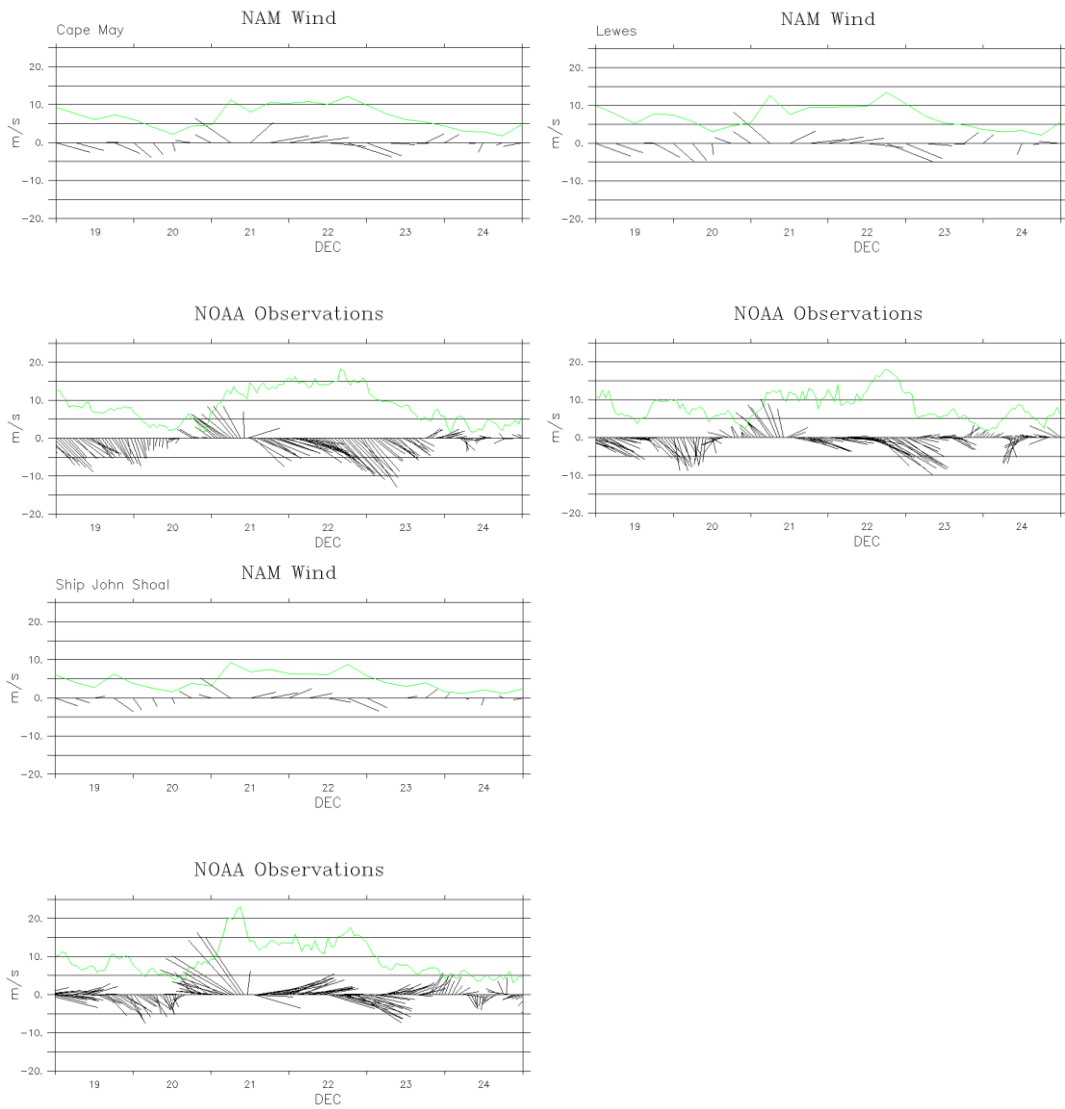


Figure B-6 – Comparison between the wind observations for the stations at Cape May, Lewes, and Ship John Shoal during the storm surge in December of 2012. The sticks represent the direction towards where the wind is going while the green line shows the wind speed in m/s.

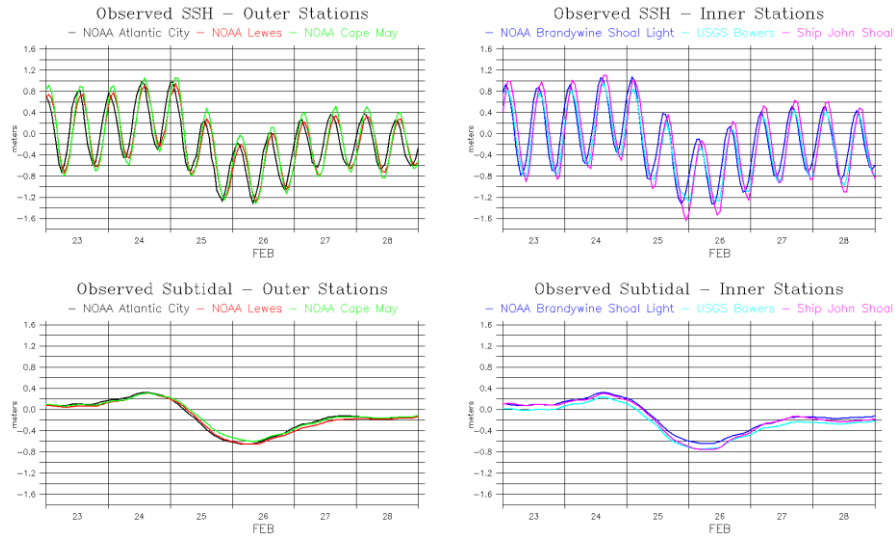


Figure B-7 – Sea surface height (top panels) and subtidal water level (bottom panels) at available water level stations inside Delaware Bay (Inner Stations, right panels) and close to the mouth of the Bay (Outer Stations, left panels) during the negative storm surge in February of 2012.

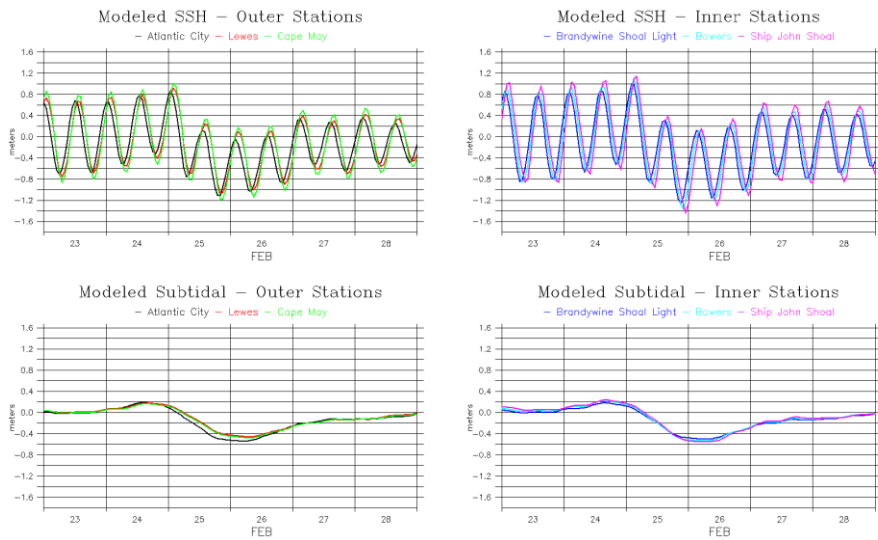


Figure B-8 – Sea surface height (top panels) and subtidal water level (bottom panels) generated by Regional Model at the measurement locations inside Delaware Bay (Inner Stations, right panels) and close to the mouth of the Bay (Outer Stations, left panels) during during the storm surge in February of 2012.

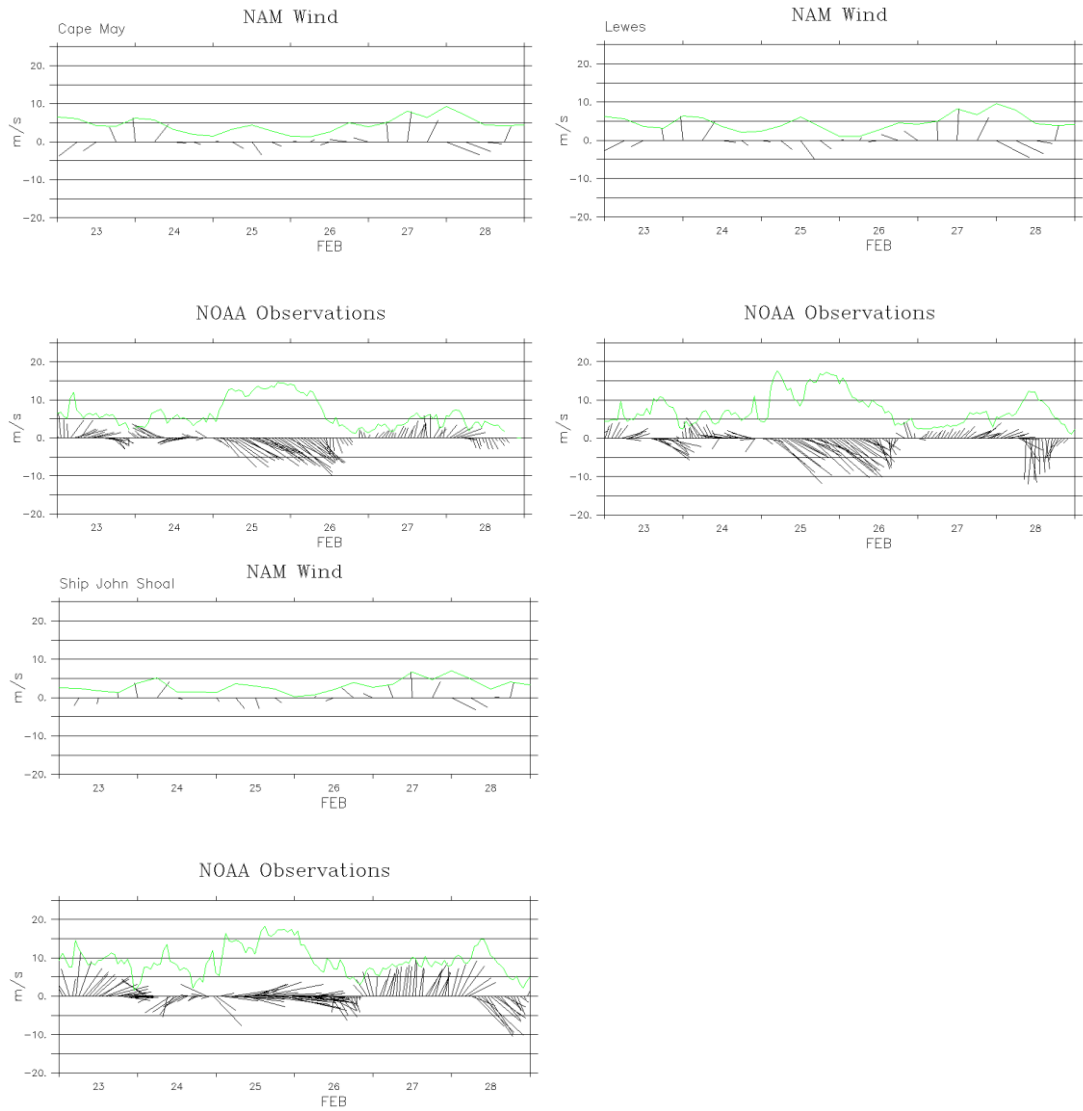


Figure B-9 – Comparison between the wind observations for the stations at Cape May, Lewes, and Ship John Shoal during the negative storm surge in February of 2012. The sticks represent the direction towards where the wind is going while the green line shows the wind speed in m/s.